Glycobiology, 2022, **32**, 12, 1116–1136
https://doi.org/10.1093/glycob/cwac050
Advance access publication date 4 August 2022
Original Article

Development and applications of sialoglycan-recognizing probes (SGRPs) with defined specificities: exploring the dynamic mammalian sialoglycome

Saurabh Srivastava[1,2], Andrea Verhagen[1,2], Aniruddha Sasmal[1,2], Brian R Wasik[3], Sandra Diaz[1,2], Hai Yu[4], Barbara A Bensing[5,6], Naazneen Khan[1,2], Zahra Khedri[1,2], Patrick Secrest[1,2], Paul Sullam[5,6], Nissi Varki[1,2], Xi Chen[4], Colin R Parrish[3], Ajit Varki[1,2,*]

[1]Department of Cellular and Molecular Medicine, School of Medicine, University of California at San Diego, San Diego, CA, USA, [2]Glycobiology Research and Training Center, University of California at San Diego, San Diego, CA, USA, [3]College of Veterinary Medicine, Cornell University, Ithaca, NY, USA, [4]Department of Chemistry, University of California at Davis, Davis, CA, USA, [5]Department of Medicine, University of California, San Francisco, CA, USA, [6]VA Medical Center, San Francisco, CA, USA

*Corresponding author: UCSD School of Medicine, La Jolla, CA 92093-0687, USA. Email: a1varki@health.ucsd.edu

Glycans that are abundantly displayed on vertebrate cell surface and secreted molecules are often capped with terminal sialic acids (Sias). These diverse 9-carbon-backbone monosaccharides are involved in numerous intrinsic biological processes. They also interact with commensals and pathogens, while undergoing dynamic changes in time and space, often influenced by environmental conditions. However, most of this sialoglycan complexity and variation remains poorly characterized by conventional techniques, which often tend to destroy or overlook crucial aspects of Sia diversity and/or fail to elucidate native structures in biological systems, i.e. in the intact sialome. To date, in situ detection and analysis of sialoglycans has largely relied on the use of plant lectins, sialidases, or antibodies, whose preferences (with certain exceptions) are limited and/or uncertain. We took advantage of naturally evolved microbial molecules (bacterial adhesins, toxin subunits, and viral hemagglutinin-esterases) that recognize sialoglycans with defined specificity to delineate 9 classes of sialoglycan recognizing probes (SGRPs: SGRP1–SGRP9) that can be used to explore mammalian sialome changes in a simple and systematic manner, using techniques common in most laboratories. SGRP candidates with specificity defined by sialoglycan microarray studies were engineered as tagged probes, each with a corresponding nonbinding mutant probe as a simple and reliable negative control. The optimized panel of SGRPs can be used in methods commonly available in most bioscience labs, such as ELISA, western blot, flow cytometry, and histochemistry. To demonstrate the utility of this approach, we provide examples of sialoglycome differences in tissues from C57BL/6 wild-type mice and human-like *Cmah*$^{-/-}$ mice.

Key words: Adhesin; acetylation; bacterial toxin; Sialoglycan-recognizing probes; Sialoglycans.

Introduction

All cells in nature are covered with a dense and complex array of sugar chains (Varki and Kornfeld 2022). In vertebrates, the outermost ends of the branches on this glycan forest are often capped with monosaccharides called sialic acids (Sias), which have enormous intrinsic complexity (Chen and Varki 2010; Schauer and Kamerling 2018). Most current methods to study this important and dynamic aspect of the glycome are too specialized for an average scientist to employ, and many aspects of the "sialome" (Altheide et al. 2006) are thus poorly studied. Given their ubiquitous presence and terminal position, Sias have been exploited as primary, transient, or co-receptors by a diverse range of commensal or pathogenic microorganisms (Severi et al. 2007; Matrosovich et al. 2015). These interactions are typically mediated by microbial proteins that have evolved high binding specificity toward sialoglycans because of the ongoing evolutionary arms race between microbes and hosts and can differentiate their target Sias by types, modifications, substitutions, and/or linkage to underlying glycans.

Here, we develop Sia-specific probes from such microbial proteins, harnessing their Sia specificity, and if found insufficient, assessed other available probes to generate a simple and reliable toolkit that can be used to easily monitor dynamic changes of Sias in normal and abnormal states. This set of sialoglycan-recognizing probes (SGRPs) can confirm whether a biological sample has any sialic acids or not; if so, the type of common Sia variations (particularly *O*-acetylation), linkage to underlying glycans, and the presence of *N*-acetyl or *N*-glycolyl groups. We assessed a number of Sia-specific binding proteins for specificity toward different mammalian Sia types and/or linkage to underlying glycans. Specifically, 9 types of SGRPs were defined from bacterial serine-rich repeat (SRR) adhesins, bacterial B5 toxins, viral hemagglutinins (HAs), and hemagglutinin-esterases (HEs) and compared with previously known invertebrate and plant lectins, selected Siglecs, and polyclonal and monoclonal antibodies. Upon identification of the best SGRP for each class of sialoglycans, a mutant inactive probe was also developed as an internal control of each probe's specificity. To ensure minimal loss of sensitive Sia modifications/substitutions, experimental conditions were optimized, and specificity of each probe was tested with positive and negative controls, such as pretreatment with specific sialidases or esterases, or mild periodate oxidation of the Sia side chain. The binding specificities of SGRPs were confirmed using a sialoglycan microarray presenting a diverse array of more than 100 mammalian sialoglycans and demonstrated by examples of laboratory methods of ELISA, western blotting,

Received: March 22, 2022. **Revised:** June 20, 2022. **Accepted:** July 14, 2022

and fluorescence detection by flow cytometry and histological analysis. An example of application of SGRPs is provided, showing sialoglycome changes in mice with human-like loss of the CMAH enzyme.

We of course realize that the absence of reactivity to a given probe is not an evidence of absence of a particular sialoglycan, and reactivity only indicates that the cognate glycan component is very likely to be present. Moreover, given the vast diversity of terminal sialoglycans in nature, we could not address all possibilities. Furthermore, our array does not represent all possible sialoglycans in nature (our estimate is >100,000 possibilities for terminal structures (Sasmal et al., BioRxiv 2021 May 28.446191)] and does not include branched structures nor some motifs found on other arrays (Fukui et al. 2002; Kletter et al. 2013; Arthur et al. 2014; Muthana and Gildersleeve 2014; Stencel-Baerenwald et al. 2014; Klamer et al. 2017). Thus, these probes are not meant to replace more rigorous chemical and structural analysis by experts. Rather they are developed for a nonexpert to discover interesting sialome patterns and changes in various biological systems, which are then worth exploring further.

Results and discussion

Defining distinct classes of SGRPs

We sought to define a set of SGRPs for detection of the most common mammalian sialoglycan variants, with nonbinding mutants as controls. This approach simplifies in-situ detection for all major types of Sias (SGRP1), typical *N*-acyl modifications at C-5 of Sias (SGRP2, SGRP5), linkages to underlying glycans (SGRP3, SGRP6, SGRP8), and occurrence of *O*-acetyl groups (SGRP4, SGRP7, SGRP9). The SGRP numbering system (see Table 1) for these probes make them easier to remember. To define a given probe, we used a superscript and added NB for the nonbinding control. Thus, for example, the *Yersinia enterocolitica* toxin B subunit (YenB) that recognizes all Neu5Ac and Neu5Gc forms and linkages is designated as SGRP1^{YenB} and the nonbinding variant as SGRP1^{YenB}NB. The current set of SGRPs does not include probes specific for 2-keto-3-deoxy-D-glycero-D-galacto-nononic acid (Kdn), which, although naturally found in mammals, occurs in limited amounts and primarily in the free form (Kawanishi et al. 2021).

Search for naturally evolved microbial molecules with defined specificity toward specific aspects of sialoglycans

SGRP candidates were defined by sialoglycan microarray studies, with a corresponding nonbinding mutant as a negative control. The essential criterion for a protein to qualify as an SGRP is that it must show specificity toward the preferred Sia modification/linkage. Detailed analyses and specificities and their practicability toward probing mammalian sialoglycans are discussed in subsequent sections. As mentioned in Table 1, we could not identify any microbial candidate having a better or broader specificity for SGRP5 (*N*-glycolyl-Sias) than our previously described affinity-purified Neu5Gc chicken polyclonal IgY, or for SGRP6 *Sambucus nigra* agglutinin (SNA), the conventionally used lectin probe for α2–6-linked Sias.

SGRP1^{YenB} detects all mammalian sialoglycans on the microarray

While α2–3Sia-binding MAL (*Maackia amurensis* lectin) and α2–6Sia-binding SNA together recognize the majority of Sia linkages, their preferences cannot be generalized for all types of Sias. Previously, Wheat germ agglutinin (WGA) and *Limax flavus* agglutinin (LFA) have been reported as having broad-spectrum Sia specificity, but their preferences toward Neu5Ac limit their utility as probes to detect all types of Sias (Bhavanandan and Katlic 1979; Miller et al. 1982; Cummings et al. 2015). For an SGRP that binds all types of Sia, we first considered YpeB (*Yersinia pestis* Toxin B subunit that recognizes both Neu5Ac- and Neu5Gc-terminated glycans [detailed sialoglycan preferences were recently reported (Khan et al. 2022), see also Fig. S1, see online supplementary material for a color version of this figure]. However, despite its ability to recognize most major classes of mammalian sialoglycans in glycan array and serum ELISAs, YpeB did not bind 4-OAc-Sias (Fig. S1, see online supplementary material for a color version of this figure). We investigated additional B subunits of AB5 bacterial toxins and selected YenB (*Y. enterocolitica* toxin B subunit) based on homology with YpeB and *Salmonella Typhimurium* ArtB, and broad host specificity (Sasmal et al., BioRxiv 2021 May 28.446191). Using His$_6$-tagged YenB (Fig. 1, also reported in Sasmal et al., bioRxiv 2021 May 28.446191), we confirmed the recognition of both Neu5Ac and Neu5Gc including 9-*O*- and 4-*O*-acetylated Sias, a clear advantage over WGA, LFA, and our initial candidate YpeB (Fig. S2, see online supplementary material for a color version of this figure). Notably, YenB did not show binding to nonsialylated glycans in the same assay. To biotinylate YenB without affecting Sia-binding, we attempted to clone with additional tags for biotinylation (SNAP, ACP, and Avi) but the modifications resulted in poor protein quality and yield, leading to reduced binding in glycan arrays. A direct *N*-hydroxysuccinimide (NHS)-biotin conjugation of YenB was therefore optimized to obtain the final biotinylated probe (SGRP1^{YenB}) that showed no change in binding in comparison to nonbiotinylated YenB. It was previously established that a serine residue contributes critically to Neu5Ac binding, while a tyrosine residue interacts with the extra OH group at the C5-acyl chain of Neu5Gc and is thus critical for its binding (Byres et al. 2008). As reported elsewhere (Sasmal et al., BioRxiv 2021 May 28.446191), we aligned the YenB sequence with those of *Escherichia coli* SubB and *S. Typhimurium* ArtB and predicted the conserved serine (S31) and tyrosine (Y100) in YenB. Mutating these critical sites for Sia recognition (YenB, S31A;Y100F) produced SGRP1^{YenB}NB as an internal control for Sia-binding SGRP1^{YenB} (Fig. S3a and b, see online supplementary material for a color version of this figure). The final binding and nonbinding specificities for SGRP1^{YenB} were tested on a sialoglycan microarray with nearly 130 mammalian sialoglycan types, suggesting all-inclusive Sia specificity in SGRP1, and a complete lack of Sia-binding by SGRP1^{YenB}NB (Fig. S4, see online supplementary material for a color version of this figure). Since there are no other molecules known to possess YenB-like Sia specificities, the pair of SGRP1^{YenB} and SGRP1^{YenB}NB are currently the most appropriate probe to detect all mammalian Sia types. The utility of SGRP1^{YenB} as a tool in situ Sia detection through ELISAs, western blotting, IHC, and flow cytometry is described and discussed below. We of course realize

Table 1. Sialoglycan recognition probes and their specificities.

Class of SialoGlycan Recognition Probe	Sialoglycans classes	Identified molecule	Pfam IDs	Sialoglycan preferences	SGRPs Nomenclature	
					Binding	Non-binding
SGRP1	All Sialic Acids (Sias)	YenB	Pertussis_S2S3 (PF02918)	All Sias	SGRP1^{YenB}	SGRP1^{YenB}NB
SGRP2	5-*N*-acetylneuraminic acid (Neu5Ac)	PltB	Pertussis_S2S3 (PF02918)	All Neu5Ac glycans	SGRP2^{PltB}	SGRP2^{PltB}NB
SGRP3	α-2-3 Linked Sialic Acids (α-2-3 Sias)	Hsa_{BR}	GspA_SrpA_N (PF20164)	All α2–3-linked Sias	SGRP3^{Hsa}	SGRP3^{Hsa}NB
SGRP4	4-O-Acetylated Sialic Acids (4-OAc Sias)	MHV	Hema_esterase (PF03996)	4-OAcetylated Neu5Ac	SGRP4^{MHV}	SGRP4^{MHV}NB
SGRP5	5-*N*- glycolylneuraminic acid (Neu5Gc)	IgY	Ig (PF00047)	All Neu5Gc glycans	SGRP5^{IgY}	SGRP5^{IgY}NB
SGRP6	α-2-6 Linked Sialic Acids (α-2-6 Sias)	SNA	Ricin_B_lectin (PF00652)	All α2–6 Linked Sia	SGRP6^{SNA}	N/A
SGRP7	7-O-Acetylated Sialic Acids (7-OAc Sias)	BCoV	Hema_esterase (PF03996)	7–9-di O-Acetylated Sia	SGRP7^{BCoV}	SGRP7^{BCoV}NB
SGRP8	α-2-8 Linked Di-Sialic Acid linkage	TeT	Toxin_R_bind_C (PF07951)	Disialic linkages	SGRP8^{TeT}	SGRP8^{TeT}NB
SGRP9	9-O-Acetylated Sialic Acids (9-OAc Sias)	PToV	Hema_esterase (PF03996)	All 9-O-Acetylated Sia	SGRP9^{PToV}	SGRP9^{PToV}NB

Table representing the classes of sialoglycan recognition probes (SGRPs), their presumed binding specificities, the most appropriate molecules as observed by assessment of sialoglycan binding by various glycomic methods, their experimentally confirmed sialoglycan preferences and defining SGRP nomenclature suggesting class of probe along with source of probe as mentioned in superscripts. The names of probes ending with NB represent the nonbinding variant of SGRPs.

that all possible sialoglycans and nonsialylated glycans have not been tested here (please see Conclusions and Perspectives section).

SGRP2^{PltB} recognizes all Neu5Ac-terminated glycans on the microarray

Neu5Ac is the most abundant Sia type and occurs in all Sia-expressing organisms. Certain mammals (including humans) lack a functional CMAH enzyme to convert cytidine 5′-monophosphate *N*-acetylneuraminic acid (CMP-Neu5Ac) into CMP-Neu5Gc and express excess Neu5Ac as a primary Sia type. Despite such wide distribution and roles in human physiology/immunity, there has so far been no direct probe to selectively detect all forms and linkages of Neu5Ac in situ. Among commonly known probes for sialoglycans, WGA shows relative specificity toward Neu5Ac-glycans, but it neither recognizes all sialoglycans terminating with Neu5Ac nor is it exclusive to Neu5Ac, showing a dual preference for Neu5Ac and GlcNAc (Bhavanandan and Katlic 1979) (Fig. S2a, see online supplementary material for a color version of this figure). Previously, we identified Neu5Ac-specific binding in PltB, the B subunit of Typhoid toxin which preferentially bound human erythrocytes and tissues rich in Neu5Ac over the corresponding Neu5Gc-rich samples from Chimpanzees (Deng et al. 2014b). Similar Neu5Ac-specific patterns of PltB binding were further studied recently by others who also reported its binding *O*-acetylated Neu5Ac in both α2–3 and α2–6-linked sialoglycans (Nguyen et al. 2020). In another paper (Sasmal et al., BioRxiv 2021 May 28.446191), we report on the binding of PltB to a range of naturally occurring Neu5Ac but not Neu5Gc-glycans, underlining PltB's appropriateness as a Neu5Ac-recognizing probe. Identifying the poor expression and purification quality of the His_6-tagged Neu5Ac-binding domain of PltB with an additional ACP tag (NEB), the final biotinylated probe version of PltB (SGRP2^{PltB}) was derived by NHS- biotinylation of PltB. This biotinylated-PltB shows comparable specificity toward Neu5Ac glycans as the unmodified protein (Fig. 1). The Neu5Ac-binding domain of PltB was characterized previously and a serine residue was reported to be critical for Neu5Ac-binding by PltB (Deng et al. 2014b). Thus, PltB^{S35A}NB, an internal nonbinding mutant control of SGRP2, was also produced, biotinylated, and included in all studies (Fig. S3c and d, see online supplementary material for a color version of this figure).

The sialoglycan microarray with mammalian sialoglycan types showed the Neu5Ac-specific binding pattern of SGRP2^{PltB}, while SGRP2^{PltB}NB completely lacks binding (Fig. S4, see online supplementary material for a color version of this figure). In agreement with previous data SGRP^{PltB} (Deng et al. 2014b), high binding preferences toward Neu5Ac were seen regardless of substitutions, modifications, or linkages to underlying glycans. SGRP2^{PltB} demonstrates comparable binding for α2–3, α2–6, and α2–8-linked Neu5Ac and distinguishes them from α2–3, α2–6, or α2–8-linked Neu5Gc (Fig. 1). Notably, SGRP2^{PltB} also exhibited recognition for Neu4,5Ac_2 and Neu5,9Ac_2. Taken together, SGRP2^{PltB} showed definite superiority over the plant lectin WGA as a Neu5Ac-binding probe (Fig. S2a, see online supplementary material for a color version of this figure).

SGRP3^{Hsa} selectively recognizes all α2–3-linked Sias on the microarray

Lectins from *M. amurensis* seeds (Kawaguchi et al. 1974) have been the gold standard for detection for Sias α2–3-linked to penultimate Gal. Initially designated as "strongly mitogenic *M. amurensis* leukoagglutinin (MAL) and 'strongly hemagglutinating *M. amurensis* hemagglutinin" (MAH), they are also known as MAL-I and MAL-II, respectively. While both lectins require at least a Siaα2–3Gal disaccharide

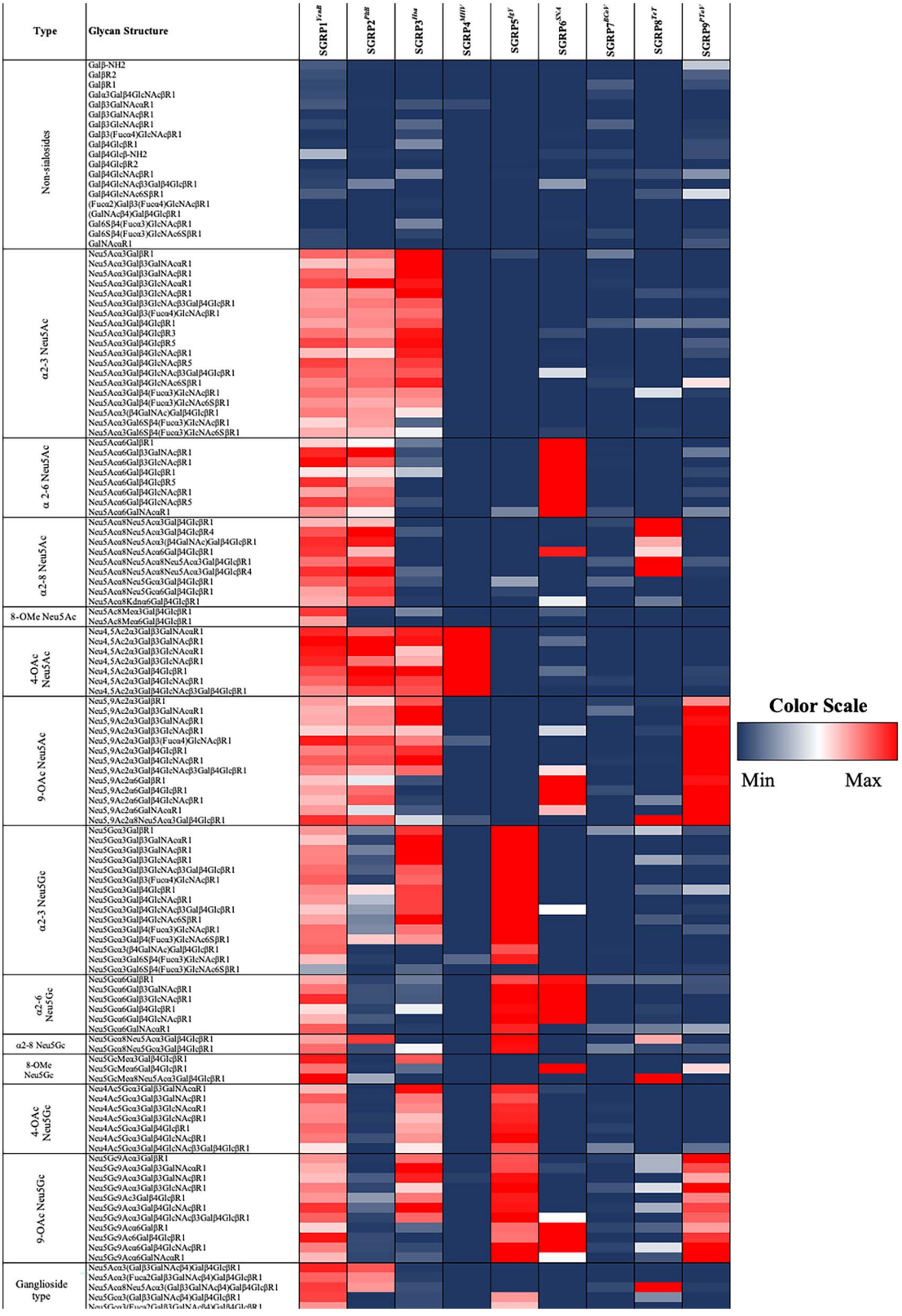

Fig. 1. Sialoglycan microarray binding studies of proposed SGRPs. Heatmap analysis of SGRPs (see Table I for details of nomenclature) binding to mammalian (sialo) glycans; SGRP1^{YenB} (30 μg/ml), SGRP2^{PltB} (30 μg/ml), SGRP3^{Hsa} (30 μg/ml), SGRP4^{MHV} (30 μg/ml), SGRP5^{IgY} (20 μg/ml), SGRP6^{SNA} (20 μg/ml), SGRP7^{BCoV} (60 μg/ml), SGRP8^{TeT} (30 μg/ml), and SGRP9^{PToV} (30 μg/ml) in microarray experiments. SGRPs binding efficiencies are displayed in red for highest binding (saturated or 100%), blue for minimum or no binding (0%), and intermediate binding represented by colors ranging between blue and red. Ranks; red (100%, or maximum), blue (0%, or minimum). Markedly reduced or absent binding was seen with the no-binding control probes studied simultaneously (see Fig. S4, see online supplementary material for a color version of this figure).

structure to bind, MAL-I shows stronger binding to Siaα2–3Galβ1-4GlcNAc/Glc (a trisaccharide common in N-glycans) and MAH (MAL-II) is selective toward Siaα2–3Galβ1-3GalNAcs (Kooner et al. 2021), typically found in *O*-linked glycans (Geisler and Jarvis 2011). Among Siaα2–3-linked structures tested, MAH prefers 9-*O*-acetyl Sias with Neu5Ac over Neu5Gc and Ser/Thr-linked *O*-glycan structures (Knibbs et al. 1991; Konami et al. 1994; Brinkman-Van der Linden et al. 2002). However, MAL-I can also recognize 3-*O*-sulfated Gal terminated oligosaccharides, i.e. it does not show exclusivity toward sialylated sequences (Bai et al. 2001). Instead, MAL-I displays widespread affinity toward α2–3-linked Neu5Ac and Neu5Gc, but with selective inclination toward Asn-linked over Ser/Thr-linked glycans. Attempts to improve *Maackia* lectins (Kaku et al. 1993) did not yield a general-purpose Siaα2–3-recognizing probe.

We looked into Sia-binding properties of previously reported Siglec-like-domain-containing ligand-binding regions (BRs) of *Streptococcus gordonii* SRR adhesins (Bensing et al. 2004; Deng et al. 2014a; Bensing et al. 2016). We selected GspB-BR of *S. gordonii* strain M99, Hsa-BR of *S. gordonii* Stain DL1 (Challis), and UB10712-BR of *S. gordonii* strain UB10712 and investigated their suitability for a comprehensive Siaα2–3-linkage identifying probe. All 3 BRs were expressed as SNAPf-His_6 fusions in the pGEX-3X vector in a bacterial expression system along with their nonbinding variants HsaBR (R340E), GspBBR (R484E), and UB10712BR (R338E) (Fig. S3, see online supplementary material for a color version of this figure).

The pairs of Hsa_{BR}/Hsa_{BR}NB, $GspB_{BR}$/$GspB_{BR}$NB, and $UB10712_{BR}$/ $UB10712_{BR}$NB were biotinylated using SNAP-benzyl guanine chemistry and tested with the sialoglycan microarray. Despite structural similarities, the 3 biotinylated BRs displayed uniquely different ligand binding profiles, including differential recognition of sialyl Lewis antigens and sulfated glycans. While $GspB_{BR}$ selectively binds sialyl-T antigen (Neu5Acα2–3Galβ1-3GalNAc) and related structures, Hsa_{BR} displays broader specificity covering NeuAcα2–3Galβ1-4GlcNAc and sialyl-T antigen (Fig. 1 and Fig. S5a, see online supplementary material for a color version of this figure) (Bensing et al. 2004; Takamatsu et al. 2005; Deng et al. 2014a). In comparison to Hsa_{BR}, $GspB_{BR}$ imparts lesser specificity toward α2–3 than α2–6 Sia linkages (Bensing et al. 2004) and falls short of the binding range of Hsa_{BR}, which not only includes trisaccharide and oligosaccharide but also disaccharide Sias. 9-*O*-Acetylation on Sia did not block $GspB_{BR}$ or Hsa_{BR} binding, but sulfation enhanced Hsa_{BR} binding (Deng et al. 2014a). Sia binding preferences of $UB10712_{BR}$ remained comparable to α2–3-linked Sia specificities of Hsa_{BR} and $GspB_{BR}$. $UB10712_{BR}$ bound to a range of α2–3-sialyl linkages including sialyl Lewis X, 3′-sialyllactosamine and their sulfated forms but preferred Neu5Ac over Neu5Gc sequences (Fig. S5a, see online supplementary material for a color version of this figure) (Bensing et al. 2016). Confirming the Sia-specificity of these BRs, the NB variants did not show any binding of Sia linkages/modifications on the array (Figs S4 and S5, see online supplementary material for a color version of these figures). The data obtained with biotinylated BRs also agree with previously published reports on GST-fusion BRs (Bensing et al. 2004, 2016; Takamatsu et al. 2005; Deng et al. 2014a), and the comparable binding abilities of these biotinylated probes with the original BRs confirmed that biotinylation did not affect the Sia specificity of these proteins.

We asked if Hsa_{BR} could be a replacement for MAL and MAH, conventional lectins for this class of probes (SGRP3). In an experiment to compare Siaα2–3-binding preferences of Biotin-Hsa_{BR}, Biotin-MAL, and Biotin-MAH, Hsa_{BR} showed significantly pronounced Siaα2–3-binding ability regardless of Sia modifications (*O*-acetylation, *O*-sulfation) or glycan structures (disaccharides, trisaccharides, oligosaccharides) (Fig. S6a, see online supplementary material for a color version of this figure). Taken together with the glycan array data, we chose biotinylated Hsa_{BR} as our SGRP 3 probe ($SGRP3^{Hsa}$) and its nonbinding variant HsaBR (R340E) as the nonbinding control ($SGRP3^{Hsa}$NB).

SGRP4^{MHV} as a probe for 4-OAc-Sias

A major contributor to mammalian sialoglycan diversity is *O*-acetylation, substituting the sialic acid hydroxyl groups at C4, C7, C8, and/or C9 (Klein and Roussel 1998; Kamerling and Gerwig 2006). The presence or absence of these *O*-acetyl moieties can block or promote the binding of cellular and microbial lectins, and their regulations through sialate-*O*-acetylesterases (SOAEs) and sialate-*O*-transferases (SOATs) act as the molecular switches to control several cellular functions and interactions (Cariappa et al. 2009; Pillai 2013). In contrast to *O*-acetylation at C7 or C9-OH, 4-*O*-acetylated Sia and its structural and functional significance have yet to be explored in detail, and 4-OAc-Sias have been difficult to study even by chemical methods, due to variable expression or absence in many animal species, dynamic occurrence in pathological conditions, resistance to conventional sialidases, lability to acidic conditions (Manzi et al. 1990), and masking of Sias from detection by some lectins. Equine erythrocytes, α2-macroglobulins, and sera were used to study 4-OAc-"HD3"-reactive antibodies due to their high 4-*O*-acetyl-*N*-acetylneuraminic acid ($Neu4,5Ac_2$) content (30–50 percent of total Sias) (Hanaoka et al. 1989). Guinea pigs are another common source of mammalian 4-OAc-Sias. $Neu4,5Ac_2$ comprises a considerable share in serum (30% of all Sias) and liver (10% of all Sias) Sias in guinea pig, besides traces of 4-*O*-acetyl-*N*-glycolylneuraminic acid (Neu5Gc4Ac) (Iwersen et al. 1998).

In humans, 4-OAc has been reported in tumor-associated antigens of colon cancers, melanomas, and gastric cancers using "HD" antigen-specific antibodies, for example a chicken antibody specific to Neu5Gc4Ac-lactosylceramide (4-OAc-HD3) recognized Neu5Gc4Ac in GM3 ganglioside fractions of human colon cancer tissues (Miyoshi et al. 1986). Similar 4-OAc-HD3-reactive HD antibodies have also been reported in sera of patients with malignancies and liver diseases (Higashihara et al. 1991). Two chicken MAbs HU/Ch2–7 and HU/Ch6–1 reacted with Neu5Gc4Ac (Asaoka et al. 1992). Despite frequent reports on heterogenous 4-OAc in HD antigens in human cancers, there has not been a reliable conventional probe for in situ detection of this entire class of sialoglycans.

Previously, a Sia-binding lectin with specificity for *O*-acetyl Sia was purified from the hemolymph of the California coastal crab *Cancer antennarius*, which was more precise than other known lectins from horseshoe crab (*Limulus Polyphemus*) and slug (*L. flavus*) but also showed affinity toward 9-*O*-acetyl in addition to 4-*O*-acetyl Sias (Ravindranath et al. 1985).

A lectin from *Tritrichomonas foetus*, a parasitic protozoan that causes abortion in cows, was reported to react preferentially with Neu4,5Ac_2 over de-*O*-acetylated Sias, and agglutinated equine erythrocytes containing Neu4,5Ac_2 efficiently, but its preferences were also not exclusive for 4-*O*-acetylated Sias (Babál et al. 1999).

In general, *O*-acetylation of Sias can be a major receptor determinant for some viruses. Among the 5 viruses shown to initiate infections via *O*-Ac-Sias were the influenza C viruses, human coronavirus OC43, Bovine Coronaviruses BCoV, and porcine encephalomyelitis virus (PToV), but none of them exhibited binding of Neu4,5Ac_2 (Herrler et al. 1985; Rogers et al. 1986; Vlasak et al. 1987; Vlasak et al. 1988; Schultze et al. 1991a). Infectious salmon anemia virus (ISAV), the causative agent of infections in Atlantic salmons, showed specificity for, and hydrolysis of 4-OAc-Sias (Hellebø et al. 2004). ISAV preferentially de-*O*-acetylated free and glycosidically bound Neu4,5Ac_2 and showed lower and no hydrolysis for free and bound Neu5,9Ac_2, respectively. ISAV exhibited hydrolysis of both Neu4,5Ac_2 and Neu5Gc4Ac at comparable efficacy, which was a significant advantage over known 4-OAc-Sia-binding molecules but its affinity for free Neu5,9Ac_2 although lower than influenza C virus (Hellebø et al. 2004), restricted possibilities to derive a comprehensive probe for 4-OAc-Sias.

Murine coronavirus mouse hepatitis virus (MHV-stain S) expresses a hemagglutinin-esterase that exhibits comparable sialate-4-*O*-acetylesterase enzymatic activity to that of ISAV (Regl et al. 1999). Unlike comparable esterases from other sources, MHV-S HE protein specifically de-*O*-acetylates Neu4,5Ac_2, but not Neu5,9Ac_2, and converts glycosidically bound Neu4,5Ac_2-rich glycoproteins from horse and guinea pigs to Neu5Ac (Regl et al. 1999). MHV-S hydrolyzes acetyl esters from free as well as glycosidically linked Neu4,5Ac_2. Interestingly, MHV-A59 and several other MHV strains do not express a HE (Luytjes et al. 1988; Shieh et al. 1989; Yokomori et al. 1991). Previously, the MHV-S HE ectodomain, released from HE-Fc by thrombin-cleavage, was reported to exhibit proper sialate-4-*O*-acetylesterase activity when assayed for substrate specificity with a synthetic di-*O*-acetylated Sia (4,9-di-*O*-acetyl-*N*-acetylneuraminic acid α-methylglycoside, Neu4,5,9$Ac_3\alpha$Me) (Langereis et al. 2012).

Our collaborators had previously expressed the esterase-inactive MHV-S-HE ectodomain as a fusion protein with a C-terminal Fc domain of human IgG1 and investigated Neu4,5Ac_2 distribution in human and mouse tissues (Langereis et al. 2015). In another study, we further modified the virolectin by fusing MHV-S-HE ectodomain-Fc to a hexahistidine (His_6) sequence and detected higher expression of 4-OAc-Sias in horse and guinea pig respiratory tract tissues than mouse, where it was mostly localized in the gastrointestinal tract. 4-OAc-Sias were also found in a small number of cells within the duck, dog, and ferret respiratory tissues screened, but not so far in the tissues of humans or pigs (Wasik et al. 2017).

To derive a stable 4-OAc-Sia-binding probe, we expressed the MHV-S-HE esterase inactive ectodomain (S45A), and the nonbinding mutant MHV-S-HE (F212A), as fusion proteins with the C-terminal Fc domain of human IgG1, along with Avi-tag for permanent biotinylation (Fig. S3, see online supplementary material for a color version of this figure). Sia-binding and nonbinding proteins MHV-S-HE protein probes were biotinylated and tested for 4-OAc-Sia specificity on sialoglycan microarray. As anticipated, biotinylated Sia-binding MHV-S-HE (S45A) exhibited very specific recognition of 4-OAc-Sias, while the nonbinding mutant MHS-S HE (F212A) did not show any binding with any sialylated or nonsialylated glycan on the microarray, confirming its suitability as a nonbinding control (Fig. 1; Fig. S4, see online supplementary material for a color version of this figure). Biotinylated MHV-S-HE (S45A) binds exclusively to Neu4,5$Ac_2\alpha$3Galβ3GalNAcαR1, Neu4,5$Ac_2\alpha$3Galβ3GalNAcβR1, Neu4,5$Ac_2\alpha$3Galβ3GlcNAcαR1, Neu4,5$Ac_2\alpha$3Galβ3GlcNAcβR1, Neu4,5$Ac_2\alpha$3Galβ4GlcβR1, Neu4,5$Ac_2\alpha$3Galβ4GlcNAcβR1, and Neu4,5$Ac_2\alpha$3Galβ4GlcNAcβ3Galβ4GlcβR1 (Fig. 1). Despite such high specificity and avidity for Neu4,5Ac_2, MHV-S-HE (S45A) did not show any binding of 4-OAc-Neu5Gc-glycans (Fig. 1). Currently, the sialoglycan microarray does not include α2–6-linked 4-OAc-Sias (Neu5Ac or Neu5Gc), hence the binding of MHV-S-HE α2–6-linked 4-OAc-Sias is not discussed here.

Considering the rarity of Neu5Gc4Ac and limited knowledge about 4-OAc-Sia-recognizing proteins, MHV-S HE-derived fusion proteins provide the most useful probes for in situ detection of 4-OAc-Sias, represented mostly by Neu4,5Ac_2. Given its exclusive preference for 4-OAc-Sias, the biotinylated MHV-S-HE esterase inactive ectodomain appears to be the best probe for this class of sialoglycans (SGRP4^{MHV} and SGRP4^{MHV}NB) and we demonstrate its utility through ELISA, western blotting, FACS, and histochemistry. We expect that SGRP4^{MHV} will facilitate research on functional significance of 4-OAc-Sias, help in finding more comprehensive 4-OAc-Sia-binding proteins, and allow us to seek an improved version of SGRP4 with recognition of both Neu4,5Ac_2 and Neu5Gc4Ac.

SGRP5^{IgY} recognizes all Neu5Gc-terminated glycans on the microarray

Humans are genetically defective in synthesizing the common mammalian Sia Neu5Gc but can metabolically incorporate small amounts of this Sia from dietary sources into glycoproteins and glycolipids of human tumors, fetuses, and some normal tissues (Tangvoranuntakul et al. 2003). A mutually nonexclusive hypothesis has been put forward to suggest endogenous Neu5Gc production by tumor cells (Bousquet et al. 2018), but supporting data is very incomplete. Regardless, Neu5Gc has been observed in breast, ovarian, prostate, colon, and lung cancers. There is also a need for sensitive and specific detection of Neu5Gc in human tissues and biotherapeutic products. Previously, a number of different monoclonal antibodies against Neu5Gc have been reported which recognized Neu5Gc only in the context of particular underlying sequences and generally lack the ability to detect Neu5Gc on other structurally related or unrelated glycans (Ohashi et al. 1983; Higashi et al. 1984; Higashi et al. 1985; Hirabayashi et al. 1987; Higashi et al. 1988; Miyake et al. 1988; Tai et al. 1988). Most microbial Neu5Gc-binding proteins binding Neu5Gc-glycans are also not completely specific for Neu5Gc, as there is always some cross-reactivity with few Neu5Ac glycans (Ohashi et al. 1983; Higashi et al. 1984; Higashi et al. 1988).

To explore Neu5Gc-specific probes from microbial sources, we considered our previously reported Neu5Gc-binding preferences of subtilase cytotoxin (SubAB), an AB5 toxin secreted by some strains of Shiga toxigenic *E. coli* (STEC)

(Byres et al. 2008). The B5 subunits of this toxin (SubB) exhibited strong preference for Neu5Gc-terminating glycans. SubB showed 20-fold less binding to Neu5Ac and over 30-fold less if the Neu5Gc linkage was changed from α2–3 to α2–6. Using molecular modeling and site directed mutations, Day and colleagues reduced the α2–3 to α2–6-linkage preference while maintaining or enhancing the selectivity of SubB for Neu5Gc over Neu5Ac (Day et al. 2017; Wang et al. 2018). This SubB analog, SubB2M (SubBΔS106/ΔT107 mutant), did display further improved specificity toward Neu5Gc, bound to α2–6-linked-Neu5Gc, and could discriminate Neu5Gc- over Neu5Ac-glycoconjugates in glycan microarrays, surface plasmon resonance and ELISA assays. SubB2M also showed promising diagnostic properties in detecting presumed Neu5Gc-glycans in serum of patients with all stages of ovarian cancer (Shewell et al. 2018) and breast cancer (Shewell et al. 2022). While the SubB2M as reported has a clear and strong preference for Neu5Gc over Neu5Ac glycans the preference is not absolute. The polyclonal chicken IgY also has the advantage of recognizing all 40+ Neu5Gc-bearing glycans, with no cross reactivity at all with Neu5Ac-glycans. Since the goal was to have as broad-spectrum a probe for Neu5Gc-glycans as possible, we chose to go with the biotinylated-IgY, using IgY from nonimmunized chickens as a negative control (Fig. S7, see online supplementary material for a color version of this figure).

Considering all results from the Neu5Gc-binding molecules discussed or tested above, there is no contemporary probe better than the affinity-purified chicken polyclonal anti-Neu5Gc-IgY to detect a broader range of Neu5Gc-glycans. Hence, we selected chicken polyclonal-specific anti-Neu5Gc-IgY as SGRP5 and biotinylated this along with its nonbinding control IgY (from nonimmunized chickens) as the final set of SGRP5^{IgY} (Fig. S4, see online supplementary material for a color version of this figure). The utility of chicken Neu5Gc-IgY as SGRP5^{IgY} in general lab-used methods including ELISA, western blotting, FACS, and histochemistry is discussed in an earlier article, and the results obtained here confirmed its Neu5Gc-specificity as previously reported (Diaz et al. 2009; Samraj et al. 2015). In a long run, it is necessary to identify a monoclonal IgY that can detect all forms of Neu5Gc-sialoglycans without any cross-reactivity with Neu5Gc.

SGRP6^{SNA} recognizes all α2–6-Sias on the array

Unlike bacteria, some viruses that cause upper respiratory infections such as human influenza A, B viruses, and human coronavirus OC43 exhibit preferential affinity toward α2–6Sias, which are abundant in the upper airway epithelial brush border in humans (Nicholls et al. 2007; Jia et al. 2020). Influenza viral haemagglutinins (HA) are the major glycoproteins that allow the recognition of cells in the upper respiratory tract or erythrocytes by binding to α2–6Sias, making them potential candidates for α2–6Sias-binding probes. We investigated a range of viral HAs in the form of HA-Fc fusion proteins (soluble HA fused to human IgG1 Fc) for their sialoglycan-binding specificity using the glycan microarray (Fig. S8, see online supplementary material for a color version of this figure). Among the tested HA-Fc fusion proteins, Cali09 HA-Fc derived from California/04/2009 H1N1 showed selective binding to α2–6-linked Sias, most prominently with Neu5Acα6Galβ4GlcNAcβR5, followed by Neu5Acα6Galβ4GlcNAcβR1 and Neu5,9Ac$_2$α6Galβ4GlcNAcβR1. Despite strong preferences for α2–6Sias, none showed binding with a full range of α2–6Sias, especially α2–6Neu5Gc glycans. The failure of Cali09-HA-Fc to recognize a number of α2–6-linked sialosides, and its binding to a few α2–3-linked sialosides, questioned its suitability as an exclusive probe for α2–6-linked Sias (Fig. S8, see online supplementary material for a color version of this figure). Aichi68-HA-Fc derived from the hemagglutinin of Aichi/2/1968 H3N2 strain also lacked robustness and specificity showing indiscriminate binding toward a number of α2–6 and α2–3Sias (Fig. S8, see online supplementary material for a color version of this figure). Surprisingly one candidate, PR8 HA-Fc derived from Influenza strain A/Puerto Rico/8/1934 (PR8 H1N1), even showed prominent binding of α2–3-sialylated glycans instead of α2–6Sias (Fig. S8, see online supplementary material for a color version of this figure). Among other tested viral haemagglutinins, SC18 HA-Fc derived from influenza A H1N1 (A/SouthCarolina/1/18) exhibited selective binding to a few α2–6Sias such as Neu5Acα6Galβ4GlcNAcβR5 and Neu5Acα6Galβ4GlcNAcβR1, while another virolectin Mem-HA-Fc from influenza A H1N1 (A/Memphis/1/1987) bound to α2–3Sias and α2–6Sias without any strong preference for either linkage (Fig. S8, see online supplementary material for a color version of this figure). Taken together, it can be inferred that the viral haemagglutinins tested exhibited promising specificity toward α2–6Sias but lacked the robustness and binding dynamics required for a probe. Our results and observations appear true for several other viral hemagglutinins not included here (Lehmann et al. 2006).

As an alternative α2–6Sia-specific microbial probe, we reviewed the α2–6Sia-binding properties of a recombinant lectin (PSL) from the mushroom *Polyporus squamosus* that was reported for its high affinity binding with Neu5Acα6Galβ4GlcNAc (Tateno et al. 2004; Kadirvelraj et al. 2011). However, PSL showed a high order preference toward α2–6 over α2–3Sias but bound exclusively to Neu5Acα6Gal on *N*-linked glycoproteins, so we did not experimentally investigate this molecule further as an α2–6Sia-specific probe.

As an α 2–6Sia-binding alternative from mammals, we considered the well-characterized vertebrate sialic acid-dependent adhesion molecule CD22/Siglec-2 a member of the immunoglobulin superfamily expressed by B lymphocytes that binds specifically to Neu5Acα6Galβ4GlcNAc (Powell et al. 1993, 1995; Kelm et al. 1994; Sjoberg et al. 1994; Brinkman-van der Linden et al. 2000). hCD22-Fc (human CD22 fused with the Fc region of human IgG1) showed high affinity for a few α2–6Sias on microarray (Fig. S9, see online supplementary material for a color version of this figure), but lacked the avidity required for a probe, particularly for α2–6-linked Neu5Gc. With a possibility to characterize 2 SGRP6 candidates: one specific for α2–6Neu5Ac and the other for α2–6Neu5Gc, we tried exploiting the evolutionary derived strong preference of mouse siglec-2 (mCD22) for α2–6Neu5Gc. mCD22-hFc showed exclusive binding toward α2–6Sias but preferred Neu5Gc in general (Fig. S9, see online supplementary material for a color version of this figure). Interestingly, 9-*O*-acetylation completely aborted hCD22's binding to α2–6Neu5Ac (Fig. S9, see online supplementary material for a color version of this figure) but did not affect mCD22 binding to α2–6Sias. Nevertheless, the relatively poor avidity and inability of hCD22 to recognize *O*-Ac-substitution in α2–6Neu5Ac and the nonspecificity of mCD22 binding

α2–3 sialyl-LNnT glycan (Neu5Gcα3Galβ4GlcNAcβ3Galβ4Glc) limited their competency as α2–6Sia-binding probes, even in combination (Fig. S9, see online supplementary material for a color version of this figure).

Among other molecules, we also analyzed the adhesin of nontypeable *Haemophilus influenzae* which was reported for high affinity toward α2–6-linked Neu5Ac (Atack et al. 2018). According to this study, HMW2 bound with high affinity to α2–6-linked Neu5Ac such as Neu5Acα6Galβ4GlcNAc (α2–6-sialyllactosamine) and could discriminate it from α2–3Sias (<120-fold lesser binding with α2–3 Sialyllactosamine). HMW2 indeed showed appreciable preference for the α2–6 over the α2–3-linkage but was not able to recognize α2–6Neu5Gc, disqualifying it from consideration as a comprehensive probe for α2–6Sias. In the absence of an evolutionarily derived microbial protein as a dynamic probe for α2–6Sias, it appears that SNA (*S. nigra* or elderberry bark lectin) is still the best available probe for α2–6Sias.

SNA exhibits high preference for the terminal Neu5Acα6Gal/GalNAc sequences in both *N*-linked and *O*-linked glycans (Shibuya et al. 1987). Due to its ability to discriminate Siaα6Gal/GalNAc from Siaα2–3Gal/GalNAc and ubiquitous binding to Neu5Ac/Gc with/without *O*-Ac substitutions, SNA has been the standard probe for studying α2–6Sias. Using Vector lab's Biotin-SNA (Catalog number B1305, lot number Z1002), we investigated SNA's Sia-binding efficiency in sialoglycan microarray and observed very high preference toward α2–6Sias for both Neu5Ac and Neu5Gc and no measurable binding to α2–3Sias (Fig. 1). Interestingly, the *O*-acetyl substitutions that were a major concern for hCD22, mCD22, viral hemagglutinins, and HMW2 did not hinder SNA's binding to α2–6Sias. Apart from its binding to 6-*O*-sulfated Galβ4GlcNAc (Yamashita et al. 1992), SNA displayed an exclusive preference for α2–6Sias in disaccharides, trisaccharides, and oligosaccharides in Asn or Ser/Thr-linked glycans. So far, there appears to be no better molecule than SNA to probe α2–6Sias, hence we selected Biotin-SNA as SGRP6 (SGRP6^{SNA}) for this study. SGRP6^{SNA} is the exception to the set of SGRPs in not having an internal control of specificity. We characterized SGRP6^{SNA} as α2–6Sia-probe without any nonbinding variant in routine lab assay methods.

SGRP7^{BCoV} recognizes 7,9-diOAc-Sias

Except for some claims in microorganisms (Lewis et al. 2004; Gurung et al. 2013) and on human lymphocytes (Wipfler et al. 2011), 7-OAc-Sias are not commonly reported in natural glycans because of their instability. During biosynthesis, the primary attachment site of *O*-acetyl groups was exclusively to the C-7 hydroxyl of Sias, and the ester group migrates from C-7 to C-9 (Vandamme-Feldhaus and Schauer 1998). A hypothesis was proposed that SOAT enzyme would effectively be a 7-*O*-acetyltransferase incorporating *O*-acetyl groups primarily at C-7 of sialic acids, followed by their migration to the primary hydroxyl group at C-9 and transfer of an additional *O*-acetyl residue to C-7, resulting in di- and tri-*O*-acetylated species (Schauer 1987). This suggests that in nature, 7-OAc will be represented as 7,9-diOAc or 7,8,9-triOAc, but largely as 7,9-diOAc in mammalian sialoglycans. Considering that there is no stable 7-OAc, there may not be a true 7-OAc-Sia-binding protein. We defined specificities of SGRP7 to 7,9-diOAc-Sias, and 7/9di,9-diOAc has traditionally been studied in bovine submaxillary mucin, where the amount of 7-OAc- and 7,9-diOAc-Sias combined is almost twice of 9-mono-*O*-Ac-Sias (Langereis et al. 2015).

We also reviewed the sialoglycan specificity of other lectins and microbial proteins, reported to bind to 7,9-diOAc-Sias. Lectins from *C. antennarius*, *Achatina fulica*, and *T. foetus* showed higher preferences for 9-OAc and somewhat to 4-OAc but negligible to poor affinities for 7,9-diOAc-Sias (Stewart et al. 1978; Ravindranath et al. 1985; Babál et al. 1999). Viruses exhibit prominent binding to *O*-Ac-Sias but most show either 9-OAc preference (Influenza C viruses, human coronavirus OC43, porcine encephalomyelitis virus) or 4-OAc preference (ISAV, Puffinosis virus, mouse hepatitis virus strains-S, DVIM, JHM) binding over 7,9-diOAc (Herrler et al. 1985; Rogers et al. 1986; Vlasak et al. 1987, 1988; Schultze et al. 1991a; Klausegger et al. 1999; Hellebø et al. 2004; Langereis et al. 2010, 2015). The hemagglutinin esterases from bovine toroviruses (BTOV-B150, BToV-Breda), bovine coronaviruses (strains; Mebus and Lun), and equine coronavirus (ECoV-NC99) preferentially cleave 7,9-diOAc substrates over mono 4- or 9-OAc-substrates (Langereis et al. 2009; Langereis et al. 2015). Bovine viruses exhibit selective binding toward 7,9-diOAc, particularly BCoV-Mebus having relatively pronounced preferences toward 7,9-diOAc variants of both Neu5Gc and Neu5Ac, but lower preferences for 9-OAcs (Langereis et al. 2015). It is interesting that BCoV esterase selectively removes all 9-OAc residues in 7,9-diOAc-Sias in BSM, leaving 7-OAc attached. The residual 7-OAc residues do not attract binding of BCoV anymore, demonstrating that Sia 9-*O*-acetylation is a strict requirement and that mono 7-OAc-Sias do not serve as ligands (Langereis et al. 2015). The S protein, another hemagglutinin in BCoV, showed high specificity exclusively for 9-OAc-Sias with no preference for 7-OAc and this raises possibility that HE is the only receptor-binding protein for 7,9-di-OAc in BCoV-Mebus (Schultze et al. 1991b; Schultze and Herrler 1992).

Since BCoV-Mebus-HE is best characterized for 7,9-diOAc-Sia specificities, we expressed its esterase inactive mutant (BCoV-Mebus-HE S40A) and corresponding nonbinding mutant (BCoV-Mebus-HE F211A), each fused to human IgG-Fc followed by a His_6-tag and an Avi-tag. Both proteins were biotinylated with an Avi-tag and tested for preferences on the sialoglycan microarray (Fig. 1, Fig. S4, see online supplementary material for a color version of this figure). While the nonbinding mutant does not show binding with any sialylated or nonsialylated glycans in the array, the Sia-binding molecule BCoV-Mebus-HE S40A exhibited some affinity for 9-OAc-Sias (Fig. 1), agreeing with its Sia-binding pattern on sialoglycan microarray reported previously (Langereis et al. 2015). However, BCoV-Mebus-HE, S40A did not exhibit any binding to 4-OAc, most 9-OAc-Sias, and nonacetylated sialyloligosaccharides. The sialoglycan microarray did not contain 7/9di-Sias, so it is not known whether the protein binds that form.

SGRP8^{TeT} binds to a major class of terminal α2–8-linked disialosides

Oligosaccharide sequences in gangliosides and a few glycoproteins that terminate in Sias are not always mono-sialylated. In addition to α2–3 or α2–6-linkage with penultimate Gal, Sia can be linked with another Sia predominantly by α2–8-linkage forming α2–8-linked di, αoligo, and polysialic acid chains. α2–8-linked disialyl structures are critical component of neuronal gangliosides and these disialyl gangliosides,

especially GD3 and GD2, have been utilized as tumor markers for melanomas, gliomas, and neuroblastomas (Miyoshi et al. 1986; Hanaoka et al. 1989; Higashihara et al. 1991; Asaoka et al. 1992). Due to their utility in cancers either as biomarker for in vivo immunolocalization or in phase I and II trials to target disseminated neuroblastoma, a range of anti-disialoganglioside monoclonal antibodies have also been generated. For example, R24 is a mouse IgG3 monoclonal antibody (MAb) that reacts with the ganglioside GD3, expressed by cells of neuroectodermal origin (Kemminer et al. 2001). Similarly, a list of anti-GD2-specific MAbs; 3F8 (Heiner et al. 1987), BW704 (Manzke et al. 2001), 14G2a, 15G2a (Castel et al. 2010), AI-201, AI-287, AI-410. AI-425 (Kawashima et al. 1988), and anti-GD3 antibodies such as MAbs AI-245 and AI-267 (Kawashima et al. 1988), Ch14.18 and Ch14.18/CHO have been characterized for their preferential binding to disialyl gangliosides. Furthermore, MAbs JONES, D1.1, and 27A showed affinity for 9-OAc-GD3 but not 9-OAc-GD2, while Mab 8A2 binds both (Sjoberg et al. 1992). Despite the large number of GD3 and GD2 MAbs, there has not been a single one that could serve as a comprehensive probe for the broader range of disialylated glycans.

Among mammalian proteins, myelin-associated glycoprotein (MAG) shows high binding for specific gangliosides in order of GQ1bα > GT1aα, GD1α > GD1a, GT1b > > GM3, GM4, but not for GM1, GD1b, GD3, and GQ1b. Despite high affinity for disia and oligosias, MAG's binding to gangliosides is not exclusive for di-Sia linkages (Ito et al. 1999; Vinson et al. 2001). Siglec-7 is also reported to react mainly with disialyl structures such as disialyl Lewis α, disialyl galactosyl globoside, and ganglioside GD3, although it also lacks the probe such as binding dynamics for this class (Hashimoto et al. 2019). Among lectins reported to bind to disialylated oligosaccharides, *C. antennarius* lectin binds with GD3 (Ravindranaths et al. 1988), *Agrocybe cylindracea* lectin binds with GD1a and GD1b while not clearly differentiating other structures containing NeuAcα3Galβ3GalNAc (Yagi et al. 1997). WGA however preferred GT1 and GD1 over other gangliosides and exhibits very high affinity for monosialylated glycans and GlcNAc also, hence cannot be used as a di-Sia linkage-specific probe (MONSIGNY et al. 1980).

Infectious microbes possess promising affinity for disialyl oligosaccharides in accordance with the glycan environment of their anchorage surfaces. Porcine sapelovirus binds specifically to GD1α (Kim et al. 2016) and *Helicobacter pylori* recognizes GD2, GD1α, and GD1β by its sialic acid-binding adhesin (SabA) (Benktander et al. 2018). In agreement with high affinity for single ganglioside as observed in *Vibrio cholerae* (GM1), the majority of gut infecting bacteria and viruses exhibit binding with a specific sialoglycan structure, and their affinity cannot be generalized for range of disialyloligosaccharide sequences.

Tetanus (TeT) and botulinum neurotoxins (BoT) are produced by anaerobic bacteria *Clostridium tetani* and *Clostridium botulinum*, respectively, and share significant structural and functional similarity (Iwamori et al. 2008). Not only do BoT (serotypes A to G) and TeT exhibit affinities for similar di and oligosialogangliosides but also share significant sequence homology. In both BoT and TeT, the 150 Kda single chain can be cleaved in to a 50-Kda N-terminal light chain and 100-Kda C-terminal heavy chain. The HC fragment plays the primary role in receptor binding and can be further cleaved into a 50-Kda N-terminal fragment (HN) and a 50-Kda C-terminal fragment (HC). HC domain or HCR is characterized by the amino acid sequence homology among BoTs and TeT, which suggests that a conserved amino acid motif in this domain may define a common carbohydrate recognition site. Since both BoT and TeT possess comparable binding specificity for gangliosides, we preferred TeT to investigate its potential for a comprehensive disialyl linkage recognizing probe. Selection of TeT over BoT was also based on detailed reports on TeT binding to gangliosides (Halpern and Loftus 1993; Louch et al. 2002; Chen et al. 2008; Chen et al. 2009), and the feasibility to select a single serotype of TeT, (where BoT has multiple serotypes). An optimal receptor-binding domain (residues 1105–1315) from TeT-HCR was expressed as SNAPf-His_6 fusion in the pGEX-3X vector in a bacterial expression system along with its mutants TeT-HCR R1226L, TeT-HCR W1289A, and TeT-HCR R1226L/W1289A (Figs S3 and S10, see online supplementary material for a color version of these figures). Expressed proteins were biotinylated by SNAP-Biotin chemistry as described in experimental procedures and tested for their sialoglycan affinity in microarray (Fig. 1, Figs S4 and S10, see online supplementary material for a color version of these figures). TeT has been shown to specifically bind gangliosides of the G1b series, GD1b or GT1b. In accordance with a published report (Chen et al. 2009), TeT-HCR bound with a range of sialogangliosides including monosialylated GM1α, fucosyl-GM1, and oligosialylated GD1α, GD3, GT3 (Fig. S10, see online supplementary material for a color version of this figure). The high affinity of TeT-HCR for GM1 and fucosyl-GM1 questioned its candidacy as di-Sia linkage-specific probe. Single mutant, TeT-HCR R1226L, and double mutant, TeT-HCR R1226L/W1289A, did not bind with any glycans on array, suggesting the significance of arginine residue at 1226 position in sialoglycan identification (Figs S4 and S10, see online supplementary material for a color version of this figure). Another single mutant TeT-HCR W1289A showed appreciable enhancement in affinity toward GD3, GT3 while loss in binding toward monosialylated and asialylated glycans on array (Fig. S10, see online supplementary material for a color version of this figure). With respect to TeT-HCR (native protein), the tryptophan mutant TeT-HCR W1289A had pronounced specificity toward disialogangliosides structures particularly Neu5Acα8Neu5Acα3Galβ4GlcβR1, Neu5Acα8Neu5Acα3Galβ4GlcβR4, Neu5Acα8Neu5Acα8 Neu5Acα3Galβ4GlcβR4, and Neu5,9Ac2α8Neu5Acα3Galb β4GlcβR1 (Fig. S10, see online supplementary material for a color version of this figure). However, we noticed that TeT-HCR W1289A exhibited some minor binding with monosialogangliosides on the array but based on its high affinity for the range of α2–8-linked disialyl oligosaccharides and lack of other available options (MAbs, plant lectins, siglecs, viral, bacterial proteins) to derive a more potent probe for this class, we selected biotinylated TeT-HCR W1289A as SGRP8 ($SGRP8^{TeT}$), and the double mutant, Biotinylated TeT-HCR R1226L/W1289A ($SGRP8^{TeT}$NB) as a nonbinding control of $SGRP8^{TeT}$ due to its complete loss of binding for any glycans on array. We excluded the potential interaction of $SGRP8^{Tet}$ toward polysialic acid by testing SGRP8 candidates in an ELISA experiment containing several gangliosides and colominic acid (Fig. S10, see online supplementary material for a color version of this figure). The broad specificity of several bacterial toxins including TeT-HCR toward GM1, GD3, GT3, and GQ series of glycans could be related with

evolutionary preference to bind with most available ligands in their neural niche. This nonexclusive binding with multiple ligands by toxins might have advantage for the microbes but reduces our possibility to derive a molecule with probe such as robustness and dynamic specificity. Here, we show that site-specific modifications could improve the binding range in otherwise "nonspecific" probe candidates and characterize $SGRP8^{TeT}$ as α2–8-disiaoligosaccharide-binding probe through general laboratory methods later in this report.

SGRP9PToV is a competent probe for all 9-OAc-Sias on the microarray

Of *all* *O*-Ac-Sia modifications in nature, 9-*O*-acetylation is the most common in cells and tissues of humans and other animals. Their distribution is highly variable and implicated in embryonic development, host–pathogen interactions, and immunity. Although there have been monoclonal antibodies against *O*-acetylated gangliosides, these MAbs remained highly specific in recognition of *O*-acetyl esters only when presented by specific underlying sugar chain (Varki 1992). Few Sia-specific lectins recognizing 9-OAc modifications have been reported, for example a lectin from the marine crab *C. antennarius* showed affinity for 9-OAc and was used to demonstrate the presence of tumor-associated 9-OAc-GD3 on human melanoma cells (Ravindranath et al. 1985). *Cancer antennarius* lectin also showed significant affinity for Neu4,5Ac_2 and did not show affinity for a broad range of 9-OAc. Achatinin-H a lectin from the hemolymph of African land snail *A. fulica* did not bind to Neu4,5Ac_2 but failed to exhibit probe-like preference for a number of 9-OAc-Sias (Mandal and Basu 1987). Another lectin from the protozoan, *T. foetus*, showed promising affinities for 9-OAc-Sias but also bound to de-O-acetylated Sias with relatively high affinity, confirming its unsuitability as a probe (Babál et al. 1999).

9-OAc-Sia-binding-specific influenza C virus hemagglutinin esterase (Inf-CHE) was previously utilized as whole virions or recombinant protein for assessing a wide spectrum of sialoglycoconjugates such as mucins, serum glycoproteins, or gangliosides containing naturally or synthetically *O*-acetylated sialic acids (Muchmore and Varki 1987). The influenza C virus hemagglutinin-esterase is a membrane-bound glycoprotein that binds specifically to 9-OAc-Sias (hemagglutinin activity) and then hydrolyzes the *O*-acetyl group (receptor-destroying activity). Inf-CHE can specifically cleave *O*-acetyl groups from Neu5,9Ac_2 but not from 7-*O*-acetyl-*N*-acetylneuraminic acid (Neu5,7Ac_2), and very slowly from Neu4,5Ac_2 (Zimmer et al. 1992). Previously, we demonstrated that inactivation of Inf-CHE esterase by treatment with the serine esterase inhibitor di-isopropyl fluorophosphate (DFP) resulted in stable and irreversible binding with 9-OAc-Sias (Muchmore and Varki 1987). However, using the whole virion as a probe was complicated due to variations in purity and stability of preparations, poor reproducibility, high nonspecific background, and lack of linearity in response. To avoid these limitations, we replaced Inf-C virions with a recombinant soluble chimeric molecule composed of the extracellular domain of Inf-CHE fused to the Fc region of human IgG1 (CHE-Fc). DFP inactivation of CHE-Fc stabilized the hemagglutinin activity and yielded the probe CHE-FcD that was more specific for 9-OAc-Sias than the whole Inf-C virion (Klein et al. 1994; Martin et al. 2003). CHE-FcD provided a better alternative but did not qualify as a standard probe for 9-OAc-Sias due to selective preference for Neu5,9Ac_2 over Neu9Ac5Gc glycans, nonspecific binding to Neu5,7Ac_2, and hazards related to use of DFP (Fig. S11, see online supplementary material for a color version of this figure) (Hellebø et al. 2004).

To derive a better probe for 9-OAc-Sias, we reviewed other *O*-Ac-esterases from Inf-C such as mammalian coronaviruses: bovine (bovine coronaviruses; BCoV strains- Mebus, LUN, Breda, B150), birds (puffinosis virus), human (human coronaviruses, strains-OC43, HKU1), equine (ECoV-NC99), murine (mouse hepatitis virus strains-S, DVIM, JHM), and porcine (porcine torovirus strains; PToV, strains- Markelo, P4), reported previously (Klausegger et al. 1999; Langereis et al. 2010, 2015). Based on these reports, which also includes previous studies on OAc-Sia specificity of nidovirus HEs, we selected Porcine Torovirus P4 strain (PToV) hemagglutinin esterase to investigate as a probe, expressing the PToV HE ectodomain in insect Hi-five cells as fusion proteins with a C-terminal Fc domain of human IgG1 (PToV-HE-Fc). Instead of DFP, we used site-directed mutagenesis (S46A) to inactivate the esterase activity in PToV-HE-Fc fusion protein. PToV-HE-Fc showed high selectivity toward 9-OAc-Sias and demonstrated applicability to revealing the 9-OAc-Sia in human and animal tissues and cell lines (Langereis et al. 2015; Wasik et al. 2017).

We expressed 9-OAc-Sia-binding protein (PToV-HE-Fc, S46A) and nonbinding protein (PToV-HE-Fc, F271A) fused to human IgG-Fc followed by a His_6 tag and an Avi-tag (Fig. S3, see online supplementary material for a color version of this figure). Both binding and nonbinding proteins were biotinylated using the Avi-tag and investigated for their affinities in a sialoglycan microarray. The esterase-inactive probe, PToV-HE-Fc (S46A), bound exclusively with 9-OAc-Sias including Neu5Ac and Neu5Gc, while hemagglutinin inactive nonbinding PToV-HE-Fc (F271A) did not bind any sialylated or nonsialylated glycans (Fig. 1, Fig. S4, see online supplementary material for a color version of this figure). PToV-HE-Fc (S46A) showed binding toward 9-OAc Neu5Ac and Neu5Gc α2–3, α2–6 and α2–8-linked to their penultimate sugars. In a similar microarray, CHE-FcD showed efficient binding with a number of Neu5,9Ac_2-glycans but did not show similar affinity for Neu5Gc9Ac and remained a weaker binder to 9-OAc-Sias in general (Fig. S11, see online supplementary material for a color version of this figure). PToV-HE-Fc (S46A) exhibited significantly stronger binding toward a wide range of 9-OAc-Sia-glycans in comparison with CHE-FcD. Taken together, the efficacy, exclusivity, and reproducibility of PToV-HE-Fc (S46A), we selected biotinylated PToV-HE-Fc (S46A) as comprehensive probe ($SGRP9^{PToV}$) for 9-OAc-Sia and biotinylated nonbinding PToV-HE-Fc (F271A) as $SGRP9^{PToV}$NB, the internal control of $SGRP9^{PToV}$'s specificity. We characterize the utility of PToV-HE-Fc (S46A) as $SGRP9^{PToV}$ in general laboratory methods in sections below.

Use of the panel of SGRPs in common methods

Although detailed sialoglycan microarray analysis provides insights into the Sia specificity of SGRPs, it is essential for SGRPs to exhibit equally precise affinities toward their ligands in ensemble of glycans represented in biological samples. In particular, the multi-antennary sialoglycans and structurally overlapping sialoglycans in biological samples may have different interactions with probes than observed with individual

sialoglycans in the glycan arrays. Qualitative Sia binding and ligand specificity of SGRPs were therefore tested by ELISA experiments with blood sera from 9 animal species, each signifying diverse sialoglycan composition in terms of the presence or absence of *N*-glycolyl at C5 of Sia, *O*-acetylation, types of glycosidic bonds to penultimate sugars, and overall oligosaccharide sequence. For example, mouse serum is high in Neu5Gc-Sias in comparison with *Cmah*$^{-/-}$ mouse that remain exclusive for Neu5Ac-Sias and have relatively higher *O*-acetylation. Horse and guinea pig sera were included for their high representation of 4-OAc-Sias which was absent in other sera, as observed in HPLC analysis of Sias (Table S1). Similarly, we included erythrocytes from 9 animal species, expecting to derive a relatable pattern of SGRPs binding with sera and RBCs. HPLC analysis of surface sialome of erythrocytes (Table S2) suggests high variance in Sia diversity among animals which would be interesting to detect with SGRPs. We emphasized minimal loss of heat and pH labile *O*-Acs during assays and modified procedures accordingly.

SGRP1^{YenB} exhibits Sia-specific binding to all mammalian sera

As results summarized in Fig. 2 suggest, SGRP1^{YenB} exhibits comparable affinity to all sera, indicating its broad range of Sia specificities. In accordance with the glycan array (Fig. 1), SGRP1^{YenB} exhibits strong binding toward sera whether it is Neu5Gc rich (mouse, goat) or Neu5Ac abundant (human, rat, and *Cmah*$^{-/-}$ mouse). Furthermore, high proportions of Sia modifications such as 9-OAc substitutions (rat, rabbit, and *Cmah*$^{-/-}$ mouse) and, more prominently, 4-OAc substitutions (guinea pig and horse serum) did not inhibit SGRP1^{YenB}'s binding to serum sialoglycans (Fig. 2a). To exclude the potential contribution of serum protein interactions with SGRP1^{YenB} from our observations, we performed binding assays with sera after mild periodate oxidation of sera followed by borohydride reduction, generaing side-chain truncated-Sias with a terminal hydroxyl at the 7th carbon. SGRP1^{YenB} showed significantly reduced binding to periodate oxidized sera that was proportional to the loss of desired Sia ligands after the truncation (Fig. S12a, see online supplementary material for a color version of this figure). The question remained as to whether the residual binding of SGRP1^{YenB} to sera, observed even after periodate treatment was due to the interaction with nonsialylated structures in serum, or *O*-acetyl substitutions protecting Sias from complete oxidation. When *O*-acetyl esters were removed by mild base treatment before periodate oxidation, the residual SGRP1^{YenB} binding was completely abolished, thereby excluding the role of protein–protein interaction in SGRP1^{YenB}'s binding to mammalian sera (Fig. S12a, see online supplementary material for a color version of this figure). In the same experiment, base treatment without periodate oxidation did not significantly influence SGRP1^{YenB} binding to sera, confirming the probe's unbiased preference for Sias as seen in glycan array also (Fig. 1). Significantly, the nonbinding variant SGRP1^{YenB} did not show any binding with any serum at all tested concentrations (Fig. 2a).

SGRP2^{PltB} exhibits Neu5Ac-specific binding to mammalian sera

SGRP2^{PltB} binds to Neu5Ac and its derivatives that constitute a major fraction of Sia population in mammalian sera. Accordingly, SGRP2^{PltB} exhibited binding to all serum types tested in a concentration dependent manner (Fig. 2b). However, SGRP2^{PltB} exhibits an interesting pattern of binding toward Neu5Gc rich mouse serum vs. Neu5Ac-rich sera, especially human and *Cmah*$^{-/-}$ mouse sera. The nonbinding mutant SGRP2^{PltB}NB failed to bind serum from any animal source. Binding assays with mild base and periodate-treated sera confirmed that SGRP2^{PltB}'s binding toward serum was exclusively to Sia and was devoid of nonspecific interactions (Fig. S12b, see online supplementary material for a color version of this figure). The SGRP2^{PltB} also exhibited residual binding after periodate oxidation that was further reduced with prior base treatments, but base treatment alone did not noticeably influence the SGRP2^{PltB} binding to sera.

SGRP3^{Hsa} exhibits α2–3Sia-specific binding to mammalian sera

SGRP3^{Hsa} is specific toward Sias linked to underlying glycans with α2–3-linkage that coexist with α2–6Sias and α2–8Sias in cells, tissues, and other biological samples. SGRP3^{Hsa} bound all sera in a concentration dependent manner. In a different experiment to test Sia-specific binding of SGRP3^{Hsa}, the probe exhibited sera binding directly proportionate to their Sia constituents (Fig. S12c, see online supplementary material for a color version of this figure), excluding nonspecific interaction with nonsialylated structures in serum. Collectively, the results demonstrate SGRP3^{Hsa}'s indiscriminate binding to α2–3Sia in serum, irrespective of *O*-acetylation, Neu5Ac, or Neu5Gc, a finding that agrees with observations from sialoglycan microarray (Fig. 1). SGRP3^{Hsa}NB, the nonbinding version of SGRP3^{Hsa} showed no binding with any serum at tested concentrations (Fig. 2c).

SGRP4^{MHV} exhibits 4-OAc-Sia-specific binding to mammalian sera

SGRP4^{MHV} represents a probe for an exclusive class of 4-*O*-acetylated sialoglycans, which show a high abundance in blood components and tissues of certain animals. In our collection of sera, 4-OAc is represented by guinea pig and horse (38.7% and 32.4% of total Sia content, respectively, Table S1) and accordingly SGRP4^{MHV} exhibited strong binding to these sera (Fig. 2d). The negligible binding of SGRP4^{MHV} to other sera suggests that its specific binding to guinea pig and horse serum was due to 4-OAc-Sias exclusively found in these samples. Importantly, SGRP4^{MHV} exhibited no binding to serum rich in 9-OAc-Sias (*Cmah*$^{-/-}$, rat, and rabbit). confirming its ability to detect 4-OAc-Sias over 9-OAc-Sias. In similar experiments, SGRP4^{MHV}NB did not bind to any serum, confirming its utility as a nonbinding control. Periodate treatment did not have much effect on SGRP4^{MHV}'s binding toward guinea pig and horse serum, but base treatment followed by periodate oxidation completely blocked Sia detection (Fig. S12d, see online supplementary material for a color version of this figure). These results, along with sialoglycan glycan microarray confirm that even in complex biological samples such as serum, SGRP4^{MHV} binds only to 4-OAc-Sias.

SGRP5^{IgY} exhibits Neu5Gc-specific binding to mammalian sera

While 5-*N*-glycolyl-Sias (Neu5Gc) are a major component of Sia diversity in mammals, Neu5Gc is absent in humans

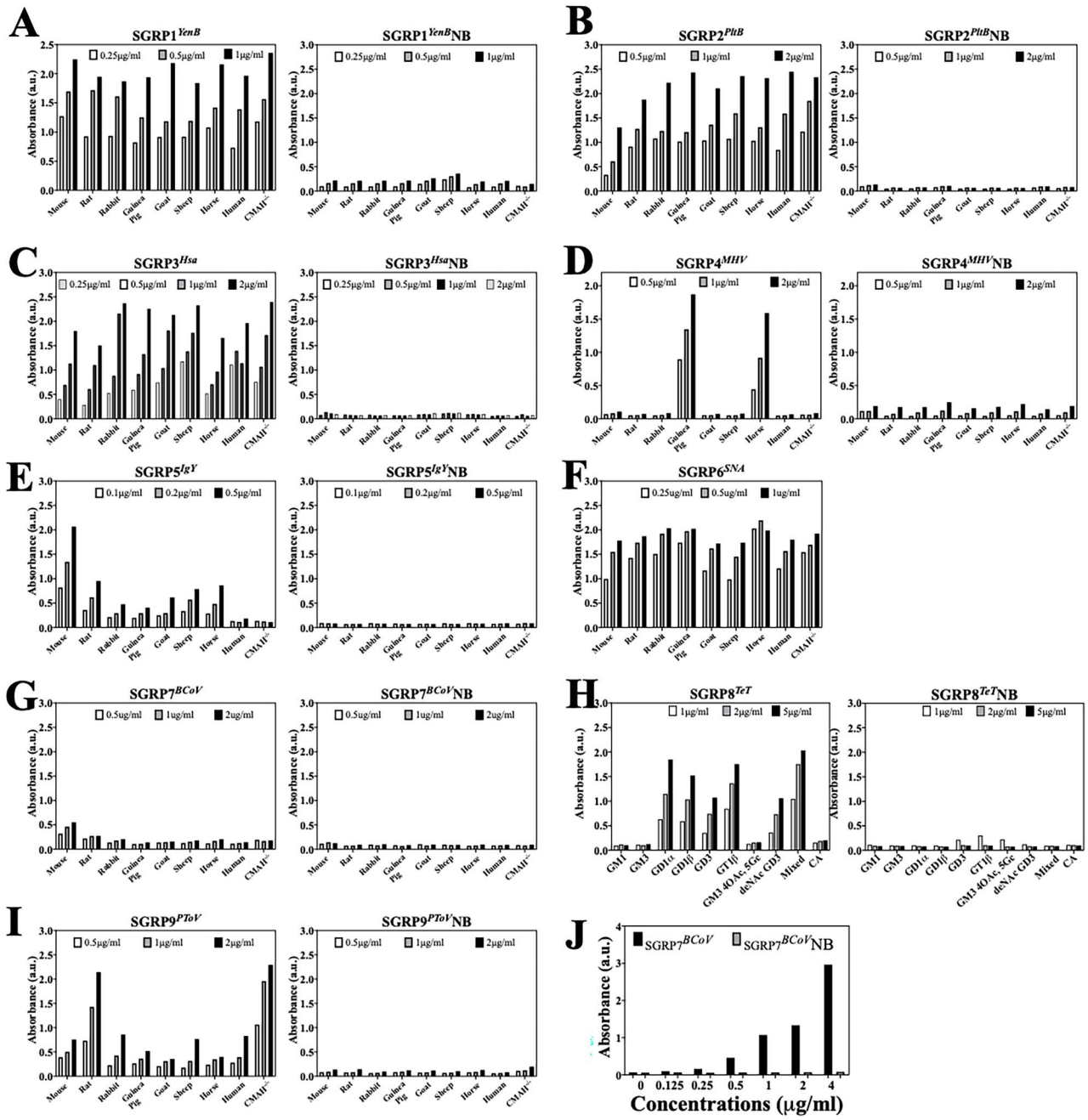

Fig. 2. Specific binding of SGRPs to sialoglycans in mammalian sera. The figure presents SGRPs binding of sialoglycans in biological samples, here represented by mammalian sera from mouse, rat, rabbit, Guinea pig, goat, sheep, horse, human, and *Cmah*$^{-/-}$ mouse. Panels A–I (except panel H) show binding efficiency of SGRPs and their nonbinding controls toward sera in concentration-dependent manner, as marked in individual panels. Panel H shows binding of SGRP8^{TeT} and SGRP8^{TeT}NB of purified gangliosides at concentrations mentioned in panel. Panel J demonstrates the 7,9-diOAc-Sia-specific binding of SGRP7^{BCoV} with bovine submaxillary mucin, while its mutant SGRP7^{BCoV}NB shows no affinity toward BSM. Binding of biotinylated SGRPs was detected and developed using Avidin-HRP (1:1,500). ELISA for each SGRP pair was performed under the same experimental conditions and validity of binding was confirmed by background signal wells treated only with secondary antibody (Avidin-HRP), not shown here.

due to loss of functional *Cmah*, and also in *Cmah* $^{-/-}$ mice. The serum binding assay (Fig. 2e) showed that SGRP5^{IgY} had very strong affinity for the WT mouse serum and also bound to all sera except human and *Cmah* $^{-/-}$ mouse. Significantly, SGRP5^{IgY} showed a reverse binding pattern to that observed with SGRP2^{PltB} (Fig. 2b), suggesting an approach to double-check the specificity of such complimentary probes. SGRP5^{IgY}NB did not bind any serum tested in similar experiments, as anticipated. A binding assay with base- and periodate-treated sera supported the specificity of SGRP5^{IgY}, as removal of OAc esters did not affect its binding to serum, while removal of Sias abolished binding (Fig. S12e, see online supplementary material for a color version of this figure).

SGRP6^{SNA} exhibits α2–6-specific binding to mammalian sera

SGRP6^{SNA} exhibits strong and general binding with all mammalian sera in binding experiments, suggesting its robustness as α2–6Sia-recognition probe. As observed in

glycan array (Fig. 1), SGRP6^{SNA} does not discriminate between α2–6Neu5Ac and α2–6Neu5Gc, with or without OAc esters. Similarly, the serum binding data (Fig. 2f) shows the binding of SGRP6^{SNA} to mouse, rabbit, guinea pig, human, or *Cmah*$^{-/-}$ mouse sera which contain Neu5Gc, Neu5Ac and Neu5,9Ac$_2$, Neu4,5Ac$_2$, Neu5Ac, Neu5Ac, and Neu5,9Ac$_2$, respectively. An experiment with periodate oxidized serum confirmed that SGRP6^{SNA} binds to sera in a Sia-specific manner and does not bind serum proteins (Fig. S12f, see online supplementary material for a color version of this figure).

SGRP7^{BCoV} exhibits 7,9-diOAc-Sia-specific binding to bovine submaxillary mucin

SGRP7^{BCoV} exhibited insignificant binding to tested mammalian sera, likely due to very strong preference toward 7,9-diOAc-Sias, absent in these sera (Fig. 2g). The probe does possess inconsistent and minor binding toward 9-OAc-Sias but those were not detected in the sera sialoglycans. To confirm SGRP7^{BCoV}'s recognition of 7, 9-diOAc-Sias, we studied binding with immobilized BSM, enriched in di- and tri-OAc-sialoglycans. As anticipated, SGRP7^{BCoV} showed dose-dependent binding patterns to BSM, while the nonbinding mutant SGRP7^{BCoV}NB showed no detectable signals (Fig. 2j). We confirmed its specificity toward OAc-Sias in base and mild periodate-oxidized BSM. The data (Fig. S12g, see online supplementary material for a color version of this figure) shows that SGRP7^{BCoV} binds BSM in OAc-dependent manner, and depletion of OAc esters resulted in dramatic reduction in SGRP7^{BCoV}'s binding, comparable to loss after complete depletion of Sias.

SGRP8^{TeT} exhibits DiSia linkage-specific binding to gangliosides

SGRP8^{TeT} exhibits very specific binding toward di-Sia linkages, the sialoglycan moieties mostly represented by gangliosides in biological system. As a result, SGRP8^{TeT} showed no detectable binding when tested against sera in ELISA experiment (Fig. S13a, see online supplementary material for a color version of this figure). In an ELISA experiment with immobilized purified gangliosides, SGRP8^{TeT} showed dose-dependent binding toward di-Sia oligosaccharide (GD1, GD3, GT1) discriminating from the mono-Sia oligosaccharides (GM1, GM3) and polySia oligosaccharides conformations (Colominic acid) (Fig. 2h). The observd results from ganglioside binding experiments are in complete agreement with the sialoglycan microarrays performed with SGRP8^{TeT} and confirm the advantage of the probe over native TeT-HCR (Fig. 1, Fig. S10a and b, see online supplementary material for a color version of this figure). The nonbinding mutant SGRP8^{TeT}NB showed no detectable signals, signifying its utility as a control for SGRP8^{TeT}'s specificity (Fig. 2h).

SGRP9^{PToV} exhibits 9-OAc-Sia-specific binding to mammalian sera

SGRP9^{PToV} binds to 9-OAc-Sias that are represented by all mammalian sera included for binding assays (Table S1). In observed results, SGRP9^{PToV} demonstrated remarkably high affinity toward rat and *Cmah*$^{-/-}$ mouse serum, suggesting their high proportions of Neu5,9Ac$_2$ (Fig. 2i). However, relatively lower binding to rabbit serum was interesting as rabbit serum contained the highest fraction of Neu5,9Ac$_2$ among the tested sera, but the basis of such variance is not known. It is clear from the serum-binding data of SGRPs that they can demonstrate the presence or absence of the preferred ligand, but that may not always measure the proportions relative to other Sia types within the serum. No detectable signals from similar binding assays with SGRP9^{PToV}NB confirm that SGRP9^{PToV} binding was specific. As observed in different ELISA experiments with OAc-depleted sera, SGRP9^{PToV}'s binding to mammalian sera including rat and *Cmah*$^{-/-}$ mouse showed a linear and reproducible binding exclusive to base labile OAc esters (Fig. S12h, see online supplementary material for a color version of this figure). The data showed that depletion of non-*O*-acetylated Sias does not influence SGRP9^{PToV} binding significantly while removal of OAc esters from Sias or complete diminution of Sia population abolished its binding to sera (Fig. S12h, see online supplementary material for a color version of this figure). These results together with sialoglycan microarray data (Fig. 1) confirm that SGRP9^{PToV} exhibits very strong preferences toward 9-OAc-Sias and does not interact with nonsialylated structures or proteins in complex biological samples.

Western blot analysis of SGRPs specificity toward sialoglycans in mammalian sera

To confirm that SGRPs are applicable to routine methods of glycoprotein analysis, we assessed SGRP's qualitative detection of sialoglycoproteins by western blots. The gel electrophoresis and western blotting protocol were modified to minimize the loss of sensitive OAc-Sias (Varki and Diaz 1984; Higa et al. 1989). SGRP1^{YenB} bound to all 9 sera included in the experiment, which is consistent with the serum binding ELISA experiments (Fig. 3a). SGRP2^{PltB} also bound to sera in accordance with their Neu5Ac contents, with a noticeable difference between its affinity for WT and *Cmah*$^{-/-}$ mouse sera (Fig. 3c). SGRP3^{Hsa} and SGRP6^{SNA} showed binding to all sera, a pattern also observed in serum binding ELISAs (Fig. 3e and k). SGRP4^{MHV} exclusively bound to guinea pig and horse sera (Fig. 3g), while SGRP9^{PToV} exhibited high binding toward rat, rabbit, and *Cmah*$^{-/-}$ mouse sera (Fig. 3n), corresponding to OAc-Sia contents of these sera (Table S1). Interestingly, SGRP7^{BCOV} showed a weak nonspecific binding with multiple sera in western blots (Fig. 3) and also showed a comparable weak nonspecificity in ELISA, which is likely due to its specificity toward 7,9-diOAc-Sias. We speculate that changes in pH and temperature during gel electrophoresis or blotting may result in migration of OAc esters, resulting in binding in western blotting, but we did not investigate this in detail. Blots, interrogated with nonbinding variants of SGRPs (Fig. 3) did not show any binding to sera, suggesting Sia-specific binding of SGRPs to sera. As SGRP8^{TeT} did not bind sera in ELISA, it was excluded from western blot analysis of serum.

SGRPs binding to frozen tissue sections: testing utility for in situ detection of Sias

The panel shows the typical binding patterns observed with each of the probes (red color indicates binding) (Fig. 4). The nonbinding control shows no binding to any of the sections, as expected. SGRP1^{YenB} detects mucins and blood vessels in many organs, and this is best demonstrated in the sections of kidney, where glomeruli are highlighted (Fig. 4a). The glomeruli as well as the capillary blood vessels between the

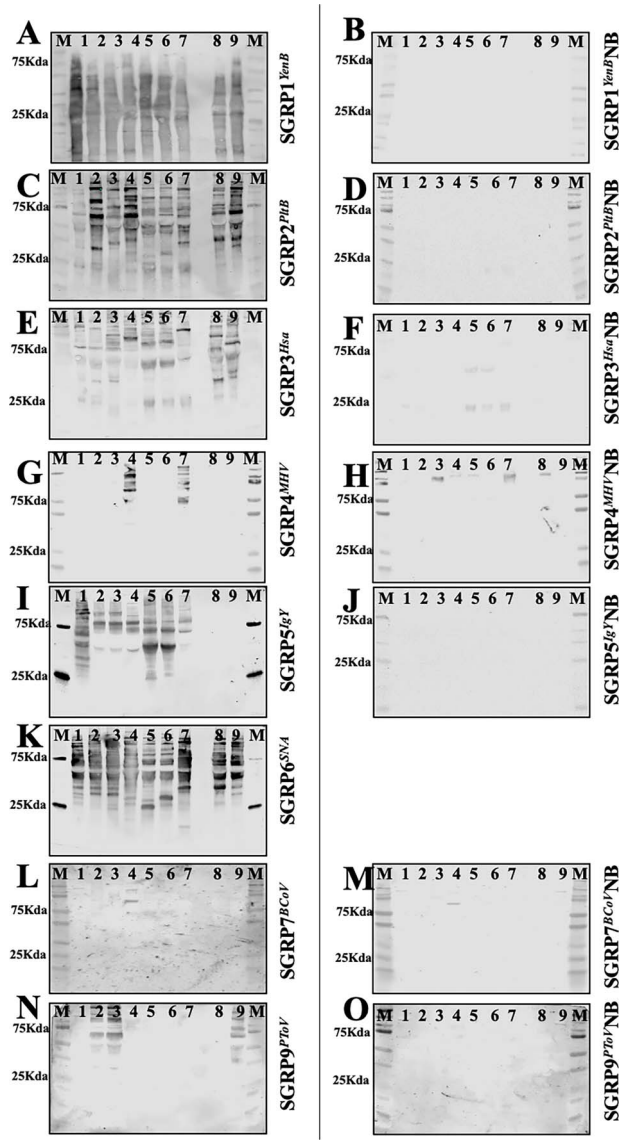

Fig. 3. Specific recognition of sialoglycoproteins in mammalian sera by SGRPs in western blots. Mammalian sera from mouse (1), rat (2), rabbit (3), Guinea pig (4), goat (5), sheep (6), horse (7), human (8), and *Cmah*$^{-/-}$ mouse (9) were subjected to SDS-PAGE under conditions that protect labile *O*-acetyl groups immunoblotted and probed with SGRPs. M in each blot represents the molecular weight marker. Panels a and b show blots interrogated with SGRP1YenB and SGRP1YenBNB (both at 1 μg/ml); panels c and d show blots interrogated with 1-μg/ml SGRP2PltB and SGRP2PltBNB; panels e and f represent SGRP3Hsa and SGRP3HsaNB (both at 1 μg/ml); panels g and h show blots probed with 1 μg/ml of SGRP4MHV and SGRP4MHVNB; panels i and j show blot probed with 0.33-μg/ml SGRP5IgY and SGRP5IgYNB; panels k is blot interrogated by 1-μg/ml SGRP6SNA; panels l and m show blots probed by 1-μg/ml SGRP7BCoV and SGRP7BCoVNB, and panels n and o represent blots interrogated with 2-μg/ml SGRP9PToV and SGRP9PToVNB. Binding of biotinylated SGRPs was detectable and developed using streptavidin IRDye 680 (1:10,000). Analysis was done on a LiCor odyssey infrared imager. Both blots for each SGRP set were detected at the same time using the same conditions.

tubules are prominent in the wild-type mouse, while in the *Cmah*$^{-/-}$ mouse, the capillaries between tubules are not as prominent (Fig. 4b). The nonbinding control shows no reactivity to any of the sections, as expected (Fig. 4c). SGRP2^{PltB} detects mucins and blood vessels in many organs, and this is best demonstrated in the sections of kidney, where the glomeruli are highlighted, and also the capillaries in between the tubules are visible (Fig. 4d and e). The nonbinding control shows no binding to any of the sections, as expected (Fig. 4f). SGRP3^{Hsa} detects mucins and blood vessels in many organs, and this is best demonstrated in the sections of kidney, where the glomeruli are prominently highlighted (Fig. 4g). The binding to the kidney glomeruli in *Cmah*$^{-/-}$ mouse is slightly more prominent (Fig. 4h). The nonbinding control shows no binding to any of the sections, as expected (Fig. 4i). SGRP4^{MHV} showed selective detection of mucins, and this is best demonstrated here in the mucin contained within the acini of pancreas. Staining was faint in wild type and was much more prominent in the *Cmah* null animal (Fig. 4j and k). Islets of the pancreas (the endocrine portion) and the nonbinding control show no binding (Fig. 4l). SGRP5^{IgY} detects blood vessels in many organs and demonstrated here by the detection of the capillaries within the sections from the pancreas in wild type, but not in *Cmah*$^{-/-}$mice (Fig. 4m and n). The nonbinding control shows no binding to any of the sections (Fig. 4o). SGRP6^{SNA} detects mucins and blood vessels in many organs. Here, we observe that SGRP6^{SNA} detects blood vessels in the pancreas of the *Cmah*$^{-/-}$mouse much better than it does in the wild-type animal (Fig. 4p and q). The tissue sections were incubated with secondary antibody Cy3-SA and served as control for SGRP6^{SNA} specificity, and show no binding to any of the sections, as expected (Fig. 4r). SGRP7^{BCoV} detects blood vessels in some organs but also detected white matter in the brain of the *Cmah*$^{-/-}$mouse extremely well (Fig. 4t). The nonbinding control shows no binding to any of the sections (Fig. 4u). SGRP8^{TeT} detected large areas of the nonnuclear neuropil in the brain from both the wild type and in the *Cmah*$^{-/-}$mouse. The white matter in the brain from the *Cmah*$^{-/-}$mouse was even more prominent, and the nonbinding control showed no binding to any of the sections (Fig. 4v, w, and x). SGRP9^{PToV} detected mucins and also red blood cells in many of the organs. However, in sections of liver from the *Cmah*$^{-/-}$mouse, there was an abnormally high expression in the sinusoidal endothelial cells around the central vein, indicating right heart failure in the *Cmah*$^{-/-}$mouse (the portal triads have two sources of blood supply and are thus the better perfused areas in the liver) (Fig. 4y and z). The nonbinding control showed no binding to any of the sections, as expected (Fig. 4z1).

SGRPs binding to mammalian erythrocytes in flow cytometry

We performed flow cytometry experiments with mammalian RBCs to demonstrate in situ detection of extracellular Sias by SGRPs (Fig. 5 and Fig. S14, see online supplementary material for a color version of this figure). As shown in Fig. 5a, SGRP1^{YenB} bound to RBCs from all 9 animal sources tested, while its nonbinding version SGRP1^{YenB}NB did not show any binding (Fig. 5a). In general, the total fluorescence intensity for nonbinder probes remained comparable to autofluorescence (RBCs without any treatment) and antibody control (RBCs detected with SA-PE only). SGRP2^{PltB} bound with all RBCs except wild-type mouse. The most robust bindings of SGRP2^{PltB} were detected with *Cmah*$^{-/-}$mouse, guinea pig, rabbit, and rat followed by goat and human RBCs (Fig. 5b). SGRP2^{PltB}NB did not show any noticeable binding with RBCs from any source. SGRP3^{Hsa} bound with all types of RBCs with

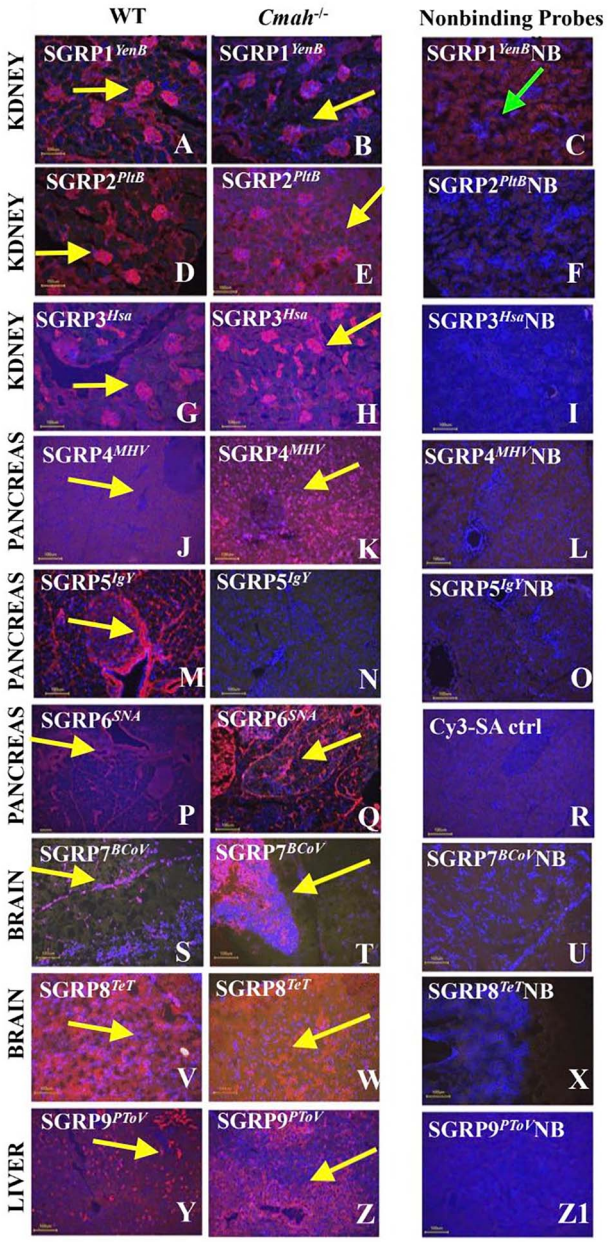

Fig. 4. Histological analysis of frozen mouse tissues by SGRPs. Examples of binding patterns (red-Cy3 streptavidin) observed with each SGRP probe (on different organs of the wild-type and the cmah null mouse strain). Panels a, b, d, e, g, and h show the detection of kidney glomeruli, (yellow arrows) by SGRP1^{YenB} and SGRP2^{PltB} (each used at 5 μg/ml) and SGRP3^{Hsa}, used at 3 μg/ml. In contrast, the nonbinding probe does not bind to glomeruli, as shown in panels c, f, and i. Pancreas exocrine mucin producing glands and intervening fibrous stroma are recognized by SGRP4^{MHV} (used at 5 μg/ml), SGRP5^{IgY} (used at 1 μg/ml) and SGRP6^{SNA} (used at 2 μg/ml) indicated by arrows in panels g, h, j, k, and m. However, with SGRP5^{IgY} as expected, there is no binding to *Cmah* null tissues; (panel n), the nonbinding controls also do not bind, as shown in panels l and o. Panel r represents secondary only control for SNA, with no binding. Brain meninges and white matter are recognized by SGRP7^{BCov} (used at 10 μg/ml) and SGRP8^{TeT} (used at 5 μg/ml), demonstrated with arrows on panels s, t, v, and w. The nonbinding controls do not bind shown in panels u and x. Liver macrophages are recognized in the wild-type animal by SGRP^{PToV}, and interestingly, in the *Cmah* null animal, SGRP^{PToV} binds to hepatocyte membranes closest to the central vein, indicating a different pathology in this genetically altered animal strain. The nonbinding control shows no binding (panel Zl). Nuclei are designated blue color by Hoechst stain.

maximum binding detected on guinea pig, goat, and rat RBCs and minimum with rabbit, indicating variable abundance of α2–3Sias on these erythrocytes (Fig. 5c). SGRP3^{Hsa}NB did not significantly bind to any RBC type. SGRP4^{MHV} showed no noticeable binding to any RBC type included in the experiment, and the binding as detected from SGRP4^{MHV} and SGRP4^{MHV}NB remained comparable, suggesting absence of 4OAc-Sias on the extracellular surface of these RBCs (Fig. 5d). SGRP5^{IgY} bound with all RBCs except from *Cmah*$^{-/-}$ mouse as anticipated (Fig. 5e). SGRP5^{IgY} also did not bind strongly to guinea pig and rat RBCs, suggesting less abundant Neu5Gc in these RBCs in comparison to mouse, horse, and rabbit. SGRP5^{IgY}NB showed negligible detection, as expected from a nonbinding control probe. A stronger SGRP6^{SNA} binding was detected with human, guinea pig, and rabbit in comparison to goat, sheep, and horse (Fig. 5f). Taking together with SGRP3^{Hsa}'s binding to RBCs, the relative abundance of α2–3Sias over α2–6Sias can be inferred for certain mammalian RBCs such as goat, sheep, and guinea pig. In absence of nonbinding mutant of SGRP6^{SNA}, the results are provided with autofluorescence and fluorescence antibody controls. The 7,9-diOAc-Sia-specific binder SGRP7^{BCoV} showed no appreciable binding in flow cytometry experiments, suggesting undetectable amounts of its ligand in tested RBCs (Fig. 5g). The resultant binding of SGRP7^{BCoV} and SGRP7^{BCOV}NB remains comparable with RBCs; consistent with the probe's response in the serum ELISA experiments, suggesting lack of SGRP7^{BCoV} binding in absence of its exclusive ligand 7,9-diOAc-Sia. α2–8-linked disialyl-oligosaccharides-specific probe SGRP8^{TeT} did not show any binding with RBCs tested (Fig. S13b, see online supplementary material for a color version of this figure), and hence, a set of GD3 transfected CHOK1 cells were used to investigate efficiency of SGRP8^{TeT} in flow cytometry experiment. As shown in Fig. 5i, SGRP8^{TeT} exhibited appreciable binding to GD3 expressing CHOK1 cells (CHOK1-GD3$^{+/+}$) compared with normal CHOK1 cells. The nonbinding SGRP8^{TeT}NB showed relatively minor binding with cells that was not affected by expression of GD3 gangliosides. As presented in Fig. 5h, SGRP9^{PToV} showed remarkable binding with rat RBCs among all tested erythrocytes and its nonbinder probe SGRP9^{PToV}NB remained completely undetectable. This experiment demonstrates the utility of SGRPs in the characterization of the extracellular sialome of cells, for example, showing that rat RBCs possess a dense Sia population that contains varying amounts of α2–3Sias, Neu5Ac, and 9-OAc-Sias than α2–6-Sias, Neu5Gc, and 4-OAc-Sias.

Conclusions and perspectives

Here, we exploited naturally evolved Sia-recognizing microbial proteins to develop an approach to design and derive sialoglycan-detecting probes. We developed and characterized a set of practicable probes recognizing the most predominant classes of mammalian Sia types. The study also reviewed and re-examined the current standing of traditional probes or probe-like molecules that have been reported against known diversity of mammalian Sia types. We reviewed, assessed, and experimentally analyzed several probes to compare their suitability for use as updated SGRPs. In this process, we successfully identified an alternative for *Maackia* lectins in the form of SGRP3^{Hsa}. This is important because these plant lectins can also recognize 3-*O*-sulfated glycans.

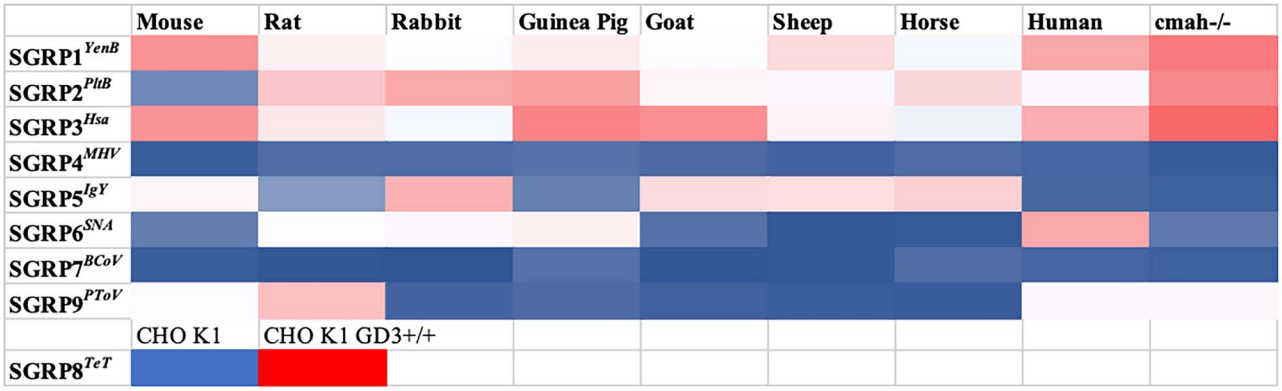

Fig. 5. SGRPs recognize specific sialoglycans on mammalian erythrocytes. Comprehensive heat map representation of SGRP's binding to mammalian erythrocytes and CHO-K1 cell line (SGRP8^{Tet}); colors red and blue represent maximum and minimum binding efficiencies, respectively. The heat map represents the comprehensive binding pattern of SGRPs (5 μg/ml) to mammalian erythrocytes and CHO-K1 cell line (SGRP8^{Tet}). SGRPs binding efficiencies are shown in red for highest binding (saturated or 100%), blue for minimum or no binding (0%), and intermediate binding represented by cells displaying colors between blue and red. As consistent with sialoglycan microarray data, no-binding control probes demonstrated significantly reduced or no binding in the same experiment.

In most instances, we found that probes from microbes that infect mammals were superior to the cross-reacting plant lectins. A striking exception was utility of conventional α2–6Sia-binding *S. nigra* lectin elderberry which appeared to be better than several microbial and mammalian proteins tested or reviewed in this study. Among developed probes; SGRP2^{PltB}, SGRP4^{MHV}, SGRP8^{TeT}, and SGRP9^{PToV} represent novel probes for their class of Sia molecules, while SGRP1^{YenB} and SGRP3^{Hsa} showed substantial improvement over previously known probes. SGRP5^{IgY} was also included in the final set, and SGRP6^{SNA} remained unique as we could not identify better alternative from microbial sources. Neu5Gc-specific microbial proteins showed utility but could not match the specificity and robustness of anti-Neu5Gc IgY that was finally selected as SGRP5^{IgY}. An exception to SGRPs set, SGRP7^{BCoV} is characterized as an imperfect probe that is not completely selective for 7-OAcSias and that must be updated with a more precise SGRP7 if one is identified in the future.

There are efforts ongoing by other groups, both in academic and industry to provide state-of-the-art sialoglycan detecting probes, and we attempted to review most of such studies and theoretically compared SGRPs with those molecules. While we appreciate the alternate approaches developed and adopted by other groups (Yabe et al. 2007; Imamura et al. 2011; Dabelsteen et al. 2020; Büll et al. 2021; Nason et al. 2021), we remained focused on naturally evolved molecules to find probes toward predominant class of mammalian sialoglycan. This study advances the merits of proposed SGRPs and their utilities for a biological science investigator. To have a consolidated assumption about the "best" available probe for any given sialoglycan class, a real-time comparison is required which is outside the scope of this study. Also not addressed here are sulfate esters, which can substitute for sialic acids in some glycans.

In conclusion, this study provides a comprehensive set of probes for many (but not all) mammalian Sia types, designed and developed for the nonsialic acid experts. Several tests to demonstrate SGRPs specificity confirm their utility as practicable probes. We expect SGRPs to be adapted by both experts and nonexperts as tools of Sia recognition in their studies. In closing, we re-emphasize that all possible terminal glycan sequences cannot be studied at this time for cross-reactivity with the SGRPs. Also, this SGRP set is not meant to give definite proof of the presence of the sialoglycans in question. Rather, binding of each probe strongly suggests that a particular component (e.g. 9-*O*-acetyl-Sias with SGRP9) is present in the sample being probed. Absence of reactivity is not evidence of absence, and presence of reactivity only indicates that the component is very likely to be present. Moreover, given the vast diversity of sialic acids in nature, we cannot address all possibilities. For example, it is possible that a 9-*O*-lactyl group (known to be present in nature but very poorly studied, and not available synthetically at this time) might cross-react. On the other hand, the presence of an 8-*O*-methyl group (also known to be present in nature but again very poorly studied, and not easily available synthetically at this time) might disrupt the recognition of a 9-*O*-acetyl group by SGRP9. Thus, these probes are not meant to substitute for more rigorous chemical and structural analysis by experts. Rather, they are meant for the nonexpert to find interesting sialome patterns in various biological systems that are then worth pursuing further. The class of probes such as SGRP1, SGRP2, SGRP4, SGRP8 and SGRP9 described in this report are novel for their target sialoglycan types. The study is based on glycomic methods to identify probe candidates and demonstrate their applications through very generic laboratory methods that can be used even by nonglycobiologists. This approach is interesting as plenty of glycan profiling methods in trends are only useful for investigators with some background in glycobiology.

Materials and methods

Sialoglycan microarray with SGRPs

The sialoglycan microarray method was adapted and modified from the literature published earlier (Deng et al. 2014b). Briefly, defined sialosides with amine linker were chemoenzymatically synthesized and then quantitated utilizing an improved DMB-HPLC method (Ji et al. 2021), and 100 μM of sialoglycan solution (in 300-mM Na-phosphate buffer, pH 8.4) was printed in quadruplets on NHS-functionalized glass slides (PolyAn 3D-NHS; catalog# PO-10400401) using an ArrayIt SpotBot®Extreme instrument. The slides were blocked (0.05-M ethanolamine solution in 0.1 M Tris–HCl,

pH 9.0), washed with warm Milli-Q water, and dried. The slides were rehydrated with 400 μl of ovalbumin (1% w/v, PBS) for 1 h in a humid chamber with gentle shaking, followed by incubating the SGRPs/proteins for 2 h at room temperature (gentle shaking). The slides were then washed with PBS-Tween (0.1% v/v). Following washes, the wells were then treated with Cy3-conjugated anti-His (Rockland Antibodies & Assays; Cat# 200-304-382) secondary antibody, for 1 h, followed by washing and scanning with a Genepix 4000B scanner (Molecular Devices Corp., Union City, CA) at a wavelength of 532 nm. Data analysis was performed using the Genepix Pro 7.3 software (Molecular Devices Corp., Union City, CA). The raw data analysis and sorting using the numerical codes were performed on Microsoft Excel. Every siaologlycan microarray experiment was repeated at least 3 times for reproducibility, and typical results are provided in the manuscript.

Serum binding assay with SGRPs

A saturable amount of sera (equivalent to 50-μg proteins), reconstituted in PBST (0.1% Tween 20), were added to individual wells in ELISA plates (Corning, 9018) and kept overnight at 4 °C for adherence. Unattached sera were removed, and wells were briefly rinsed with PBST before addition of 200 μl, 0.5% cold fish gelatin (Sigma- G7765-1 L, diluted in PBST) for blocking. Lectins, SGRPs, or other probes were reconstituted in diluting buffer (PBST with 0.05% cold fish gelatin) at desired concentrations and added to serum-coated wells for 1 h (or otherwise specified) at room temperature. Specifically, for MAL-I (VECTOR LAB, B1315) and MAL-II (B1265), 10-mM $CaCl_2$ and 10-mM $MnCl_2$ were added to diluting buffer to maximize lectin binding. Post-incubation, wells were vigorously washed with 250-μl PBST, 5 times and then incubated with Avidin-HRP (Biolegend, 405,103) for biotinylated probes at 1:2,000 dilution for 45 min at room temperature. Wells were again washed vigorously with 250-μl PBST 6–7 times, and 100 μl of TMB (BD OptEIA-55,214) was added to each well as substrate for HRP's enzymatic activities and incubated for color development. The reactions were stopped by adding 40 μl of 2 N H_2SO_4 after 30 min, or if the wells specified as negative controls begin to develop color. Plates were read at 450 nm and readings were processed to observe binding patterns of tested molecules (Perkin Elmer, Enspire Alpha). For every experiment, wells treated with avidin-HRP only served as negative control of binding, along with nonbinding mutants of probes, whenever applicable.

For serum binding experiments with nonbiotinylated proteins, Fc-tagged or His_6-conjugated proteins were probed. His_6 detection was determined by anti-His antibody (mouse, Gene Script, #A00186, 1:4,000) followed by anti-mouse-HRP (CTS, #7076S, 1:1,500). In certain probes discussed in this article, for example LFA (EY Lab, BA1501–1, CHE-FcD etc.), the preconjugated combination of probe and secondary antibody was adopted for stronger signals, as mentioned in corresponding figure legends. Every serum binding ELISA experiment was repeated at least 3 times for reproducibility, and typical results are provided with the manuscript.

Western blotting

Commercial animal sera (rat, equine, goat, guinea pig, rabbit, sheep; Sigma, St.Louis, MO), wt mouse and human serum (Valley Biomedical, Winchester, VA) and in house $Cmah^{-/-}$ mouse serum were chromatographed on 12% CosmoPAGE Bis-Tris precast gels (Nacalai, USA, NU00212). The gels were run in CosmoPAGE MOPS running buffer pH 7 (Nacalai, USA, NU01004), with ice packs to keep running buffer temperature below 23 °C. The proteins were transferred to Immobilon FL (EMD Millipore Corp IPFL00010) membrane in transfer buffer containing 10% methanol and 0.2% SDS. Membranes were blocked overnight at 4 °C with 0.5% Cold water fish skin gelatin in PBST (PBS pH 7.4 with 0.1% Tween 20), with gentle agitation. The membranes were incubated at room temperature for 2 h with 1 μg/ml of all probes, except $SGRP5^{IgY}$, which was used at 0.33 μg/ml, diluted in blocking buffer without Tween. Also, $SGRP4^{MHV}$ and $SGRP9^{PToV}$ were used at 2 μg/ml. Amounts of serum proteins immunoblotted for each SGRP were adjusted to highlight their ligand preferences. Specifically, 25-μg protein per well was loaded for $SGRP1^{YenB}$, $SGRP2^{PltB}$, and their nonbinding variants, 50-μg protein per well was loaded for $SGRP3^{Hsa}$, $SGRP4^{MHV}$, $SGRP7^{BCoV}$, $SGRP9^{PToV}$, and their nonbinding mutants, while 12.5-μg protein per well was loaded for $SGRP5^{IgY}$, $SGRP5^{IgY}$NB, and $SGRP6^{SNA}$ (Vector lab, B1305, lot number Z1002). Secondary antibody incubation was with Streptavidin IRDye 680 (Licor, 925–68,079) at 1:10,000 dilution in PBST at room temperature. Signal was read with Odyssey infrared imager (Licor Biosciences, Lincoln, NE). Interrogating SGRPs and corresponding nonbinding SGRPs were used at the same concentration and all images were obtained at the same time using the same imager settings.

Histology procedure

Frozen sections of various organs from the wild type and $Cmah^{-/-}$ mouse were air dried for 30 min, rehydrated in Tris-Buffered Saline pH 7.5, and overlaid with 0.5% Fish gelatin, which was then tipped off for blocking the endogenous biotin using the Avidin Biotin blocking kit from Vector labs (SP-2001). Sections were then fixed for 30 min in 10% Neutral buffered formalin (VWR-89370-094), washed and overlaid with either the binding or nonbinding probes, each used 5 μg/μl. Separate slides (Globe, 1358 W) were then overlaid with each of the Biotinylated probes and incubated in a humid chamber at room temperature for 30 min. Washing was then performed in TBS, followed by incubation with Cy3 Streptavidin (Red, Jackson Laboratory, 016-160-084) for 30 min. After washing again, nuclei were counterstained with Hoechst (Blue, Molecular Probes, H3570) for 2 min, washed and cover-slipped using an aqueous mounting medium (Vector lab H5501). Digital images were captured using the Keyence microscope and organized using Adobe Photoshop.

Flow cytometry

SGRPs were used at 5 μg/ml (or otherwise, mentioned in figure legends) for their RBC binding properties. For this experiment, blood from several animal species was resuspended in PBS (4°C) to make a 2% volume/volume dilution, and 200 μl of this blood suspension was supplemented with 200 μl of 10 μg/ml probe dilution in PBS (4°C) to make a final blood suspension and probe dilution of 1% and 5 μg/ml respectively (unless mentioned otherwise)· 400 μl of this blood suspension was incubated on ice for 1 h with intermittent gentle mixing to avoid settlement of RBCs. After incubation, 1 ml ice cold PBS was added to each tube and centrifuged at 1,000 RPM, 3 min at 4°C. The washing was repeated 2 more times, and then the pellet was gently resuspended in 300 μl of 1 μg/ml dilution of Streptavidin Cy3 (Jackson

016-170-084) and incubated for 45 min on ice. For autofluorescence control of RBCs, blood suspension was never treated either by probe or fluorescence antibody, while for fluorescent secondary antibody control, mock treated blood was incubated with the equivalent streptavidin-Cy3 dilution in similar conditions. After incubation, 1-ml ice cold PBS was added to each tube and the washes were repeated for a total of 3 times.The final pellet was gently resuspended in 500 μl of PBS and fluorescence was analyzed on FL2 channel on the FACS Caliber flow cytometer. The settings for acquisition of data and analysis remained the same for all probes and their nonbinding mutants in an experiment. Binding efficiencies of SGRPs and their nonbinding probes were plotted in red for highest binding (saturated or 100%), blue for minimum or no binding (0%), and intermediate binding represented by cells displaying colors between blue and red.

Supplementary material

Supplementary material is available at *Glycobiology Journal* online.

Data availability

All data are contained within the article and supporting information.

Funding

This work was supported by the National Institutes of Health Grants U01CA199792 and R01GM32373 (to AV), and additional generous financial support from BioLegend, San Diego.

Conflicts of interest statement: The authors declare no competing financial interests.

References

Altheide TK, Hayakawa T, Mikkelsen TS, Diaz S, Varki N, Varki A. System-wide genomic and biochemical comparisons of sialic acid biology among primates and rodents: Evidence for two modes of rapid evolution. *J Biol Chem*. 2006:**281**(35):25689–25702.

Arthur CM, Cummings RD, Stowell SR. Using glycan microarrays to understand immunity. *Curr Opin Chem Biol*. 2014:**18**: 55–61.

Asaoka H, Nishinaka S, Wakamiya N, Matsuda H, Murata M. Two chicken monoclonal antibodies specific for heterophil Hanganutziu-Deicher antigens. *Immunol Lett*. 1992:**32**(1):91–96.

Atack JM, Day CJ, Poole J, Brockman KL, Bakaletz LO, Barenkamp SJ, Jennings MP. The HMW2 adhesin of non-typeable Haemophilus influenzae is a human-adapted lectin that mediates high-affinity binding to 2-6 linked N-acetylneuraminic acid glycans. *Biochem Biophys Res Commun*. 2018:**503**(2):1103–1107.

Babál P, Pindak FF, Russell LC, Gardner WA Jr. Sialic acid-specific lectin from Tritrichomonas foetus. *Biochim Biophys Acta*. 1999:**1428**(1):106–116.

Bai X, Brown JR, Varki A, Esko JD. Enhanced 3-O-sulfation of galactose in Asn-linked glycans and Maackia amurensis lectin binding in a new Chinese hamster ovary cell line. *Glycobiology*. 2001:**11**(8): 621–632.

Benktander J, Barone A, Johansson MM, Teneberg S. Helicobacter pylori SabA binding gangliosides of human stomach. *Virulence*. 2018:**9**(1):738–751.

Bensing BA, Lopez JA, Sullam PM. The Streptococcus gordonii surface proteins GspB and Hsa mediate binding to sialylated carbohydrate epitopes on the platelet membrane glycoprotein Ibalpha. *Infect Immun*. 2004:**72**(11):6528–6537.

Bensing BA, Khedri Z, Deng L, Yu H, Prakobphol A, Fisher SJ, Chen X, Iverson TM, Varki A, Sullam PM. Novel aspects of sialoglycan recognition by the Siglec-like domains of streptococcal SRR glycoproteins. *Glycobiology*. 2016:**26**(11):1222–1234.

Bhavanandan VP, Katlic AW. The interaction of wheat germ agglutinin with sialoglycoproteins. The role of sialic acid. *J Biol Chem*. 1979:**254**(10):4000–4008.

Bousquet PA, Sandvik JA, Jeppesen Edin NF, Krengel U. Hypothesis: Hypoxia induces de novo synthesis of NeuGc gangliosides in humans through CMAH domain substitute. *Biochem Biophys Res Commun*. 2018:**495**(1):1562–1566.

Brinkman-van der Linden ECM, Sjoberg ER, Juneja LR, Crocker PR, Varki N, Varki A. Loss of N-glycolylneuraminic acid in human evolution. Implications for sialic acid recognition by siglecs. *J Biol Chem*. 2000:**275**(12):8633–8640.

Brinkman-Van der Linden EC, Sonnenburg JL, Varki A. Effects of sialic acid substitutions on recognition by Sambucus nigra agglutinin and Maackia amurensis hemagglutinin. *Anal Biochem*. 2002:**303**(1): 98–104.

Büll C, Nason R, Sun L, van Coillie J, Madriz Sørensen D, Moons SJ, Yang Z, Arbitman S, Fernandes SM, Furukawa S, *et al.* Probing the binding specificities of human Siglecs by cell-based glycan arrays. *Proc Natl Acad Sci U S A*. 2021:**118**(17):e2026102118.

Byres E, Paton AW, Paton JC, Löfling JC, Smith DF, Wilce MCJ, Talbot UM, Chong DC, Yu H, Huang S, *et al.* Incorporation of a non-human glycan mediates human susceptibility to a bacterial toxin. *Nature*. 2008:**456**(7222):648–652.

Cariappa A, Takematsu H, Liu H, Diaz S, Haider K, Boboila C, Kalloo G, Connole M, Shi HN, Varki N, *et al.* B cell antigen receptor signal strength and peripheral B cell development are regulated by a 9-O-acetyl sialic acid esterase. *J Exp Med*. 2009:**206**(1):125–138.

Castel V, Segura V, Cañete A. Treatment of high-risk neuroblastoma with anti-GD2 antibodies. *Clin Transl Oncol*. 2010:**12**:788–793.

Chen X, Varki A. Advances in the biology and chemistry of sialic acids. *ACS Chem Biol*. 2010:**5**(2):163–176.

Chen C, Baldwin MR, Barbieri JT. Molecular basis for tetanus toxin coreceptor interactions. *Biochemistry*. 2008:**47**(27):7179–7186.

Chen C, Fu Z, Kim JJP, Barbieri JT, Baldwin MR. Gangliosides as high affinity receptors for tetanus neurotoxin. *J Biol Chem*. 2009:**284**(39):26569–26577.

Cummings RD, Darvill AG, Etzler ME, Hahn Ajit Varki MG, Cummings RD, Esko JD, Stanley P, Hart GW, Aebi M, *et al.* Glycan-recognizing probes as tools. In: Varki A, *et al.*, editors. *Essentials of glycobiology*. Cold Spring Harbor (NY): Cold Spring Harbor Laboratory Press; 2015

Dabelsteen S, Pallesen EMH, Marinova IN, Nielsen MI, Adamopoulou M, Rømer TB, Levann A, Andersen MM, Ye Z, Thein D, *et al.* Essential functions of Glycans in human epithelia dissected by a CRISPR-Cas9-engineered human Organotypic skin model. *Dev Cell*. 2020:**54**(5):669–684.e7.

Day CJ, Paton AW, Higgins MA, Shewell LK, Jen FEC, Schulz BL, Herdman BP, Paton JC, Jennings MP. Structure aided design of a Neu5Gc specific lectin. *Sci Rep*. 2017:**7**(1):1495.

Deng L, Bensing BA, Thamadilok S, Yu H, Lau K, Chen X, Ruhl S, Sullam PM, Varki A. Oral streptococci utilize a Siglec-like domain of serine-rich repeat adhesins to preferentially target platelet sialoglycans in human blood. *PLoS Pathog*. 2014a:**10**(12): e1004540.

Deng L, Song J, Gao X, Wang J, Yu H, Chen X, Varki N, Naito-Matsui Y, Galán JE, Varki A. Host adaptation of a bacterial toxin from the human pathogen salmonella Typhi. *Cell*. 2014b:**159**(6): 1290–1299.

Diaz SL, Padler-Karavani V, Ghaderi D, Hurtado-Ziola N, Yu H, Chen X, Brinkman-van der Linden ECM, Varki A, Varki NM. Sensitive and specific detection of the non-human sialic acid N-glycolylneuraminic acid in human tissues and biotherapeutic products. *PLoS One*. 2009:**4**(1):e4241.

Fukui S, Feizi T, Galustian C, Lawson AM, Chai W. Oligosaccharide microarrays for high-throughput detection and specificity assignments of carbohydrate-protein interactions. *Nat Biotechnol*. 2002:**20**(10):1011–1017.

Geisler C, Jarvis DL. Effective glycoanalysis with Maackia amurensis lectins requires a clear understanding of their binding specificities. *Glycobiology*. 2011:**21**(8):988–993.

Gurung MK, Ræder ILU, Altermark B, Smalås AO. Characterization of the sialic acid synthase from Aliivibrio salmonicida suggests a novel pathway for bacterial synthesis of 7-O-acetylated sialic acids. *Glycobiology*. 2013:**23**(7):806–819.

Halpern JL, Loftus A. Characterization of the receptor-binding domain of tetanus toxin. *J Biol Chem*. 1993:**268**(15):11188–11192.

Hanaoka K, Pritchett TJ, Takasaki S, Kochibe N, Sabesan S, Paulson JC, Kobata A. 4-O-acetyl-N-acetylneuraminic acid in the N-linked carbohydrate structures of equine and Guinea pig alpha 2-macroglobulins, potent inhibitors of influenza virus infection. *J Biol Chem*. 1989:**264**(17):9842–9849.

Hashimoto N, Ito S, Tsuchida A, Bhuiyan RH, Okajima T, Yamamoto A, Furukawa K, Ohmi Y, Furukawa K. The ceramide moiety of disialoganglioside (GD3) is essential for GD3 recognition by the sialic acid-binding lectin SIGLEC7 on the cell surface. *J Biol Chem*. 2019:**294**(28):10833–10845.

Heiner JP, Miraldi F, Kallick S, Makley J, Neely J, Smith-Mensah WH, Cheung NK. Localization of GD2-specific monoclonal antibody 3F8 in human osteosarcoma. *Cancer Res*. 1987:**47**(20):5377–5381.

Hellebø A, Vilas U, Falk K, Vlasak R. Infectious salmon anemia virus specifically binds to and hydrolyzes 4-O-acetylated sialic acids. *J Virol*. 2004:**78**(6):3055–3062.

Herrler G, Rott R, Klenk HD, Müller HP, Shukla AK, Schauer R. The receptor-destroying enzyme of influenza C virus is neuraminate-O-acetylesterase. *EMBO J*. 1985:**4**(6):1503–1506.

Higa HH, Manzi A, Varki A. O-acetylation and de-O-acetylation of sialic acids. Purification, characterization, and properties of a glycosylated rat liver esterase specific for 9-O-acetylated sialic acids. *J Biol Chem*. 1989:**264**(32):19435–19442.

Higashi H, Nishi Y, Fukui Y, Ikuta K, Ueda S, Kato S, Fujita M, Nakano Y, Taguchi T, Sakai S. Tumor-associated expression of glycosphingolipid Hanganutziu-Deicher antigen in human cancers. *Gan*. 1984:**75**(11):1025–1029.

Higashi H, Hirabayashi Y, Fukui Y, Naiki M, Matsumoto M, Ueda S, Kato S. Characterization of N-glycolylneuraminic acid-containing gangliosides as tumor-associated Hanganutziu-Deicher antigen in human colon cancer. *Cancer Res*. 1985:**45**(8):3796–3802.

Higashi H, Sasabe T, Fukui Y, Maru M, Kato S. Detection of gangliosides as N-glycolylneuraminic acid-specific tumor-associated Hanganutziu-Deicher antigen in human retinoblastoma cells. *Jpn J Cancer Res*. 1988:**79**(8):952–956.

Higashihara T, Takeshima T, Anzai M, Tomioka M, Matsumoto K, Nishida K, Kitamura Y, Okinaga K, Naiki M. Survey of Hanganutziu and Deicher antibodies in operated patients. *Int Arch Allergy Appl Immunol*. 1991:**95**(2–3):231–235.

Hirabayashi Y, Kasakura H, Matsumoto M, Higashi H, Kato S, Kasai N, Naiki M. Specific expression of unusual GM2 ganglioside with Hanganutziu-Deicher antigen activity on human colon cancers. *Jpn J Cancer Res*. 1987:**78**(3):251–260.

Imamura K, Takeuchi H, Yabe R, Tateno H, Hirabayashi J. Engineering of the glycan-binding specificity of Agrocybe cylindracea galectin towards α(2,3)-linked sialic acid by saturation mutagenesis. *J Biochem*. 2011:**150**(5):545–552.

Ito H, Ishida H, Waki H, Ando S, Kiso M. Total synthesis of a cholinergic neuron-specific ganglioside GT1a alpha: a high affinity ligand for myelin-associated glycoprotein (MAG). *Glycoconj J*. 1999:**16**(10):585–598.

Iwamori M, Takamizawa K, Momoeda M, Iwamori Y, Taketani Y. Gangliosides in human, cow and goat milk, and their abilities as to neutralization of cholera toxin and botulinum type a neurotoxin. *Glycoconj J*. 2008:**25**(7):675–683.

Iwersen M, Vandamme-Feldhaus V, Schauer R. Enzymatic 4-O-acetylation of N-acetylneuraminic acid in Guinea-pig liver. *Glycoconj J*. 1998:**15**(9):895–904.

Ji Y, Sasmal A, Li W, Oh L, Srivastava S, Hargett AA, Wasik BR, Yu H, Diaz S, Choudhury B, *et al*. Reversible O-acetyl migration within the sialic acid side chain and its influence on protein recognition. *ACS Chem Biol*. 2021:**16**(10):1951–1960.

Jia N, Byrd-Leotis L, Matsumoto Y, Gao C, Wein AN, Lobby JL, Kohlmeier JE, Steinhauer DA, Cummings RD. The human lung Glycome reveals novel glycan ligands for influenza a virus. *Sci Rep*. 2020:**10**(1):5320.

Kadirvelraj R, Grant OC, Goldstein IJ, Winter HC, Tateno H, Fadda E, Woods RJ. Structure and binding analysis of Polyporus squamosus lectin in complex with the Neu5Ac{alpha}2-6Gal{beta}1-4GlcNAc human-type influenza receptor. *Glycobiology*. 2011:**21**(7):973–984.

Kaku H, Mori Y, Goldstein IJ, Shibuya N. Monomeric, monovalent derivative of Maackia amurensis leukoagglutinin. Preparation and application to the study of cell surface glycoconjugates by flow cytometry. *J Biol Chem*. 1993:**268**(18):13237–13241.

Kamerling JP, Gerwig GJ. Structural analysis of naturally occurring sialic acids. *Methods Mol Biol*. 2006:**347**:69–91.

Kawaguchi T, Matsumoto I, Osawa T. Studies on hemagglutinins from Maackia amurensis seeds. *J Biol Chem*. 1974:**249**(9):2786–2792.

Kawanishi K, Saha S, Diaz S, Vaill M, Sasmal A, Siddiqui SS, Choudhury B, Sharma K, Chen X, Schoenhofen IC, *et al*. Evolutionary conservation of human ketodeoxynonulosonic acid production is independent of sialoglycan biosynthesis. *J Clin Invest*. 2021:**131**(5):137681.

Kawashima I, Tada N, Ikegami S, Nakamura S, Ueda R, Tai T. Mouse monoclonal antibodies detecting disialogangliosides on mouse and human T lymphomas. *Int J Cancer*. 1988:**41**(2):267–274.

Kelm S, Pelz A, Schauer R, Filbin MT, Tang S, Bellard, Schnaar RL, Mahoney JA, Hartnell A, Bradfield P, *et al*. Sialoadhesin, myelin-associated glycoprotein and CD22 define a new family of sialic acid-dependent adhesion molecules of the immunoglobulin superfamily. *Curr Biol*. 1994:**4**(11):965–972.

Kemminer SE, Conradt HS, Nimtz M, Sagi D, Peter-Katalinic J, Diekmann O, Drmic I, Muthing J. Production and molecular characterization of clinical phase i anti-melanoma mouse IgG3 monoclonal antibody R24. *Biotechnol Prog*. 2001:**17**(5):809–821.

Khan N, Sasmal A, Khedri Z, Secrest P, Verhagen A, Srivastava S, Varki N, Chen X, Yu H, Beddoe T, *et al*. Sialoglycan-binding patterns of bacterial AB_5 toxin B subunits correlate with host range and toxicity, indicating evolution independent of a subunits. *J Biol Chem*. 2022:**298**(5):101900.

Kim DS, Son KY, Koo KM, Kim JY, Alfajaro MM, Park JG, Hosmillo M, Soliman M, Baek YB, Cho EH, *et al*. Porcine Sapelovirus uses α2,3-linked sialic acid on GD1a ganglioside as a receptor. *J Virol*. 2016:**90**(8):4067–4077.

Klamer Z, Staal B, Prudden AR, Liu L, Smith DF, Boons GJ, Haab B. Mining high-complexity motifs in Glycans: a new language to uncover the fine specificities of lectins and Glycosidases. *Anal Chem*. 2017:**89**(22):12342–12350.

Klausegger A, Strobl B, Regl G, Kaser A, Luytjes W, Vlasak R. Identification of a coronavirus hemagglutinin-esterase with a substrate specificity different from those of influenza C virus and bovine coronavirus. *J Virol*. 1999:**73**(5):3737–3743.

Klein A, Roussel P. O-acetylation of sialic acids. *Biochimie*. 1998:**80**(1):49–57.

Klein A, Krishna M, Varki NM, Varki A. 9-O-acetylated sialic acids have widespread but selective expression: analysis using a chimeric dual-function probe derived from influenza C hemagglutinin-esterase. *Proc Natl Acad Sci U S A*. 1994:**91**(16):7782–7786.

Kletter D, Singh S, Bern M, Haab BB. Global comparisons of lectin-glycan interactions using a database of analyzed glycan array data. *Mol Cell Proteomics*. 2013:**12**(4):1026–1035.

Knibbs RN, Goldstein IJ, Ratcliffe RM, Shibuya N. Characterization of the carbohydrate binding specificity of the leukoagglutinating lectin from Maackia amurensis. Comparison with other sialic acid-specific lectins. *J Biol Chem*. 1991:**266**(1):83–88.

Konami Y, Yamamoto K, Osawa T, Irimura T. Strong affinity of Maackia amurensis hemagglutinin (MAH) for sialic acid-containing Ser/Thr-linked carbohydrate chains of N-terminal octapeptides from human glycophorin a. *FEBS Lett*. 1994:**342**(3):334–338.

Kooner AS, Diaz S, Yu H, Santra A, Varki A, Chen X. Chemoenzymatic synthesis of Sialosides containing 7-N- or 7,9-Di-N-acetyl sialic acid as stable O-acetyl analogues for probing sialic acid-binding proteins. *J Org Chem*. 2021:**86**(21):14381–14397.

Langereis MA, Zeng Q, Gerwig GJ, Frey B, Itzstein, Kamerling JP, de Groot RJ, Huizinga EG. Structural basis for ligand and substrate recognition by torovirus hemagglutinin esterases. *Proc Natl Acad Sci U S A*. 2009:**106**(37):15897–15902.

Langereis MA, van Vliet ALW, Boot W, de Groot RJ. Attachment of mouse hepatitis virus to O-acetylated sialic acid is mediated by hemagglutinin-esterase and not by the spike protein. *J Virol*. 2010:**84**(17):8970–8974.

Langereis MA, Zeng Q, Heesters B, Huizinga EG, de Groot RJ. The murine coronavirus hemagglutinin-esterase receptor-binding site: A major shift in ligand specificity through modest changes in architecture. *PLoS Pathog*. 2012:**8**(1):e1002492.

Langereis MA, Bakkers MJG, Deng L, Padler-Karavani V, Vervoort SJ, Hulswit RJG, van Vliet ALW, Gerwig GJ, de Poot SAH, Boot W, *et al*. Complexity and diversity of the mammalian Sialome revealed by Nidovirus Virolectins. *Cell Rep*. 2015:**11**(12):1966–1978.

Lehmann F, Tiralongo E, Tiralongo J. Sialic acid-specific lectins: Occurrence, specificity and function. *Cell Mol Life Sci*. 2006:**63**(12):1331–1354.

Lewis AL, Nizet V, Varki A. Discovery and characterization of sialic acid O-acetylation in group B streptococcus. *Proc Natl Acad Sci U S A*. 2004:**101**(30):11123–11128.

Louch HA, Buczko ES, Woody MA, Venable RM, Vann WF. Identification of a binding site for ganglioside on the receptor binding domain of tetanus toxin. *Biochemistry*. 2002:**41**(46):13644–13652.

Luytjes W, Bredenbeek PJ, Noten AFH, Horzinek MC, Spaan WJM. Sequence of mouse hepatitis virus A59 mRNA 2: Indications for RNA recombination between coronaviruses and influenza C virus. *Virology*. 1988:**166**(2):415–422.

Mandal C, Basu S. An unique specificity of a sialic acid binding lectin AchatininH, from the hemolymph of Achatina fulica snail. *Biochem Biophys Res Commun*. 1987:**148**(2):795–801.

Manzi AE, Sjoberg ER, Diaz S, Varki A. Biosynthesis and turnover of O-acetyl and N-acetyl groups in the gangliosides of human melanoma cells. *J Biol Chem*. 1990:**265**(22):13091–13103.

Manzke O, Russello O, Leenen C, Diehl V, Bohlen H, Berthold F. Immunotherapeutic strategies in neuroblastoma: Antitumoral activity of deglycosylated ricin a conjugated anti-GD2 antibodies and anti-CD3xanti-GD2 bispecific antibodies. *Med Pediatr Oncol*. 2001:**36**(1):185–189.

Martin LT, Verhagen A, Varki A. Recombinant influenza C hemagglutinin-esterase as a probe for sialic acid 9-O-acetylation. *Methods Enzymol*. 2003:**363**:489–498.

Matrosovich M, Herrler G, Klenk HD. Sialic acid receptors of viruses. *Top Curr Chem*. 2015:**367**:1–28.

Miller RL, Collawn JF, Fish WW. Purification and macromolecular properties of a sialic acid-specific lectin from the slug Limax flavus. *J Biol Chem*. 1982:**257**(13):7574–7580.

Miyake M, Ito M, Hitomi S, Ikeda S, Taki T, Kurata M, Hino A, Miyake N, Kannagi R. Generation of two murine monoclonal antibodies that can discriminate N-glycolyl and N-acetyl neuraminic acid residues of GM2 gangliosides. *Cancer Res*. 1988:**48**(21):6154–6160.

Miyoshi I, Higashi H, Hirabayashi Y, Kato S, Naiki M. Detection of 4-O-acetyl-N-glycolylneuraminyl lactosylceramide as one of tumor-associated antigens in human colon cancer tissues by specific antibody. *Mol Immunol*. 1986:**23**(6):631–638.

Monsigny M, Roche AC, Sene C, Maget-Dana R, Delmotte F. Sugar-lectin interactions: how does wheat-germ agglutinin bind sialoglycoconjugates. *Eur J Biochem*. 1980:**104**(1):147–153.

Muchmore EA, Varki A. Selective inactivation of influenza C esterase: a probe for detecting 9-O-acetylated sialic acids. *Science*. 1987:**236**(4806):1293–1295.

Muthana SM, Gildersleeve JC. Glycan microarrays: powerful tools for biomarker discovery. *Cancer Biomark*. 2014:**14**(1):29–41.

Nason R, Büll C, Konstantinidi A, Sun L, Ye Z, Halim A, du W, Sørensen DM, Durbesson F, Furukawa S, *et al*. Display of the human mucinome with defined O-glycans by gene engineered cells. *Nat Commun*. 2021:**12**(1):4070.

Nguyen T, Lee S, Yang YA, Ahn C, Sim JH, Kei TG, Barnard KN, Yu H, Millano SK, Chen X, *et al*. The role of 9-O-acetylated glycan receptor moieties in the typhoid toxin binding and intoxication. *PLoS Pathog*. 2020:**16**(2):e1008336.

Nicholls JM, Bourne AJ, Chen H, Guan Y, Peiris JSM. Sialic acid receptor detection in the human respiratory tract: Evidence for widespread distribution of potential binding sites for human and avian influenza viruses. *Respir Res*. 2007:**8**(1):73.

Ohashi Y, Sasabe T, Nishida T, Nishi Y, Higashi H. Hanganutziu-Deicher heterophile antigen in human retinoblastoma cells. *Am J Ophthalmol*. 1983:**96**(3):321–325.

Pillai S. Rethinking mechanisms of autoimmune pathogenesis. *J Autoimmun*. 2013:**45**:97–103.

Powell LD, Sgroi D, Sjoberg ER, Stamenkovic I, Varki A. Natural ligands of the B cell adhesion molecule CD22beta carry N-linked oligosaccharides with alpha-2,6-linked sialic acids that are required for recognition. *J Biol Chem*. 1993:**268**(10):7019–7027.

Powell LD, Jain RK, Matta KL, Sabesan S, Varki A. Characterization of sialyloligosaccharide binding by recombinant soluble and native cell-associated CD22. Evidence for a minimal structural recognition motif and the potential importance of multisite binding. *J Biol Chem*. 1995:**270**(13):7523–7532.

Ravindranath MH, Higa HH, Cooper EL, Paulson JC. Purification and characterization of an O-acetylsialic acid-specific lectin from a marine crab Cancer antennarius. *J Biol Chem*. 1985:**260**(15):8850–8856.

Ravindranaths MH, Paulson JC, Irie RF. Human melanoma antigen O-acetylated ganglioside GD3 is recognized by Cancer antennarius lectin. *J Biol Chem*. 1988:**263**(4):2079–2086.

Regl G, Kaser A, Iwersen M, Schmid H, Kohla G, Strobl B, Vilas U, Schauer R, Vlasak R. The hemagglutinin-esterase of mouse hepatitis virus strain S is a sialate-4-O-acetylesterase. *J Virol*. 1999:**73**(6):4721–4727.

Rogers GN, Herrler G, Paulson JC, Klenk HD. Influenza C virus uses 9-O-acetyl-N-acetylneuraminic acid as a high affinity receptor determinant for attachment to cells. *J Biol Chem*. 1986:**261**(13):5947–5951.

Samraj AN, Pearce OMT, Läubli H, Crittenden AN, Bergfeld AK, Banda K, Gregg CJ, Bingman AE, Secrest P, Diaz SL, *et al*. A red meat-derived glycan promotes inflammation and cancer progression. *Proc Natl Acad Sci U S A*. 2015:**112**(2):542–547.

Schauer R. Sialic acids: metabolism of O-acetyl groups. *Methods Enzymol*. 1987:**138**:611–626.

Schauer R, Kamerling JP. Exploration of the sialic acid world. *Adv Carbohydr Chem Biochem*. 2018:**75**:1–213.

Schultze B, Herrler G. Bovine coronavirus uses N-acetyl-9-O-acetylneuraminic acid as a receptor determinant to initiate the infection of cultured cells. *J Gen Virol*. 1992:**73**(Pt 4):901–906.

Schultze B, Gross HJ, Brossmer R, Herrler G. The S protein of bovine coronavirus is a hemagglutinin recognizing 9-O-acetylated sialic acid as a receptor determinant. *J Virol*. 1991a:**65**(11):6232–6237.

Schultze B, Wahn K, Klenk HD, Herrler G. Isolated HE-protein from hemagglutinating encephalomyelitis virus and bovine coronavirus has receptor-destroying and receptor-binding activity. *Virology*. 1991b:**180**(1):221–228.

Severi E, Hood DW, Thomas GH. Sialic acid utilization by bacterial pathogens. *Microbiology*. 2007:**153**(Pt 9):2817–2822.

Shewell LK, Wang JJ, Paton JC, Paton AW, Day CJ, Jennings MP. Detection of N-glycolylneuraminic acid biomarkers in sera from patients with ovarian cancer using an engineered N-glycolylneuraminic acid-specific lectin SubB2M. *Biochem Biophys Res Commun*. 2018:**507**(1–4):173–177.

Shewell LK, Day CJ, Kutasovic JR, Abrahams JL, Wang J, Poole J, Niland C, Ferguson K, Saunus JM, Lakhani SR, *et al.* N-glycolylneuraminic acid serum biomarker levels are elevated in breast cancer patients at all stages of disease. *BMC Cancer*. 2022: **22**(1):334.

Shibuya N, Goldstein IJ, Broekaert WF, Nsimba-Lubaki M, Peeters B, Peumans WJ. The elderberry (Sambucus nigra L.) bark lectin recognizes the Neu5Ac(alpha 2-6)gal/GalNAc sequence. *J Biol Chem*. 1987:**262**(4):1596–1601.

Shieh CK, Lee HJ, Yokomori K, la Monica N, Makino S, Lai MM. Identification of a new transcriptional initiation site and the corresponding functional gene 2b in the murine coronavirus RNA genome. *J Virol*. 1989:**63**(9):3729–3736.

Sjoberg ER, Manzi AE, Khoo KH, Dell A, Varki A. Structural and immunological characterization of O-acetylated GD2. Evidence that GD2 is an acceptor for ganglioside O-acetyltransferase in human melanoma cells. *J Biol Chem*. 1992:**267**(23):16200–16211.

Sjoberg ER, Powell LD, Klein A, Varki A. Natural ligands of the B cell adhesion molecule CD22 beta can be masked by 9-O-acetylation of sialic acids. *J Cell Biol*. 1994:**126**(2):549–562.

Stencel-Baerenwald JE, Reiss K, Reiter DM, Stehle T, Dermody TS. The sweet spot: defining virus-sialic acid interactions. *Nat Rev Microbiol*. 2014:**12**(11):739–749.

Stewart AD, Batty J, Harkiss GD. Genetic variation in plasma thyroxine levels and minimal metabolic rates of the mouse, Mus musculus. *Genet Res*. 1978:**31**(3):303–306.

Tai T, Kawashima I, Furukawa K, Lloyd KO. Monoclonal antibody R24 distinguishes between different N-acetyl- and N-glycolylneuraminic acid derivatives of ganglioside GD3. *Arch Biochem Biophys*. 1988:**260**(1):51–55.

Takamatsu D, Bensing BA, Cheng H, Jarvis GA, Siboo IR, López JA, Griffiss JML, Sullam PM. Binding of the Streptococcus gordonii surface glycoproteins GspB and Hsa to specific carbohydrate structures on platelet membrane glycoprotein Ibalpha. *Mol Microbiol*. 2005:**58**(2):380–392.

Tangvoranuntakul P, Gagneux P, Diaz S, Bardor M, Varki N, Varki A, Muchmore E. Human uptake and incorporation of an immunogenic nonhuman dietary sialic acid. *Proc Natl Acad Sci U S A*. 2003: **100**(21):12045–12050.

Tateno H, Winter HC, Goldstein IJ. Cloning, expression in Escherichia coli and characterization of the recombinant Neu5Acalpha2,6Galbeta1,4GlcNAc-specific high-affinity lectin and its mutants from the mushroom Polyporus squamosus. *Biochem J*. 2004: **382**(Pt 2):667–675.

Vandamme-Feldhaus V, Schauer R. Characterization of the enzymatic 7-O-acetylation of sialic acids and evidence for enzymatic O-acetyl migration from C-7 to C-9 in bovine submandibular gland. *J Biochem*. 1998:**124**(1):111–121.

Varki A. Diversity in the sialic acids. *Glycobiology*. 1992:**2**(1): 25–40.

Varki A, Diaz S. The release and purification of sialic acids from glycoconjugates: Methods to minimize the loss and migration of O-acetyl groups. *Anal Biochem*. 1984:**137**(1):236–247.

Varki A, Kornfeld S. Historical background and overview. In: Varki A, *et al*., editors. *Essentials of glycobiology*. Cold Spring Harbor (NY): Cold Spring Harbor Laboratory Press; 2022

Vinson M, Strijbos PJLM, Rowles A, Facci L, Moore SE, Simmons DL, Walsh FS. Myelin-associated glycoprotein interacts with ganglioside GT1b. A mechanism for neurite outgrowth inhibition. *J Biol Chem*. 2001:**276**(23):20280–20285.

Vlasak R, Krystal M, Nacht M, Palese P. The influenza C virus glycoprotein (HE) exhibits receptor-binding (hemagglutinin) and receptor-destroying (esterase) activities. *Virology*. 1987:**160**(2): 419–425.

Vlasak R, Luytjes W, Spaan W, Palese P. Human and bovine coronaviruses recognize sialic acid-containing receptors similar to those of influenza C viruses. *Proc Natl Acad Sci U S A*. 1988:**85**(12): 4526–4529.

Wang J, Shewell LK, Paton AW, Paton JC, Day CJ, Jennings MP. Specificity and utility of SubB2M, a new N-glycolylneuraminic acid lectin. *Biochem Biophys Res Commun*. 2018:**500**(3):765–771.

Wasik BR, Barnard KN, Ossiboff RJ, Khedri Z, Feng KH, Yu H, Chen X, Perez DR, Varki A, Parrish CR. Distribution of O-acetylated sialic acids among target host tissues for influenza virus. *mSphere*. 2017:**2**(5):e00379–e00316.

Wipfler D, Srinivasan GV, Sadick H, Kniep B, Arming S, Willhauck-Fleckenstein M, Vlasak R, Schauer R, Schwartz-Albiez R. Differentially regulated expression of 9-O-acetyl GD3 (CD60b) and 7-O-acetyl-GD3 (CD60c) during differentiation and maturation of human T and B lymphocytes. *Glycobiology*. 2011:**21**(9): 1161–1172.

Yabe R, Suzuki R, Kuno A, Fujimoto Z, Jigami Y, Hirabayashi J. Tailoring a novel sialic acid-binding lectin from a ricin-B chain-like galactose-binding protein by natural evolution-mimicry. *J Biochem*. 2007:**141**(3):389–399.

Yagi F, Miyamoto M, Abe T, Minami Y, Tadera K, Goldstein IJ. Purification and carbohydrate-binding specificity of Agrocybe cylindracea lectin. *Glycoconj J*. 1997:**14**(2):281–288.

Yamashita K, Umetsu K, Suzuki T, Ohkura T. Purification and characterization of a Neu5Ac alpha 2–>6Gal beta 1–>4GlcNAc and HSO3(−)–>6Gal beta 1–>GlcNAc specific lectin in tuberous roots of Trichosanthes japonica. *Biochemistry*. 1992:**31**(46): 11647–11650.

Yokomori K, Banner LR, Lai MM. Heterogeneity of gene expression of the hemagglutinin-esterase (HE) protein of murine coronaviruses. *Virology*. 1991:**183**(2):647–657.

Zimmer G, Reuter G, Schauer R. Use of influenza C virus for detection of 9-O-acetylated sialic acids on immobilized glycoconjugates by esterase activity. *Eur J Biochem*. 1992:**204**(1):209–215.

SUPPORTING INFORMATION

Development and applications of sialoglycan-recognizing probes (SGRPs) with defined specificities: exploring the dynamic mammalian sialoglycome

Saurabh Srivastava[1,2], Andrea Verhagen[1,2], Aniruddha Sasmal[1,2,] Brian R. Wasik[3], Sandra Diaz[1,2], Hai Yu[4], Barbara A. Bensing[5], Naazneen Khan[1,2], Zahra Khedri[1,2], Patrick Secrest[1,2], Paul Sullam[5], Nissi Varki[1,2], Xi Chen[4], Colin R. Parrish[3] and Ajit Varki[1,2]*

[1]Department of Cellular and Molecular Medicine, School of Medicine, and [2]Glycobiology Research and Training Center, University of California, San Diego, San Diego, CA, [3]College of Veterinary Medicine, Cornell University, Ithaca, NY, [4]Department of Chemistry, University of California, Davis, Davis, CA, [5]Department of Medicine, University of California, San Francisco and VA Medical Center, San Francisco, CA

Supplementary Table -SI

	Mouse	Rat	Rabbit	Guinea Pig	Goat	Sheep	Horse	Human	CMAH$^{-/-}$ Mouse
Neu5Ac	4.1	67.7	40.9	49.8	62.4	62.8	50.8	92.5	68.2
Neu5Gc	78.0	8.1	6.5	5.7	28.5	25.7	11.3	0.0	0.0
Neu5Gc,7Ac	1.9	0.0	0.0	0.0	0.0	0.0	0.0	0.0	0.0
Neu5,7Ac$_2$	0.0	1.5	3.8	0.0	0.0	0.0	1.2	0.0	2.6
Neu5Gc,4Ac	0.0	0.0	0.0	0.0	0.0	0.0	0.0	0.0	0.0
Neu5Gc,9Ac	8.3	0.0	0.0	0.0	0.0	0.2	0.2	0.0	0.0
Neu5,9Ac$_2$	7.2	19.8	40.8	4.3	8.6	10.5	4.2	6.8	25.2
Neu4,5Ac$_2$	0.0	0.0	0.0	38.7	0.0	0.0	32.4	0.0	0.0

Distribution of Sialic acids in serum. Percentages of the Sialic Acids, highlighting the 5-N Acetylation, 5-N-Glycolylation and O-Acetyl substitutions in mammalian sera, considered in this study. Percentage values have been calculated for individual type by comparing it with total Sias amount, obtained by analysis of HPLC chromatograms as mentioned in method section.

Supplementary Table- SII

	Rat	Rabbit	Guinea Pig	Goat	Sheep	Horse
Neu5Ac	8.4	69.7	0.6	75.3	77.9	87.3
Neu5Gc	44.9	11.4	92.8	15.8	9.7	2.3
Neu5Gc7Ac	1.7	0	0	0	0.5	0.6
Neu5,7Ac$_2$	1.8	0	0	7.3	8.4	0
Neu5Gc4Ac	4.6	4.5	1.3	0	0.6	0.2
Neu5Gc9Ac	0	0	0	0	0.9	8.0
Neu5,9Ac$_2$	15.7	4.8	1.5	0	0.4	0.8
Neu4,5Ac$_2$	0	0	0	0	0	0.4

Ratio of cell surface sialoglycans in erythrocytes: Percentages of sialic acids, highlighting the 5-*N*-acetylation, 5-*N*-glycolylation and *O*-acetyl substitutions in mammalian RBCs, considered in this study. Percentage values have been calculated for individual type by comparing it with total Sias amount, obtained by analysis of HPLC chromatograms as mentioned in method section.

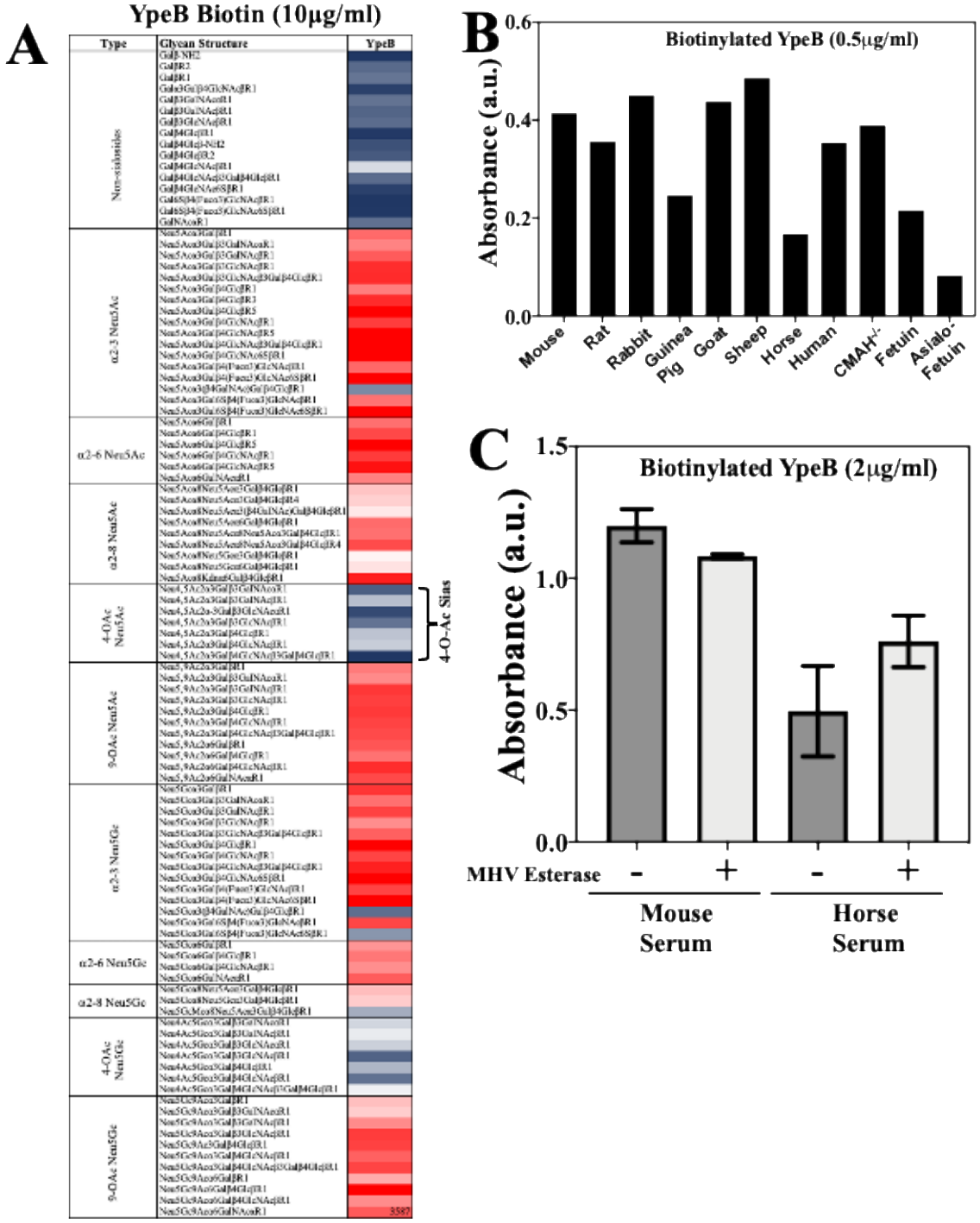
A
YpeB Biotin (10μg/ml)
Type
Glycan Structure
YpeB
Non-sialosides
α2-3 Neu5Ac
α2-6 Neu5Ac
α2-8 Neu5Ac
4-OAc Neu5Ac
9-OAc Neu5Ac
α2-3 Neu5Gc
α2-6 Neu5Gc
α2-8 Neu5Gc
4-OAc Neu5Gc
9-OAc Neu5Gc
4-O-Ac Sias
3587
B
Biotinylated YpeB (0.5μg/ml)
Absorbance (a.u.)
0.0
0.2
0.4
0.6
Mouse
Rat
Rabbit
Guinea Pig
Goat
Sheep
Horse
Human
CMAH-/-
Fetuin
Asialo-Fetuin
C
Biotinylated YpeB (2μg/ml)
Absorbance (a.u.)
0.0
0.5
1.0
1.5
MHV Esterase
-
+
-
+
Mouse Serum
Horse Serum

Figure S1. YpeB does not recognize 4-OAc-Sias efficiently. *Panel A* demonstrates Sia specificity of YpeB (10 μg/ml), as observed in a sialoglycan microarray experiment. The data suggests towards YpeB affinity towards all major types of Sia substitutions except 4-OAc. Similar to observation in an ELISA experiment (*Panel B*), where biotinylated YpeB (0.5 μg/ml) binds to all tested animal serum, with selective non-preference towards guinea pig and horse serum, particularly enriched in 4-OAc-Sias. In accordance to sialoglycan microarray results, YpeB didn't bind with non-sialylated glycans represented by asialofetuin. Results described in *Panel C* underlines that YpeB's binding towards 4-OAc Sia rich horse serum but not towards mouse serum can be restored by selective removal of 4-OAcs by active acetylesterases from MHV (5μg/ml). Binding efficiencies are displayed in red for highest binding (saturated or 100%), blue for minimum or no binding (0%) and intermediate binding represented by colors ranging between blue and red. Ranks; Red (100%, or maximum), Blue (0%, or minimum).

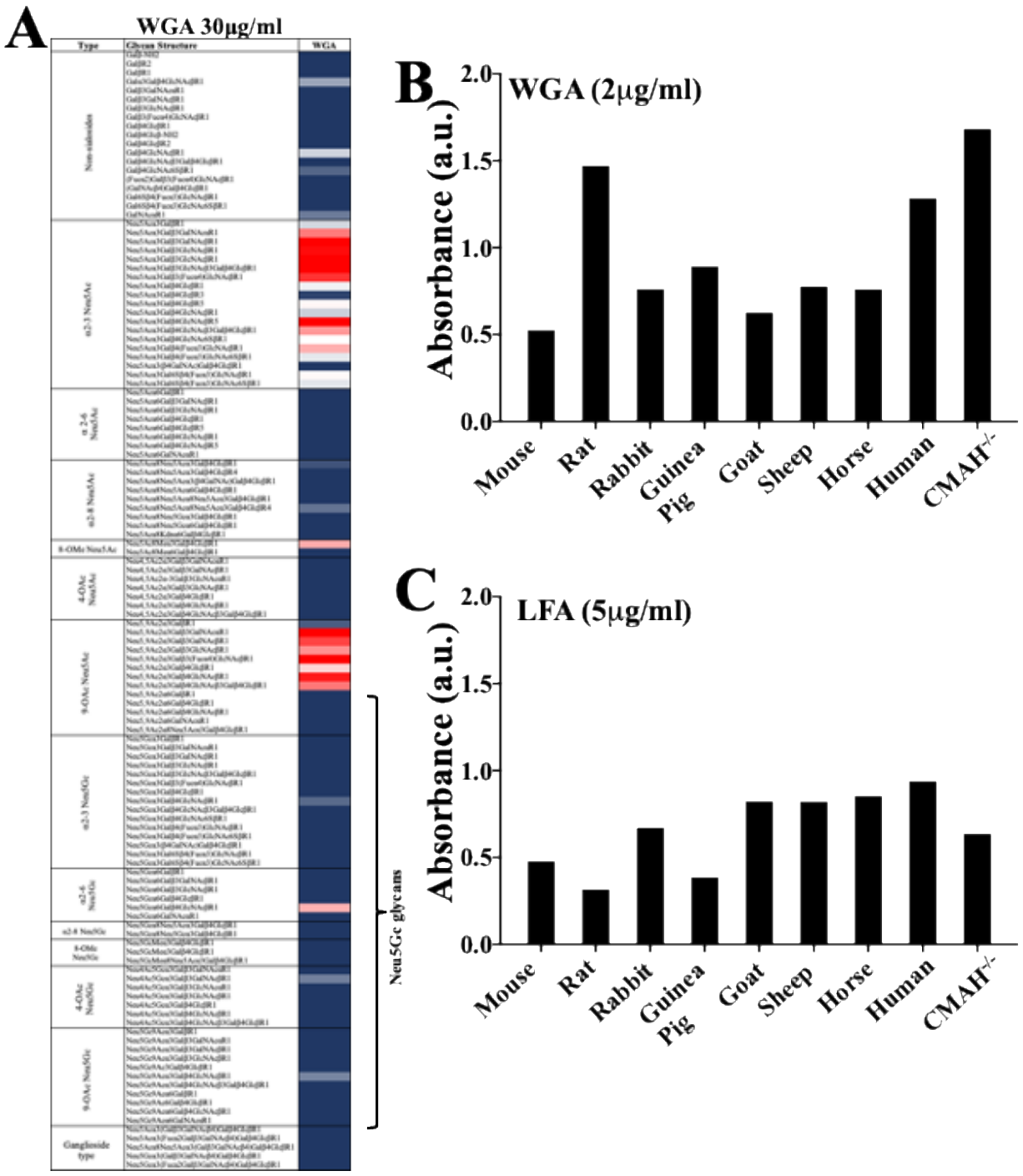
A
WGA 30μg/ml
Type
Glycan Structure
WGA
Non-sialosides
α2-3 Neu5Ac
α-2-6 Neu5Ac
α2-8 Neu5Ac
8-OMe Neu5Ac
4-OAc Neu5Ac
9-OAc Neu5Ac
α2-3 Neu5Gc
α2-6 Neu5Gc
α2-8 Neu5Gc
8-OMe Neu5Gc
4-OAc Neu5Gc
9-OAc Neu5Gc
Ganglioside type
Neu5Gc glycans
B
WGA (2μg/ml)
Absorbance (a.u.)
2.0
1.5
1.0
0.5
0.0
Mouse
Rat
Rabbit
Guinea Pig
Goat
Sheep
Horse
Human
CMAH-/-
C
LFA (5μg/ml)
Absorbance (a.u.)
2.0
1.5
1.0
0.5
0.0
Mouse
Rat
Rabbit
Guinea Pig
Goat
Sheep
Horse
Human
CMAH-/-

Figure S2. WGA and LFA lacks the specificity and robustness required for SGRP1; the probe for all major mammalian sialoglycan types. *Panel A,* the sialoglycan microarray data with Biotin-WGA (30 μg/ml) demonstrate the sia preferences of WGA. WGA does not bind to wide range of glycans terminating with Neu5Gc while shows selective preference towards few Neu5Ac terminating glycans. The data also suggest WGA's preference towards GlcNAc, available in our ensemble of glycans on sialoglycan microarray. Binding efficiencies are displayed in red for highest binding (saturated or 100%), blue for minimum or no binding (0%) and intermediate binding represented by colors ranging between blue and red. Ranks; Red (100%, or maximum), Blue (0%, or minimum). *Panel B* shows the WGA binding with mammalian (sialo)glycans present in various animal sera. WGA selective binding towards Neu5Ac over Neu5Gc can be observed in higher signals for Neu5Ac-rich CMAH$^{-/-}$ than WT mouse serum. *Panel C* represents the LFA binding to serum sialoglycans. LFA, although promising probe, lacks the avidity required for a comprehensive Sia-binding probe. To obtain this data, Biotin LFA (5 μg/ml) was pre complexed with Avidin-HRP (1:1500) to minimize loss of binding in washing steps, the signals otherwise remained weak and inconclusive.

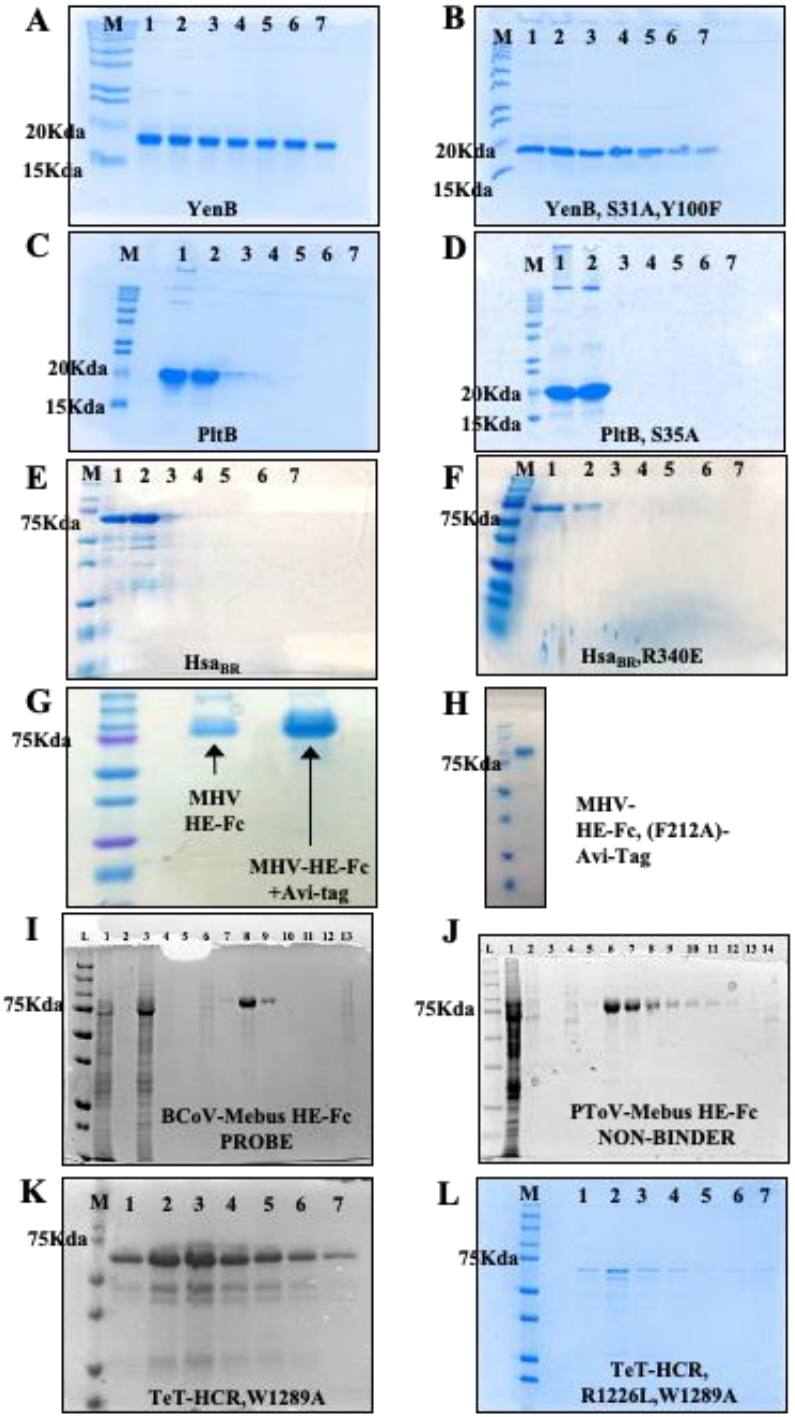
A
M 1 2 3 4 5 6 7
20Kda
15Kda
YenB
B
M 1 2 3 4 5 6 7
20Kda
15Kda
YenB, S31A,Y100F
C
M 1 2 3 4 5 6 7
20Kda
15Kda
PltB
D
M 1 2 3 4 5 6 7
20Kda
15Kda
PltB, S35A
E
M 1 2 3 4 5 6 7
75Kda
Hsa$_{BR}$
F
M 1 2 3 4 5 6 7
75Kda
Hsa$_{BR}$,R340E
G
75Kda
MHV
HE-Fc
MHV-HE-Fc
+Avi-tag
H
75Kda
MHV-
HE-Fc, (F212A)-
Avi-Tag
I
75Kda
BCoV-Mebus HE-Fc
PROBE
J
75Kda
PToV-Mebus HE-Fc
NON-BINDER
K
M 1 2 3 4 5 6 7
75Kda
TeT-HCR,W1289A
L
M 1 2 3 4 5 6 7
75Kda
TeT-HCR,
R1226L,W1289A

Figure S3. SDS-PAGE analysis results for the purification of protein candidates of SGRPs.

Panels A-L, demonstrating elution profiles of purified proteins, as mentioned in figure. In every gel, *lane M* stands for protein molecular weight standard and *lanes 1-7* represent protein samples eluted by corresponding purification methods for YenB, PltB, Hsa_{BR}, TeT-HCR (W1289A) and their non-binding mutants. Panel G shows the eluted protein MHV-HE-Fc (no Avi-tag) and MHV-HE-Fc with Avi tag, comparing the quality of purification of protein after introducing Avi-tag. Panel F represents eluted MHV-HE-Fc (F212A) with Avi tag, the nonbinding control for MHV-HE-Fc. Panels I & J represent purification profiles for SGRPs 7 and 9, showed by BCoV-Mebus HE-Fc binder probe ($SGRP7^{BCoV}$) and PToV-Mebus HE-Fc nonbinder molecule ($SGRP9^{PToV}$NB). *For Panel I,* lane L is BioRad PrecisionPlus ladder, lanes 1is culture pellet 1, lane 2 is culture harvest supernatant 1, lane 3 is culture pellet 2 and lane 4 is culture harvest supernatant 2. Lanes 5 and 6 are dialysate and dialyzed Super / Column Load, while lanes 7-11 are elution column volumes. Lane 12 is pre-elution wash and lane 13 is sample load flow-through. For *Panel J*- lane L is BioRad PrecisionPlus Ladder, lanes 1 is culture pellet 1, lane 2 is culture harvest supernatant 1, lane 3 is dialysate and lane 4 is dialyzed Super / Column Load. Lanes 5–12 are elution column volumes. Lane 13 is pre-elution wash and lane 14 is sample load flow-through.

Type
Glycan Structure
SGRP1 Tyr48
SGRP1 Tyr48 NB
SGRP2 P88
SGRP2 P88 NB
SGRP3 R86
SGRP3 R86 NB
SGRP4 H89
SGRP4 H89 NB
SGRP5 K87
SGRP5 K87 NB
SGRP7 R143
SGRP7 R143 NB
SGRP8 T47
SGRP8 T47 NB
SGRP9 T143
SGRP9 T143 NB
Non-sialosides
Galβ-NH2
GalβR2
GalβR1
Galα3Galβ4GlcNAcβR1
Galβ3GalNAcαR1
Galβ3GalNAcβR1
Galβ3GlcNAcβR1
Galβ3(Fucα4)GlcNAcβR1
Galβ4GlcβR1
Galβ4Glcβ-NH2
Galβ4GlcβR2
Galβ4GlcNAcβR1
Galβ4GlcNAcβ3Galβ4GlcβR1
Galβ4GlcNAcα6SβR1
(Fucα2Galβ3)Fucα4GlcNAcβR1
(GalNAcβ4)Galβ4GlcβR1
Galα6Sβ4(Fucα3)GlcNAcβR1
Galα6Sβ4(Fucα3)GlcNAcα6SβR1
GalNAcαR1
α2-3 Neu5Ac
Neu5Acα3Galβ1R1
Neu5Acα3Galβ3GalNAcαR1
Neu5Acα3Galβ3GalNAcβR1
Neu5Acα3Galβ3GlcNAcβR1
Neu5Acα3Galβ3GlcNAcβR1
Neu5Acα3Galβ3GlcNAcβ3Galβ4GlcβR1
Neu5Acα3Galβ3(Fucα4)GlcNAcβR1
Neu5Acα3Galβ4GlcβR1
Neu5Acα3Galβ4GlcβR3
Neu5Acα3Galβ4GlcβR5
Neu5Acα3Galβ4GlcNAcβR1
Neu5Acα3Galβ4GlcNAcβR5
Neu5Acα3Galβ4GlcNAcβ3Galβ4GlcβR1
Neu5Acα3Galβ4GlcNAcα6SβR1
Neu5Acα3Galβ4(Fucα3)GlcNAcβR1
Neu5Acα3Galβ4(Fucα3)GlcNAcα6SβR1
Neu5Acα3β4GalNAcβ3Galβ4GlcβR1
Neu5Acα3Galα6Sβ4(Fucα3)GlcNAcβR1
Neu5Acα3Galα6Sβ4(Fucα3)GlcNAcα6SβR1
α 2-6 Neu5Ac
Neu5Acα6GalβR1
Neu5Acα6Galβ3GalNAcβR1
Neu5Acα6Galβ3GlcNAcβR1
Neu5Acα6Galβ4GlcβR1
Neu5Acα6Galβ4GlcβR5
Neu5Acα6Galβ4GlcNAcβR1
Neu5Acα6Galβ4GlcNAcβR5
Neu5Acα6GalNAcαR1
α2-8 Neu5Ac
Neu5Acα8Neu5Acα3Galβ4GlcβR1
Neu5Acα8Neu5Acα3Galβ4GlcβR4
Neu5Acα8Neu5Acα3(β4GalNAcα)Galβ4GlcβR1
Neu5Acα8Neu5Acα6Galβ4GlcβR1
Neu5Acα8Neu5Acα8Neu5Acα3Galβ4GlcβR1
Neu5Acα8Neu5Acα8Neu5Acα3Galβ4GlcβR4
Neu5Acα8Neu5Gcα3Galβ4GlcβR1
Neu5Acα8Neu5Gcα6Galβ4GlcβR1
Neu5Acα8Kdnα6Galβ4GlcβR1
8-OMe Neu5Ac
Neu5Acα8Meα3Galβ4GlcβR1
Neu5Acα8Meα6Galβ4GlcβR1
4-OAc Neu5Ac
Neu4,5Ac2α3Galβ3GalNAcαR1
Neu4,5Ac2α3Galβ3GalNAcβR1
Neu4,5Ac2α-3Galβ3GlcNAcαR1
Neu4,5Ac2α3Galβ3GlcNAcβR1
Neu4,5Ac2α3Galβ4GlcβR1
Neu4,5Ac2α3Galβ4GlcNAcβR1
Neu4,5Ac2α3Galβ4GlcNAcβ3Galβ4GlcβR1
9-OAc Neu5Ac
Neu5,9Ac2α3GalβR1
Neu5,9Ac2α3Galβ3GalNAcαR1
Neu5,9Ac2α3Galβ3GalNAcβR1
Neu5,9Ac2α3Galβ3GlcNAcβR1
Neu5,9Ac2α3Galβ3(Fucα4)GlcNAcβR1
Neu5,9Ac2α3Galβ4GlcβR1
Neu5,9Ac2α3Galβ4GlcNAcβR1
Neu5,9Ac2α3Galβ4GlcNAcβ3Galβ4GlcβR1
Neu5,9Ac2α6GalβR1
Neu5,9Ac2α6Galβ4GlcβR1
Neu5,9Ac2α6Galβ4GlcNAcβR1
Neu5,9Ac2α6GalNAcαR1
Neu5,9Ac2αNeu5Acα3Galβ4GlcβR1
α2-3 Neu5Gc
Neu5Gcα3GalβR1
Neu5Gcα3Galβ3GalNAcαR1
Neu5Gcα3Galβ3GalNAcβR1
Neu5Gcα3Galβ3GlcNAcβR1
Neu5Gcα3Galβ3GlcNAcβ3Galβ4GlcβR1
Neu5Gcα3Galβ3(Fucα4)GlcNAcβR1
Neu5Gcα3Galβ4GlcβR1
Neu5Gcα3Galβ4GlcNAcβR1
Neu5Gcα3Galβ4GlcNAcβ3Galβ4GlcβR1
Neu5Gcα3Galβ4GlcNAcα6SβR1
Neu5Gcα3Galβ4(Fucα3)GlcNAcβR1
Neu5Gcα3Galβ4(Fucα3)GlcNAcα6SβR1
Neu5Gcα3β4GalNAcβ3Galβ4GlcβR1
Neu5Gcα3Galα6Sβ4(Fucα3)GlcNAcβR1
Neu5Gcα3Galα6Sβ4(Fucα3)GlcNAcα6SβR1
α2-6 Neu5Gc
Neu5Gcα6GalβR1
Neu5Gcα6Galβ3GalNAcβR1
Neu5Gcα6Galβ3GlcNAcβR1
Neu5Gcα6Galβ4GlcβR1
Neu5Gcα6Galβ4GlcNAcβR1
Neu5Gcα6GalNAcαR1
α2-8 Neu5Gc
Neu5Gcα8Neu5Acα3Galβ4GlcβR1
Neu5Gcα8Neu5Gcα3Galβ4GlcβR1
8-OMe Neu5Gc
Neu5GcMeα3Galβ4GlcβR1
Neu5GcMeα8Neu5Acα3Galβ4GlcβR1
4-OAc Neu5Gc
Neu4Ac5Gcα3Galβ3GalNAcαR1
Neu4Ac5Gcα3Galβ3GalNAcβR1
Neu4Ac5Gcα3Galβ3GlcNAcαR1
Neu4Ac5Gcα3Galβ3GlcNAcβR1
Neu4Ac5Gcα3Galβ4GlcβR1
Neu4Ac5Gcα3Galβ4GlcNAcβR1
Neu4Ac5Gcα3Galβ4GlcNAcβ3Galβ4GlcβR1
9-OAc Neu5Gc
Neu5Gc9Acα3GalβR1
Neu5Gc9Acα3Galβ3GalNAcαR1
Neu5Gc9Acα3Galβ3GalNAcβR1
Neu5Gc9Acα3Galβ3GlcNAcβR1
Neu5Gc9Acα3Galβ4GlcβR1
Neu5Gc9Acα3Galβ4GlcNAcβR1
Neu5Gc9Acα3Galβ4GlcNAcβ3Galβ4GlcβR1
Neu5Gc9Acα6GalβR1
Neu5Gc9Actα6Galβ4GlcβR1
Neu5Gc9Acα6Galβ4GlcNAcβR1
Neu5Gc9Acα6GalNAcαR1
Ganglioside type
Neu5Acα3(Galβ3GalNAcβ4)Galβ4GlcβR1
Neu5Acα3(Fucα2Galβ3GalNAcβ4)Galβ4GlcβR1
Neu5Acα8Neu5Acα3(Galβ3GalNAcβ4)Galβ4GlcβR1
Neu5Gcα3(Galβ3GalNAcβ4)Galβ4GlcβR1
Neu5Gcα3(Fucα2Galβ3GalNAcβ4)Galβ4GlcβR1

Figure S4. Sialoglycan microarray binding studies of non-binding variants of Sialoglycan Recognizing Probes (SGRPs). Heatmap analysis of SGRP-NBs binding to mammalian (sialo)glycans; SGRP1^{YenB}NB (30 μg/ml), SGRP2^{PlBt}NB (30μg/ml), SGRP3^{Hsa}NB (30 μg/ml), SGRP4^{MHV}NB (30 μg/ml), SGRP5^{IgY}NB (20 μg/ml), SGRP7^{BCoV}NB (60 μg/ml), SGRP8^{TeT}NB (30 μg/ml) and SGRP9^{PToV}NB (30 μg/ml) were characterized for the Sia-specificity in different experiments and displayed by heatmaps, colors ranging between blue, white and red. Ranks; Red (100%), Blue (0%). There was no nonbinding control molecule for SGRP6^{SNA}.

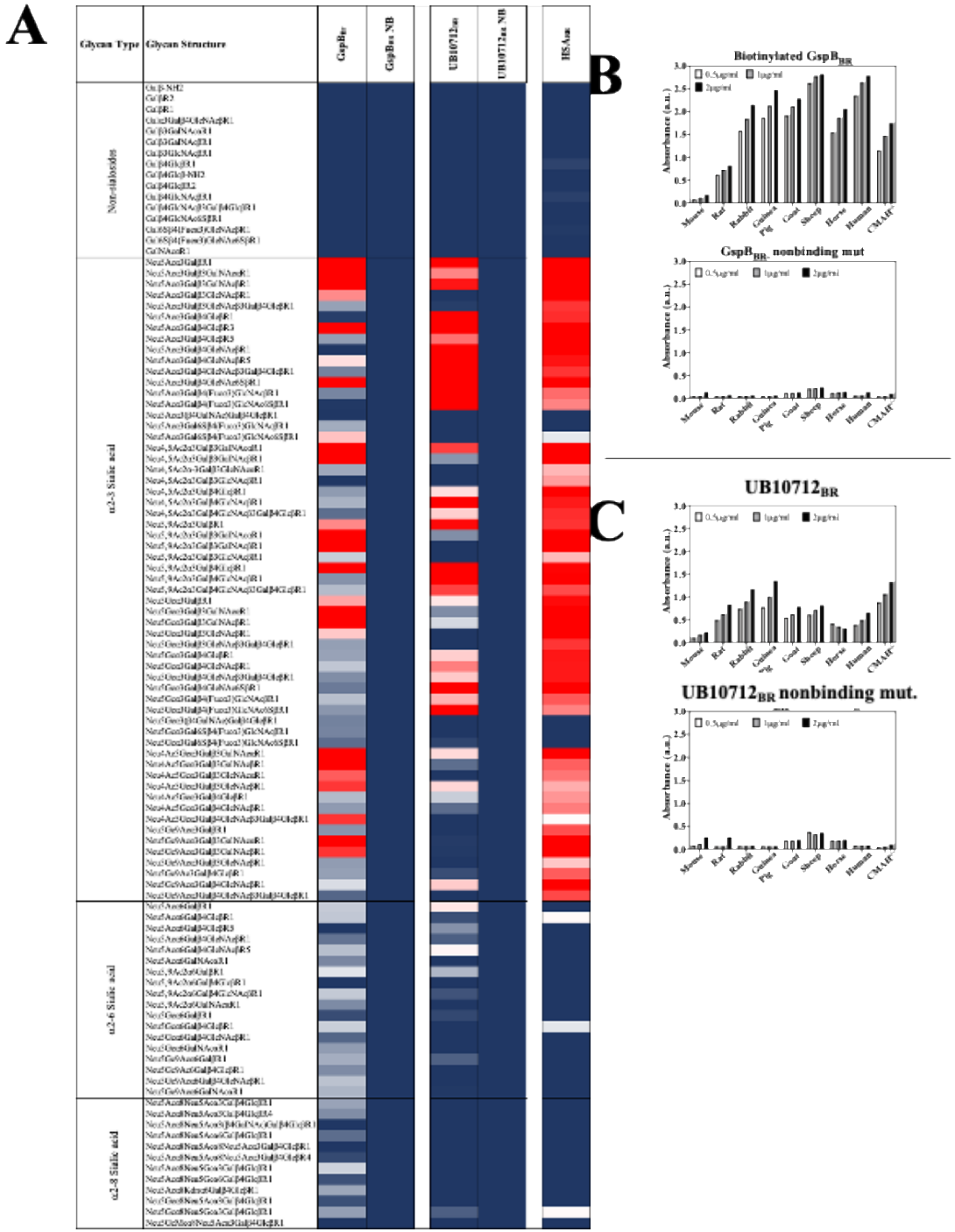
A
Glycan Type
Glycan Structure
GspB$_{BR}$
GspB$_{BR}$ NB
UB10712$_{BR}$
UB10712$_{BR}$ NB
HSAm
Non-sialosides
α2-3 Sialic acid
α2-6 Sialic acid
α2-8 Sialic acid
B
Biotinylated GspB$_{BR}$
GspB$_{BR}$ nonbinding mut
C
UB10712$_{BR}$
UB10712$_{BR}$ nonbinding mut.
0.5μg/ml
1μg/ml
2μg/ml
Absorbance (a.u.)
Mouse
Rat
Rabbit
Guinea Pig
Goat
Sheep
Horse
Human
CMAF-

Figure S5. The other *Streptococcus* SRR adhesins; GspB$_{BR}$ and UB10712$_{BR}$ demonstrate specificity towards α2-3Sias but lack the Hsa$_{BR}$ like broad range of α2-3Sia ligands. *Panel A,* the sialoglycan microarray data with Biotin-GspB$_{BR}$ and Biotin- UB10712$_{BR}$, suggesting towards their competent preference towards α2-3Sias. Both molecules, however, lacks the Hsa$_{BR}$ like binding dynamics (Hsa$_{BR}$ glycan array is same as presented in Figure 1). Binding efficiencies are displayed in red for highest binding (saturated or 100%), blue for minimum or no binding (0%) and intermediate binding represented by colors ranging between blue and red. Ranks; Red (100%, or maximum), Blue (0%, or minimum). *Panels B & C* are the ELISA experiments results highlighting the sialoglycan binding efficacy of Biotin-GspB$_{BR}$ and Biotin-UB10712$_{BR}$ towards mammalian sialoglycans represented by mammalian sera. Binding of biotinylated adhesins were diagnosed and developed using Avidin-HRP (1:1500). ELISA for each pair of proteins was performed in same experiment/conditions and goodness of experiment was confirmed by signals developed in sera treated only with secondary antibody (Avidin-HRP), not shown here.

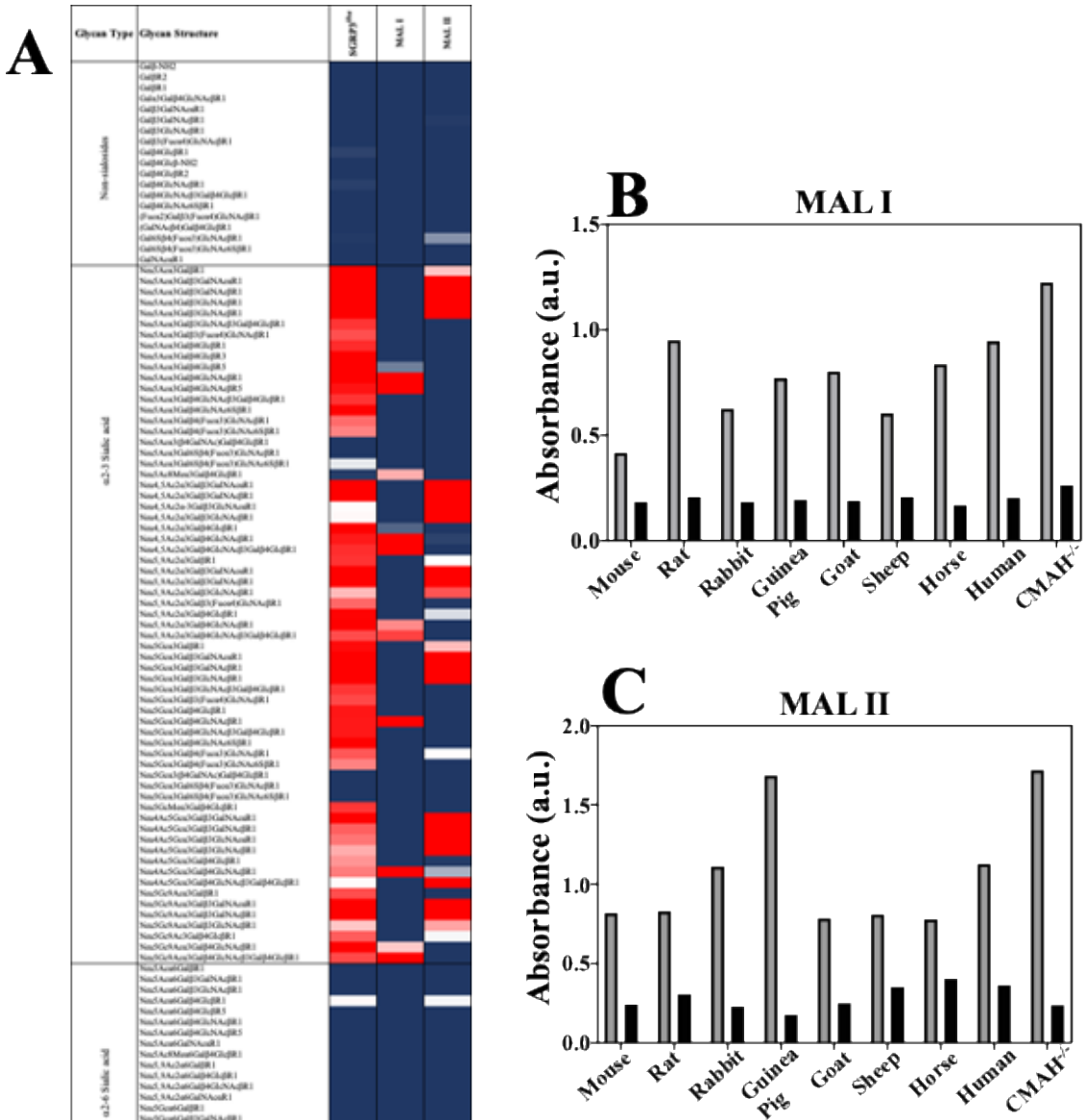
A
Glycan Type
Glycan Structure
SGE2Fc
MAL I
MAL II
Non-sialosides
α2-3 Sialic acid
α2-6 Sialic acid
α2-8 Sialic acid
B
MAL I
Absorbance (a.u.)
1.5
1.0
0.5
0.0
Mouse
Rat
Rabbit
Guinea Pig
Goat
Sheep
Horse
Human
CMAH-/-
C
MAL II
Absorbance (a.u.)
2.0
1.5
1.0
0.5
0.0
Mouse
Rat
Rabbit
Guinea Pig
Goat
Sheep
Horse
Human
CMAH-/-

Figure S6. SGRP3^{Hsa} demonstrates more predominant affinity towards α2-3Sias than MAL I and MAL II, the conventional probes for this class of sialoglycans. *Panel A*, the sialoglycan microarray data of SGRP3^{Hsa} (30 μg/ml), MAL II (40μg/ml) and MAL I (30 μg/ml) suggesting towards their preferences for α2-3-linked sialoglycans in microarray. The data clearly indicate that SGRP3^{Hsa} can identify more structural variants of α2-3Sias than MALI and MAL II with significant affinities. Binding efficiencies are displayed in red for highest binding (saturated or 100%), blue for minimum or no binding (0%) and intermediate binding represented by colors ranging between blue (minimum) and red (maximum). In a separate experiment, preincubation of mammalian serum with HsaBR significantly inhibited the binding of MAL I (*Panel B*) and MAL II (*Panel C*) respectively. The sources of serum are mentioned in panels, and goodness of experiment was confirmed by signals developed in sera treated only with secondary antibody (Avidin-HRP), not shown here

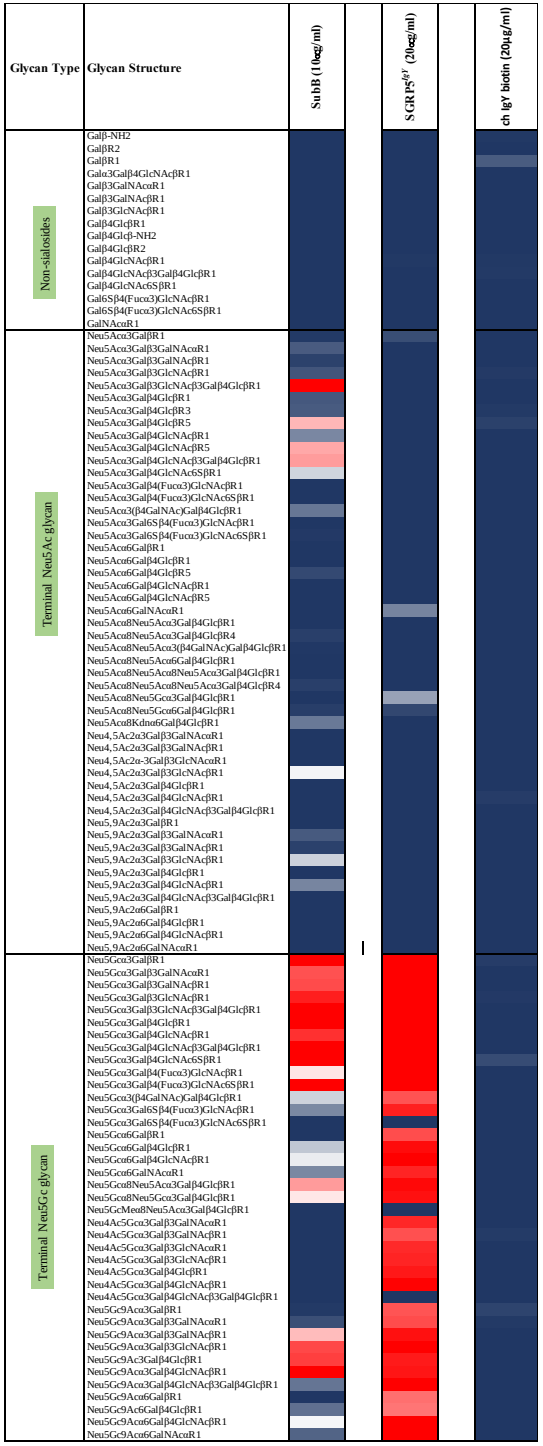
Glycan Type
Glycan Structure
SubB (10μg/ml)
SGRP$^{4/3}$ (20μg/ml)
ch IgY biotin (20μg/ml)
Non-sialosides
Galβ-NH2
GalβR2
GalβR1
Galα3Galβ4GlcNAcβR1
Galβ3GalNAcαR1
Galβ3GalNAcβR1
Galβ3GlcNAcβR1
Galβ4GlcβR1
Galβ4Glcβ-NH2
Galβ4GlcβR2
Galβ4GlcNAcβR1
Galβ4GlcNAcβ3Galβ4GlcβR1
Galβ4GlcNAc6SβR1
Galα6Sβ4(Fucα3)GlcNAcβR1
Galα6Sβ4(Fucα3)GlcNAc6SβR1
GalNAcαR1
Terminal Neu5Ac glycan
Neu5Acα3GalβR1
Neu5Acα3Galβ3GalNAcαR1
Neu5Acα3Galβ3GalNAcβR1
Neu5Acα3Galβ3GlcNAcβR1
Neu5Acα3Galβ3GlcNAcβ3Galβ4GlcβR1
Neu5Acα3Galβ4GlcβR1
Neu5Acα3Galβ4GlcβR3
Neu5Acα3Galβ4GlcβR5
Neu5Acα3Galβ4GlcNAcβR1
Neu5Acα3Galβ4GlcNAcβR5
Neu5Acα3Galβ4GlcNAcβ3Galβ4GlcβR1
Neu5Acα3Galβ4GlcNAc6SβR1
Neu5Acα3Galβ4(Fucα3)GlcNAcβR1
Neu5Acα3Galβ4(Fucα3)GlcNAc6SβR1
Neu5Acα3(β4GalNAc)Galβ4GlcβR1
Neu5Acα3Gal6Sβ4(Fucα3)GlcNAcβR1
Neu5Acα3Gal6Sβ4(Fucα3)GlcNAc6SβR1
Neu5Acα6GalβR1
Neu5Acα6Galβ4GlcβR1
Neu5Acα6Galβ4GlcβR5
Neu5Acα6Galβ4GlcNAcβR1
Neu5Acα6Galβ4GlcNAcβR5
Neu5Acα6GalNAcαR1
Neu5Acα8Neu5Acα3Galβ4GlcβR1
Neu5Acα8Neu5Acα3Galβ4GlcβR4
Neu5Acα8Neu5Acα3(β4GalNAc)Galβ4GlcβR1
Neu5Acα8Neu5Acα6Galβ4GlcβR1
Neu5Acα8Neu5Acα8Neu5Acα3Galβ4GlcβR1
Neu5Acα8Neu5Acα8Neu5Acα3Galβ4GlcβR4
Neu5Acα8Neu5Gcα3Galβ4GlcβR1
Neu5Acα8Neu5Gcα6Galβ4GlcβR1
Neu5Acα8Kdnα6Galβ4GlcβR1
Neu4,5Ac2α3Galβ3GalNAcαR1
Neu4,5Ac2α3Galβ3GalNAcβR1
Neu4,5Ac2α-3Galβ3GlcNAcαR1
Neu4,5Ac2α3Galβ3GlcNAcβR1
Neu4,5Ac2α3Galβ4GlcβR1
Neu4,5Ac2α3Galβ4GlcNAcβR1
Neu4,5Ac2α3Galβ4GlcNAcβ3Galβ4GlcβR1
Neu5,9Ac2α3GalβR1
Neu5,9Ac2α3Galβ3GalNAcαR1
Neu5,9Ac2α3Galβ3GalNAcβR1
Neu5,9Ac2α3Galβ3GlcNAcβR1
Neu5,9Ac2α3Galβ4GlcβR1
Neu5,9Ac2α3Galβ4GlcNAcβR1
Neu5,9Ac2α3Galβ4GlcNAcβ3Galβ4GlcβR1
Neu5,9Ac2α6GalβR1
Neu5,9Ac2α6Galβ4GlcβR1
Neu5,9Ac2α6Galβ4GlcNAcβR1
Neu5,9Ac2α6GalNAcαR1
Terminal Neu5Gc glycan
Neu5Gcα3GalβR1
Neu5Gcα3Galβ3GalNAcαR1
Neu5Gcα3Galβ3GalNAcβR1
Neu5Gcα3Galβ3GlcNAcβR1
Neu5Gcα3Galβ3GlcNAcβ3Galβ4GlcβR1
Neu5Gcα3Galβ4GlcβR1
Neu5Gcα3Galβ4GlcNAcβR1
Neu5Gcα3Galβ4GlcNAcβ3Galβ4GlcβR1
Neu5Gcα3Galβ4GlcNAc6SβR1
Neu5Gcα3Galβ4(Fucα3)GlcNAcβR1
Neu5Gcα3Galβ4(Fucα3)GlcNAc6SβR1
Neu5Gcα3(β4GalNAc)Galβ4GlcβR1
Neu5Gcα3Gal6Sβ4(Fucα3)GlcNAcβR1
Neu5Gcα3Gal6Sβ4(Fucα3)GlcNAc6SβR1
Neu5Gcα6GalβR1
Neu5Gcα6Galβ4GlcβR1
Neu5Gcα6Galβ4GlcNAcβR1
Neu5Gcα6GalNAcαR1
Neu5Gcα8Neu5Acα3Galβ4GlcβR1
Neu5Gcα8Neu5Gcα3Galβ4GlcβR1
Neu5GcMeα8Neu5Acα3Galβ4GlcβR1
Neu4Ac5Gcα3Galβ3GalNAcαR1
Neu4Ac5Gcα3Galβ3GalNAcβR1
Neu4Ac5Gcα3Galβ3GlcNAcαR1
Neu4Ac5Gcα3Galβ3GlcNAcβR1
Neu4Ac5Gcα3Galβ4GlcβR1
Neu4Ac5Gcα3Galβ4GlcNAcβR1
Neu4Ac5Gcα3Galβ4GlcNAcβ3Galβ4GlcβR1
Neu5Gc9Acα3GalβR1
Neu5Gc9Acα3Galβ3GalNAcαR1
Neu5Gc9Acα3Galβ3GalNAcβR1
Neu5Gc9Acα3Galβ3GlcNAcβR1
Neu5Gc9Ac3Galβ4GlcβR1
Neu5Gc9Acα3Galβ4GlcNAcβR1
Neu5Gc9Acα3Galβ4GlcNAcβ3Galβ4GlcβR1
Neu5Gc9Acα6GalβR1
Neu5Gc9Ac6Galβ4GlcβR1
Neu5Gc9Acα6Galβ4GlcNAcβR1
Neu5Gc9Acα6GalNAcαR1

Figure S7. SGRP5^{IgY} shows prominent binding towards Neu5Gc in comparison to subtilis toxin SubB: The sialoglycan microarray data of subtilis toxin subunits- SubB (native protein; 10 μg/ml), compared the SGRP5^{IgY} (20 μg/ml-data same as presented in Figure 1). The results suggest towards more prominent Neu5Gc recognition by SGRP5^{IgY} than SubB. Ch. IgY Biotin (20 μg/ml) served as internal control for SGRP5^{IgY} binding. Binding efficiencies are displayed in red for highest binding (saturated or 100%), blue for minimum or no binding (0%) and intermediate binding represented by colors ranging between blue (minimum) and red (maximum).

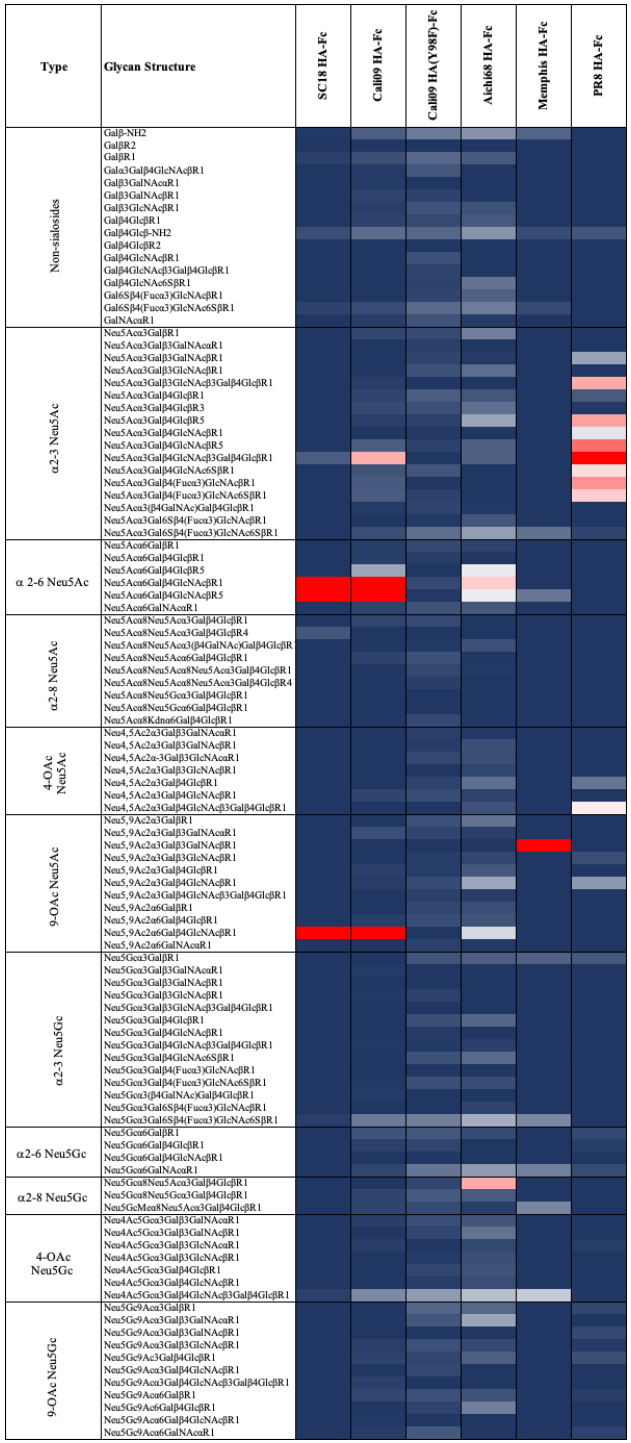
Type
Glycan Structure
SC18 HA-Fc
Cal09 HA-Fc
Cal09 HA(Y98F)-Fc
Aichi68 HA-Fc
Memphis HA-Fc
PR8 HA-Fc
Non-sialosides
Galβ-NH2
GalβR2
GalβR1
Galα3Galβ4GlcNAcβR1
Galβ3GalNAcαR1
Galβ3GalNAcβR1
Galβ3GlcNAcβR1
Galβ4GlcβR1
Galβ4Glcβ-NH2
Galβ4GlcβR2
Galβ4GlcNAcβR1
Galβ4GlcNAcβ3Galβ4GlcβR1
Galβ4GlcNAc6SβR1
Gal6Sβ4(Fucα3)GlcNAcβR1
Gal6Sβ4(Fucα3)GlcNAc6SβR1
GalNAcαR1
α2-3 Neu5Ac
Neu5Acα3GalβR1
Neu5Acα3Galβ3GalNAcαR1
Neu5Acα3Galβ3GalNAcβR1
Neu5Acα3Galβ3GlcNAcβR1
Neu5Acα3Galβ3GlcNAcβ3Galβ4GlcβR1
Neu5Acα3Galβ4GlcβR1
Neu5Acα3Galβ4GlcβR3
Neu5Acα3Galβ4GlcβR5
Neu5Acα3Galβ4GlcNAcβR1
Neu5Acα3Galβ4GlcNAcβR5
Neu5Acα3Galβ4GlcNAcβ3Galβ4GlcβR1
Neu5Acα3Galβ4GlcNAc6SβR1
Neu5Acα3Galβ4(Fucα3)GlcNAcβR1
Neu5Acα3Galβ4(Fucα3)GlcNAc6SβR1
Neu5Acα3(β4GalNAc)Galβ4GlcβR1
Neu5Acα3Gal6Sβ4(Fucα3)GlcNAcβR1
Neu5Acα3Gal6Sβ4(Fucα3)GlcNAc6SβR1
α 2-6 Neu5Ac
Neu5Acα6GalβR1
Neu5Acα6Galβ4GlcβR1
Neu5Acα6Galβ4GlcβR5
Neu5Acα6Galβ4GlcNAcβR1
Neu5Acα6Galβ4GlcNAcβR5
Neu5Acα6GalNAcαR1
α2-8 Neu5Ac
Neu5Acα8Neu5Acα3Galβ4GlcβR1
Neu5Acα8Neu5Acα3Galβ4GlcβR4
Neu5Acα8Neu5Acα3(β4GalNAc)Galβ4GlcβR
Neu5Acα8Neu5Acα6Galβ4GlcβR1
Neu5Acα8Neu5Acα8Neu5Acα3Galβ4GlcβR1
Neu5Acα8Neu5Acα8Neu5Acα3Galβ4GlcβR4
Neu5Acα8Neu5Gcα3Galβ4GlcβR1
Neu5Acα8Neu5Gcα6Galβ4GlcβR1
Neu5Acα8Kdnα6Galβ4GlcβR1
4-OAc Neu5Ac
Neu4,5Ac2α3Galβ3GalNAcαR1
Neu4,5Ac2α3Galβ3GalNAcβR1
Neu4,5Ac2α-3Galβ3GlcNAcαR1
Neu4,5Ac2α3Galβ3GlcNAcβR1
Neu4,5Ac2α3Galβ4GlcβR1
Neu4,5Ac2α3Galβ4GlcNAcβR1
Neu4,5Ac2α3Galβ4GlcNAcβ3Galβ4GlcβR1
9-OAc Neu5Ac
Neu5,9Ac2α3GalβR1
Neu5,9Ac2α3Galβ3GalNAcαR1
Neu5,9Ac2α3Galβ3GalNAcβR1
Neu5,9Ac2α3Galβ3GlcNAcβR1
Neu5,9Ac2α3Galβ4GlcβR1
Neu5,9Ac2α3Galβ4GlcNAcβR1
Neu5,9Ac2α3Galβ4GlcNAcβ3Galβ4GlcβR1
Neu5,9Ac2α6GalβR1
Neu5,9Ac2α6Galβ4GlcβR1
Neu5,9Ac2α6Galβ4GlcNAcβR1
Neu5,9Ac2α6GalNAcαR1
α2-3 Neu5Gc
Neu5Gcα3GalβR1
Neu5Gcα3Galβ3GalNAcαR1
Neu5Gcα3Galβ3GalNAcβR1
Neu5Gcα3Galβ3GlcNAcβR1
Neu5Gcα3Galβ3GlcNAcβ3Galβ4GlcβR1
Neu5Gcα3Galβ4GlcβR1
Neu5Gcα3Galβ4GlcNAcβR1
Neu5Gcα3Galβ4GlcNAcβ3Galβ4GlcβR1
Neu5Gcα3Galβ4GlcNAc6SβR1
Neu5Gcα3Galβ4(Fucα3)GlcNAcβR1
Neu5Gcα3Galβ4(Fucα3)GlcNAc6SβR1
Neu5Gcα3(β4GalNAc)Galβ4GlcβR1
Neu5Gcα3Gal6Sβ4(Fucα3)GlcNAcβR1
Neu5Gcα3Gal6Sβ4(Fucα3)GlcNAc6SβR1
α2-6 Neu5Gc
Neu5Gcα6GalβR1
Neu5Gcα6Galβ4GlcβR1
Neu5Gcα6Galβ4GlcNAcβR1
Neu5Gcα6GalNAcαR1
α2-8 Neu5Gc
Neu5Gcα8Neu5Acα3Galβ4GlcβR1
Neu5Gcα8Neu5Gcα3Galβ4GlcβR1
Neu5GcMeα8Neu5Acα3Galβ4GlcβR1
4-OAc Neu5Gc
Neu4Ac5Gcα3Galβ3GalNAcαR1
Neu4Ac5Gcα3Galβ3GalNAcβR1
Neu4Ac5Gcα3Galβ3GlcNAcαR1
Neu4Ac5Gcα3Galβ3GlcNAcβR1
Neu4Ac5Gcα3Galβ4GlcβR1
Neu4Ac5Gcα3Galβ4GlcNAcβR1
Neu4Ac5Gcα3Galβ4GlcNAcβ3Galβ4GlcβR1
9-OAc Neu5Gc
Neu5Gc9Acα3GalβR1
Neu5Gc9Acα3Galβ3GalNAcαR1
Neu5Gc9Acα3Galβ3GalNAcβR1
Neu5Gc9Acα3Galβ3GlcNAcβR1
Neu5Gc9Ac3Galβ4GlcβR1
Neu5Gc9Acα3Galβ4GlcNAcβR1
Neu5Gc9Acα3Galβ4GlcNAcβ3Galβ4GlcβR1
Neu5Gc9Acα6GalβR1
Neu5Gc9Ac6Galβ4GlcβR1
Neu5Gc9Acα6Galβ4GlcNAcβR1
Neu5Gc9Acα6GalNAcαR1

Figure S8. Sialoglycan microarray of influenza virus hemagglutinins included in the study: The glycan array data suggest towards very selective Sia-binding of influenza virus hemagglutinins that cannot be generalized towards the broader class of α2-6Sialoglycans. All viral HA-Fc were tested at 5 μg/ml concentration. Binding efficiencies are displayed in red for highest binding (saturated or 100%), blue for minimum or no binding (0%) and intermediate binding represented by colors ranging between blue (minimum) and red (maximum).

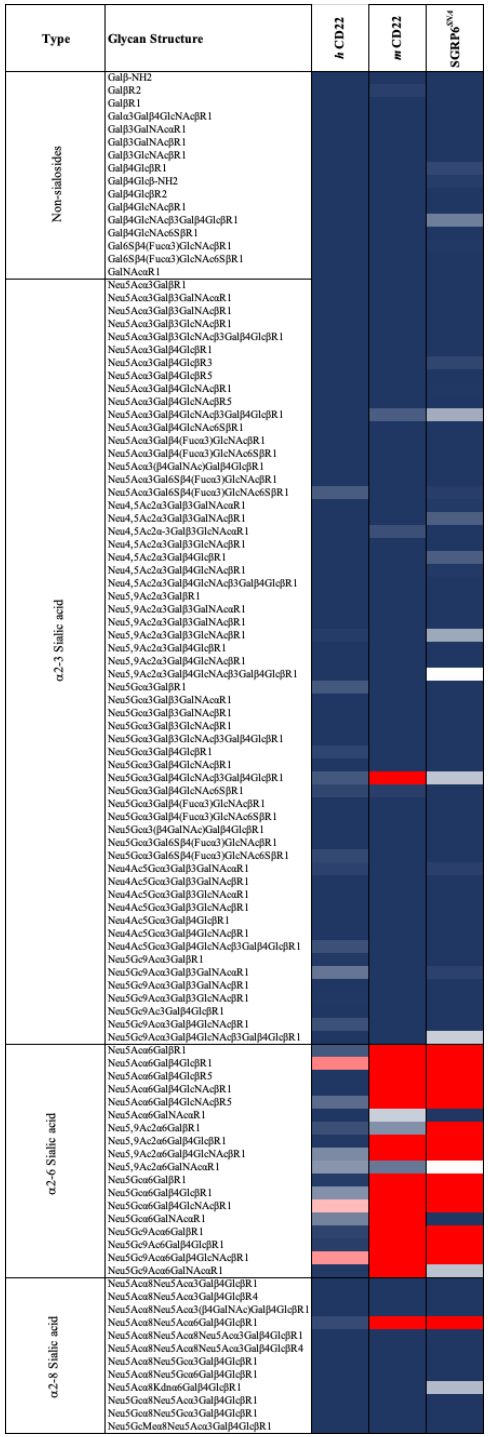
Type
Glycan Structure
h CD22
m CD22
SGRP6 N/A
Non-sialosides
α2-3 Sialic acid
α2-6 Sialic acid
α2-8 Sialic acid
Galβ-NH2
GalββR2
GalββR1
Galα3Galβ4GlcNAcβR1
Galβ3GalNAcαR1
Galβ3GalNAcβR1
Galβ3GlcNAcβR1
Galβ4GlcβR1
Galβ4Glcβ-NH2
Galβ4GlcβR2
Galβ4GlcNAcβR1
Galβ4GlcNAcβ3Galβ4GlcβR1
Galβ4GlcNAc6SβR1
Gal6Sβ4(Fucα3)GlcNAcβR1
Gal6Sβ4(Fucα3)GlcNAc6SβR1
GalNAcαR1
Neu5Acα3Galβ3GalNAcαR1
Neu5Acα3Galβ3GalNAcβR1
Neu5Acα3Galβ3GlcNAcβR1
Neu5Acα3Galβ3GlcNAcβ3Galβ4GlcβR1
Neu5Acα3Galβ4GlcβR1
Neu5Acα3Galβ4GlcβR3
Neu5Acα3Galβ4GlcβR5
Neu5Acα3Galβ4GlcNAcβR1
Neu5Acα3Galβ4GlcNAcβR5
Neu5Acα3Galβ4GlcNAcβ3Galβ4GlcβR1
Neu5Acα3Galβ4GlcNAc6SβR1
Neu5Acα3Galβ(Fucα3)GlcNAcβR1
Neu5Acα3Galβ(Fucα3)GlcNAc6SβR1
Neu5Acα3Galβ4GlcNAcβ3Galβ4GlcβR1
Neu5Acα3Gal6Sβ4(Fucα3)GlcNAcβR1
Neu5Acα3Gal6Sβ4(Fucα3)GlcNAc6SβR1
Neu4,5Ac2α3Galβ3GalNAcαR1
Neu4,5Ac2α3Galβ3GalNAcβR1
Neu4,5Ac2α-3Galβ3GlcNAcαR1
Neu4,5Ac2α3Galβ3GlcNAcβR1
Neu4,5Ac2α3Galβ4GlcβR1
Neu4,5Ac2α3Galβ4GlcNAcβR1
Neu4,5Ac2α3Galβ4GlcNAcβ3Galβ4GlcβR1
Neu5,9Ac2α3GalβR1
Neu5,9Ac2α3Galβ3GalNAcαR1
Neu5,9Ac2α3Galβ3GalNAcβR1
Neu5,9Ac2α3Galβ3GlcNAcβR1
Neu5,9Ac2α3Galβ4GlcβR1
Neu5,9Ac2α3Galβ4GlcNAcβR1
Neu5,9Ac2α3Galβ4GlcNAcβ3Galβ4GlcβR1
Neu5Gcα3GalβR1
Neu5Gcα3Galβ3GalNAcαR1
Neu5Gcα3Galβ3GalNAcβR1
Neu5Gcα3Galβ3GlcNAcβR1
Neu5Gcα3Galβ3GlcNAcβ3Galβ4GlcβR1
Neu5Gcα3Galβ4GlcβR1
Neu5Gcα3Galβ4GlcNAcβR1
Neu5Gcα3Galβ4GlcNAcβ3Galβ4GlcβR1
Neu5Gcα3Galβ4GlcNAc6SβR1
Neu5Gcα3Galβ4(Fucα3)GlcNAcβR1
Neu5Gcα3Galβ4(Fucα3)GlcNAc6SβR1
Neu5Gcα3(β4GalNAc)Galβ4GlcβR1
Neu5Gcα3Gal6Sβ4(Fucα3)GlcNAcβR1
Neu5Gcα3Gal6Sβ4(Fucα3)GlcNAc6SβR1
Neu4Ac5Gcα3Galβ3GalNAcαR1
Neu4Ac5Gcα3Galβ3GalNAcβR1
Neu4Ac5Gcα3Galβ3GlcNAcαR1
Neu4Ac5Gcα3Galβ3GlcNAcβR1
Neu4Ac5Gcα3Galβ4GlcβR1
Neu4Ac5Gcα3Galβ4GlcNAcβR1
Neu4Ac5Gcα3Galβ4GlcNAcβ3Galβ4GlcβR1
Neu5Gc9Acα3GalβR1
Neu5Gc9Acα3Galβ3GalNAcαR1
Neu5Gc9Acα3Galβ3GalNAcβR1
Neu5Gc9Acα3Galβ3GlcNAcβR1
Neu5Gc9Ac3Galβ4GlcβR1
Neu5Gc9Acα3Galβ4GlcNAcβR1
Neu5Gc9Acα3Galβ4GlcNAcβ3Galβ4GlcβR1
Neu5Acα6GalβR1
Neu5Acα6Galβ4GlcβR1
Neu5Acα6Galβ4GlcβR5
Neu5Acα6Galβ4GlcNAcβR1
Neu5Acα6Galβ4GlcNAcβR5
Neu5Acα6GalNAcαR1
Neu5,9Ac2α6GalβR1
Neu5,9Ac2α6Galβ4GlcβR1
Neu5,9Ac2α6Galβ4GlcNAcβR1
Neu5,9Ac2α6GalNAcαR1
Neu5Gcα6GalβR1
Neu5Gcα6Galβ4GlcβR1
Neu5Gcα6Galβ4GlcNAcβR1
Neu5Gcα6GalNAcαR1
Neu5Gc9Acα6GalβR1
Neu5Gc9Ac6Galβ4GlcβR1
Neu5Gc9Acα6Galβ4GlcNAcβR1
Neu5Gc9Acα6GalNAcαR1
Neu5Acα8Neu5Acα3Galβ4GlcβR1
Neu5Acα8Neu5Acα3Galβ4GlcβR4
Neu5Acα8Neu5Acα3(β4GalNAc)Galβ4GlcβR1
Neu5Acα8Neu5Acα6Galβ4GlcβR1
Neu5Acα8Neu5Acα8Neu5Acα3Galβ4GlcβR1
Neu5Acα8Neu5Acα8Neu5Acα3Galβ4GlcβR4
Neu5Acα8Neu5Gcα3Galβ4GlcβR1
Neu5Acα8Neu5Gcα6Galβ4GlcβR1
Neu5Acα8Kdnα6Galβ4GlcβR1
Neu5Gcα8Neu5Acα3Galβ4GlcβR1
Neu5Gcα8Neu5Gcα3Galβ4GlcβR1
Neu5GcMeα8Neu5Acα3Galβ4GlcβR1

Figure S9. Sialoglycan microarray results of hCD22 and mCD22: The data shows that hCD22 and mCD22 lack the range and robustness of SNA, required in a probe for class of α2-6-linked sialoglycans. hCD22 (30 μg/ml) failed to recognize *N*-glycolyl Sias and Sias with *O*-acetyl substitutions. mCD22 (30 μg/ml) despite having more promising affinities and avidity than hCD22, but bound to few α2-3Sias and remained less selective than $SGRP6^{SNA}$, which is also the conventional probe for this class of sialoglycans. Sialoglycan microarray data for $SGRP6^{SNA}$ is same as presented in figure 1. Binding efficiencies are displayed in red for highest binding (saturated or 100%), blue for minimum or no binding (0%) and intermediate binding represented by colors ranging between blue (minimum) and red (maximum).

A

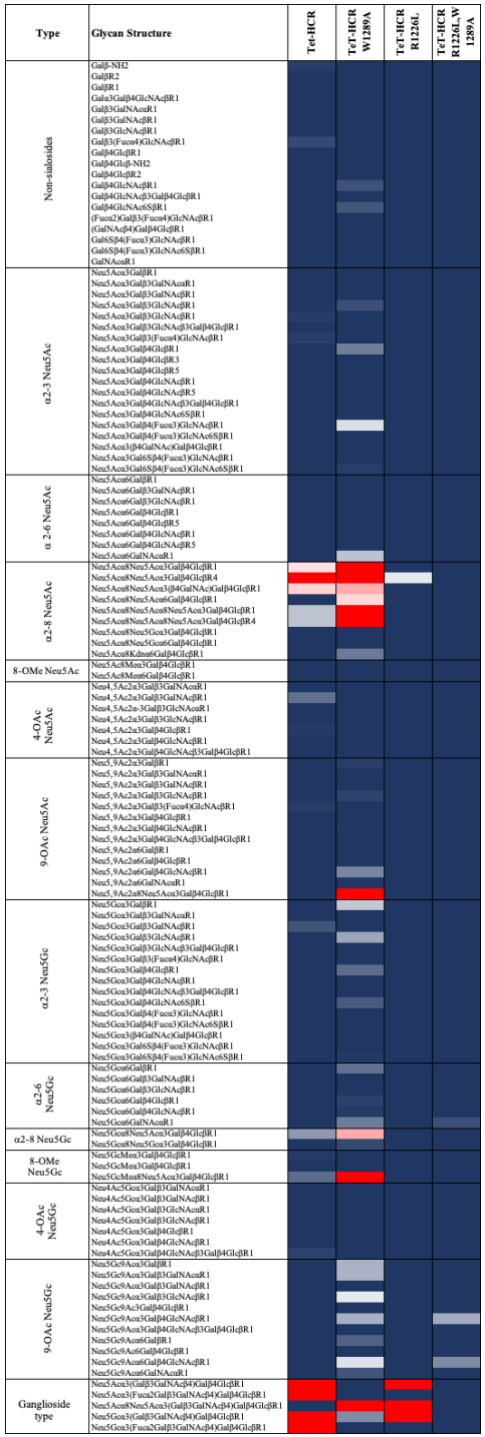
Type
Glycan Structure
Tet-HCR
TeT-HCR W1289A
TeT-HCR R1226L
TeT-HCR R1226L,W 1289A
Non-sialosides
α2-3 Neu5Ac
α 2-6 Neu5Ac
α2-8 Neu5Ac
8-OMe Neu5Ac
4-OAc Neu5Ac
9-OAc Neu5Ac
α2-3 Neu5Gc
α2-6 Neu5Gc
α2-8 Neu5Gc
8-OMe Neu5Gc
4-OAc Neu5Gc
9-OAc Neu5Gc
Ganglioside type

B

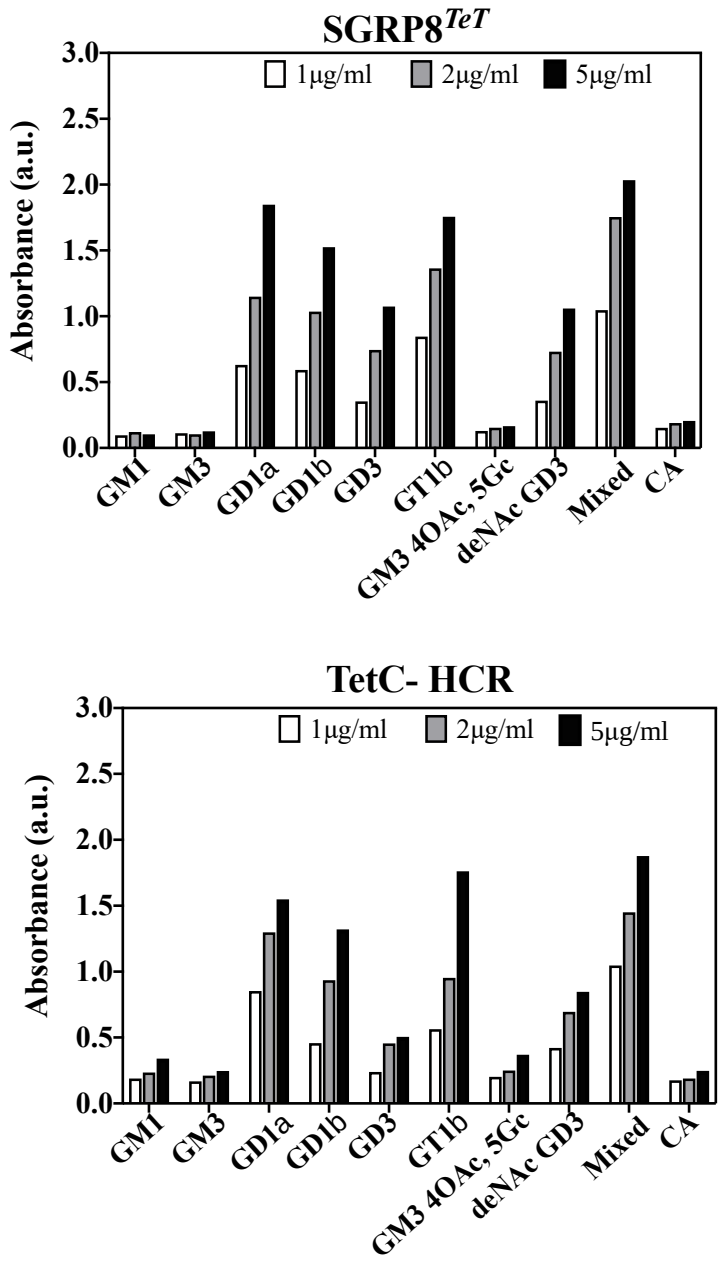
SGRP8TeT
1μg/ml
2μg/ml
5μg/ml
Absorbance (a.u.)
3.0
2.5
2.0
1.5
1.0
0.5
0.0
GM1
GM3
GD1a
GD1b
GD3
GT1b
GM3 4OAc, 5Gc
deNAc GD3
Mixed
CA
TetC- HCR
1μg/ml
2μg/ml
5μg/ml
Absorbance (a.u.)
GM1
GM3
GD1a
GD1b
GD3
GT1b
GM3 4OAc, 5Gc
deNAc GD3
Mixed
CA

Figure S10. Comparison of sialoglycan specificity between TeT-HCR variants. Sialoglycan microarray suggests better recognition of di-sia linkages by TeT-HCR W1289A than native TeT-HCR. The data also indicates towards negligible binding towards sialoglycans upon arginine substitutions at position 1226 with leucine, that further reduces when simultaneous substitutions of arginine (1226) and tryptophan (1289). All 4 proteins were tested at 30 μg/ml concentration and the results for TeT-HCR W1289A and TeT-HCR R1226L/W1289A are same as presented in Figure 1 and Suppl Fig S4. Binding efficiencies are displayed in red for highest binding (saturated or 100%), blue for minimum or no binding (0%) and intermediate binding represented by colors ranging between blue (minimum) and red (maximum). *Panel B* demonstrates the relative improvement in diSia specific binding in the W1289A mutant over TeT-HCR when tested with purified gangliosides, as described in methods section.

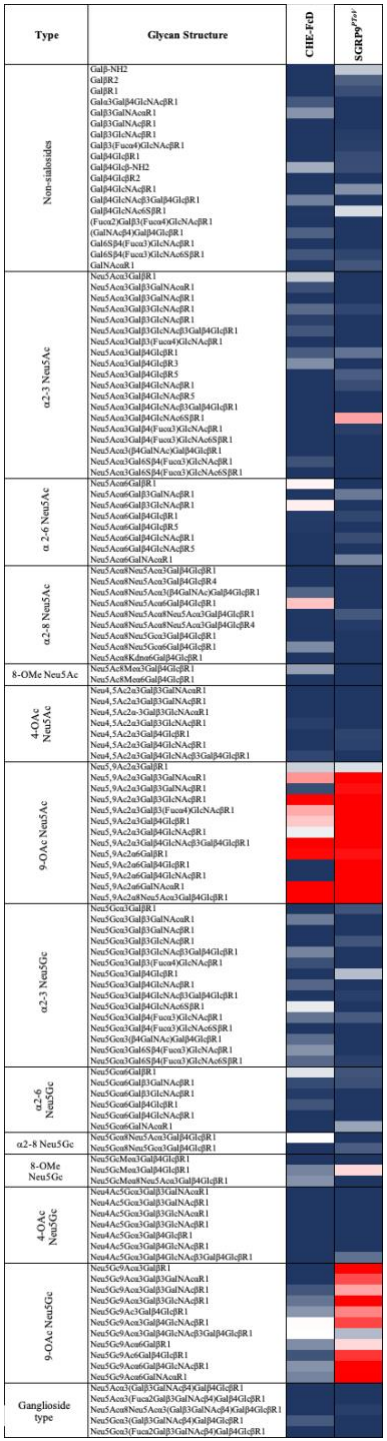
Type
Glycan Structure
CHE-FcD
SCRPsgGta1
Non-sialosides
Galβ-NH2
Galβ1R2
Galβ1R1
Galα3Galβ4GlcNAcβ1R1
Galβ3GalNAcα1R1
Galβ3GalNAcβ1R1
Galβ3GlcNAcβ1R1
Galβ3(Fucα4)GlcNAcβ1R1
Galβ4Glcβ1R1
Galβ4Glcβ-NH2
Galβ4Glcβ1R2
Galβ4GlcNAcβ1R1
Galβ4GlcNAcβ3Galβ4Glcβ1R1
Galβ4GlcNAc6Sβ1R1
(Fucα2)Galβ3(Fucα4)GlcNAcβ1R1
(GalNAcβ4)Galβ4Glcβ1R1
Galα6Sβ4(Fucα3)GlcNAcβ1R1
Galα6Sβ4(Fucα3)GlcNAc6Sβ1R1
GalNAcα1R1
α2-3 Neu5Ac
Neu5Acα3Galβ1R1
Neu5Acα3Galβ3GalNAcα1R1
Neu5Acα3Galβ3GalNAcβ1R1
Neu5Acα3Galβ3GlcNAcβ1R1
Neu5Acα3Galβ3GlcNAcβ1R1
Neu5Acα3Galβ3GlcNAcβ3Galβ4Glcβ1R1
Neu5Acα3Galβ3(Fucα4)GlcNAcβ1R1
Neu5Acα3Galβ4Glcβ1R1
Neu5Acα3Galβ4Glcβ1R3
Neu5Acα3Galβ4Glcβ1R5
Neu5Acα3Galβ4GlcNAcβ1R1
Neu5Acα3Galβ4GlcNAcβ1R5
Neu5Acα3Galβ4GlcNAcβ3Galβ4Glcβ1R1
Neu5Acα3Galβ4GlcNAc6Sβ1R1
Neu5Acα3Galβ4(Fucα3)GlcNAcβ1R1
Neu5Acα3Galβ4(Fucα3)GlcNAc6Sβ1R1
Neu5Acα3(β4GalNAcα)Galβ4Glcβ1R1
Neu5Acα3Gal6Sβ4(Fucα3)GlcNAcβ1R1
Neu5Acα3Gal6Sβ4(Fucα3)GlcNAc6Sβ1R1
α 2-6 Neu5Ac
Neu5Acα6Galβ1R1
Neu5Acα6Galβ3GalNAcβ1R1
Neu5Acα6Galβ3GlcNAcβ1R1
Neu5Acα6Galβ4Glcβ1R1
Neu5Acα6Galβ4Glcβ1R5
Neu5Acα6Galβ4GlcNAcβ1R1
Neu5Acα6Galβ4GlcNAcβ1R5
Neu5Acα6GalNAcα1R1
α2-8 Neu5Ac
Neu5Acα8Neu5Acα3Galβ4Glcβ1R1
Neu5Acα8Neu5Acα3Galβ4Glcβ1R4
Neu5Acα8Neu5Acα3(β4GalNAcα)Galβ4Glcβ1R1
Neu5Acα8Neu5Acα6Galβ4Glcβ1R1
Neu5Acα8Neu5Acα8Neu5Acα3Galβ4Glcβ1R1
Neu5Acα8Neu5Acα8Neu5Acα3Galβ4Glcβ1R4
Neu5Acα8Neu5Gcα3Galβ4Glcβ1R1
Neu5Acα8Neu5Gcα6Galβ4Glcβ1R1
Neu5Acα8Kdnα6Galβ4Glcβ1R1
8-OMe Neu5Ac
Neu5Ac8Meα3Galβ4Glcβ1R1
Neu5Ac8Meα6Galβ4Glcβ1R1
4-OAc Neu5Ac
Neu4,5Ac2α3Galβ3GalNAcα1R1
Neu4,5Ac2α3Galβ3GalNAcβ1R1
Neu4,5Ac2α-3Galβ3GlcNAcα1R1
Neu4,5Ac2α3Galβ3GlcNAcβ1R1
Neu4,5Ac2α3Galβ4Glcβ1R1
Neu4,5Ac2α3Galβ4GlcNAcβ1R1
Neu4,5Ac2α3Galβ4GlcNAcβ3Galβ4Glcβ1R1
9-OAc Neu5Ac
Neu5,9Ac2α3Galβ1R1
Neu5,9Ac2α3Galβ3GalNAcα1R1
Neu5,9Ac2α3Galβ3GalNAcβ1R1
Neu5,9Ac2α3Galβ3GlcNAcβ1R1
Neu5,9Ac2α3Galβ3(Fucα4)GlcNAcβ1R1
Neu5,9Ac2α3Galβ4Glcβ1R1
Neu5,9Ac2α3Galβ4GlcNAcβ1R1
Neu5,9Ac2α3Galβ4GlcNAcβ3Galβ4Glcβ1R1
Neu5,9Ac2α6Galβ1R1
Neu5,9Ac2α6Galβ4Glcβ1R1
Neu5,9Ac2α6Galβ4GlcNAcβ1R1
Neu5,9Ac2α6GalNAcα1R1
Neu5,9Ac2α8Neu5Acα3Galβ4Glcβ1R1
α2-3 Neu5Gc
Neu5Gcα3Galβ1R1
Neu5Gcα3Galβ3GalNAcα1R1
Neu5Gcα3Galβ3GalNAcβ1R1
Neu5Gcα3Galβ3GlcNAcβ1R1
Neu5Gcα3Galβ3GlcNAcβ3Galβ4Glcβ1R1
Neu5Gcα3Galβ3(Fucα4)GlcNAcβ1R1
Neu5Gcα3Galβ4Glcβ1R1
Neu5Gcα3Galβ4GlcNAcβ1R1
Neu5Gcα3Galβ4GlcNAcβ3Galβ4Glcβ1R1
Neu5Gcα3Galβ4GlcNAc6Sβ1R1
Neu5Gcα3Galβ4(Fucα3)GlcNAcβ1R1
Neu5Gcα3Galβ4(Fucα3)GlcNAc6Sβ1R1
Neu5Gcα3(β4GalNAcα)Galβ4Glcβ1R1
Neu5Gcα3Gal6Sβ4(Fucα3)GlcNAcβ1R1
Neu5Gcα3Gal6Sβ4(Fucα3)GlcNAc6Sβ1R1
α2-6 Neu5Gc
Neu5Gcα6Galβ1R1
Neu5Gcα6Galβ3GalNAcβ1R1
Neu5Gcα6Galβ3GlcNAcβ1R1
Neu5Gcα6Galβ4Glcβ1R1
Neu5Gcα6Galβ4GlcNAcβ1R1
Neu5Gcα6GalNAcα1R1
α2-8 Neu5Gc
Neu5Gcα8Neu5Acα3Galβ4Glcβ1R1
Neu5Gcα8Neu5Gcα3Galβ4Glcβ1R1
8-OMe Neu5Gc
Neu5Gc8Meα3Galβ4Glcβ1R1
Neu5Gc8Meα3Galβ4Glcβ1R1
Neu5Gc8Meα8Neu5Acα3Galβ4Glcβ1R1
4-OAc Neu5Gc
Neu4Ac5Gcα3Galβ3GalNAcα1R1
Neu4Ac5Gcα3Galβ3GalNAcβ1R1
Neu4Ac5Gcα3Galβ3GlcNAcα1R1
Neu4Ac5Gcα3Galβ3GlcNAcβ1R1
Neu4Ac5Gcα3Galβ4Glcβ1R1
Neu4Ac5Gcα3Galβ4GlcNAcβ1R1
Neu4Ac5Gcα3Galβ4GlcNAcβ3Galβ4Glcβ1R1
9-OAc Neu5Gc
Neu5Gc9Acα3Galβ1R1
Neu5Gc9Acα3Galβ3GalNAcα1R1
Neu5Gc9Acα3Galβ3GalNAcβ1R1
Neu5Gc9Acα3Galβ3GlcNAcβ1R1
Neu5Gc9Ac3Galβ4Glcβ1R1
Neu5Gc9Acα3Galβ4GlcNAcβ1R1
Neu5Gc9Acα3Galβ4GlcNAcβ3Galβ4Glcβ1R1
Neu5Gc9Acα6Galβ1R1
Neu5Gc9Ac6Galβ4Glcβ1R1
Neu5Gc9Acα6Galβ4GlcNAcβ1R1
Neu5Gc9Acα6GalNAcα1R1
Ganglioside type
Neu5Acα3(Galβ3GalNAcβ4Galβ4Glcβ1R1
Neu5Acα3(Fucα2Galβ3GalNAcβ4)Galβ4Glcβ1R1
Neu5Acα8Neu5Acα3(Galβ3GalNAcβ4Galβ4Glcβ1R1
Neu5Gcα3(Galβ3GalNAcβ4Galβ4Glcβ1R1
Neu5Gcα3(Fucα2Galβ3GalNAcβ4Galβ4Glcβ1R1

Figure S11. Comparison of sialoglycan specificity between CHE-FcD and SGRP9^{PToV}: Sialoglycan microarray results shows more predominant recognition of 9-OAc-Sias by SGRP9^{PToV} than previously known probe CHE-FcD for this class of sialoglycans. Both probes were tested at 30 μg/ml. SGRP9^{PToV} results used for comparison here, are the same as shown in Figure 1. Binding efficiencies are displayed in red for highest binding (saturated or 100%), blue for minimum or no binding (0%) and intermediate binding represented by colors ranging between blue (minimum) and red (maximum).

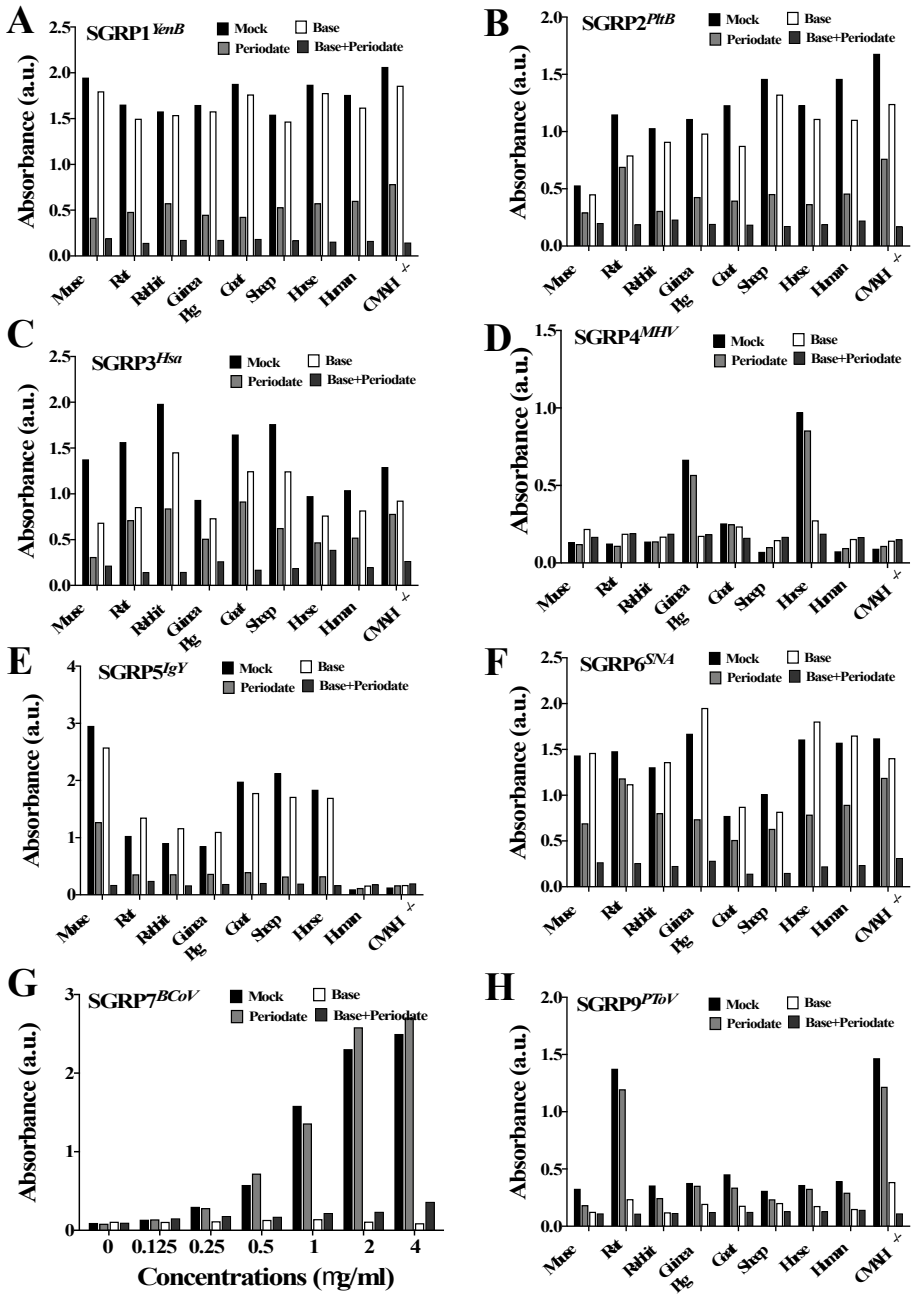
A
SGRP1 YenB
B
SGRP2 PtfB
C
SGRP3 Hsa
D
SGRP4 MHV
E
SGRP5 IgY
F
SGRP6 SNA
G
SGRP7 BCoV
H
SGRP9 PToV
Mock
Base
Periodate
Base+Periodate
Absorbance (a.u.)
Concentrations (mg/ml)
0
0.125
0.25
0.5
1
2
4
Muse
Rat
Rbbit
Guinea Pig
Cat
Sheep
Hrse
Hmn
CMH1 +

Figure S12. SGRPs confirmed their efficacy to bind target sialoglycans without any binding with serum glycoproteins: SGRPs 1, 2, 3, 5, and 6 exhibited their binding to serum sialoglycan that varied corresponding to depletion in Sia, while SGRP4^{MHV}, SGRP7^{BCoV} and SGRP9^{PToV} have exclusive affinity for their O-Ac-ligands. Mild periodate and base treatments were used to generate Sia and O-Ac-depleted samples for ELISA experiments.

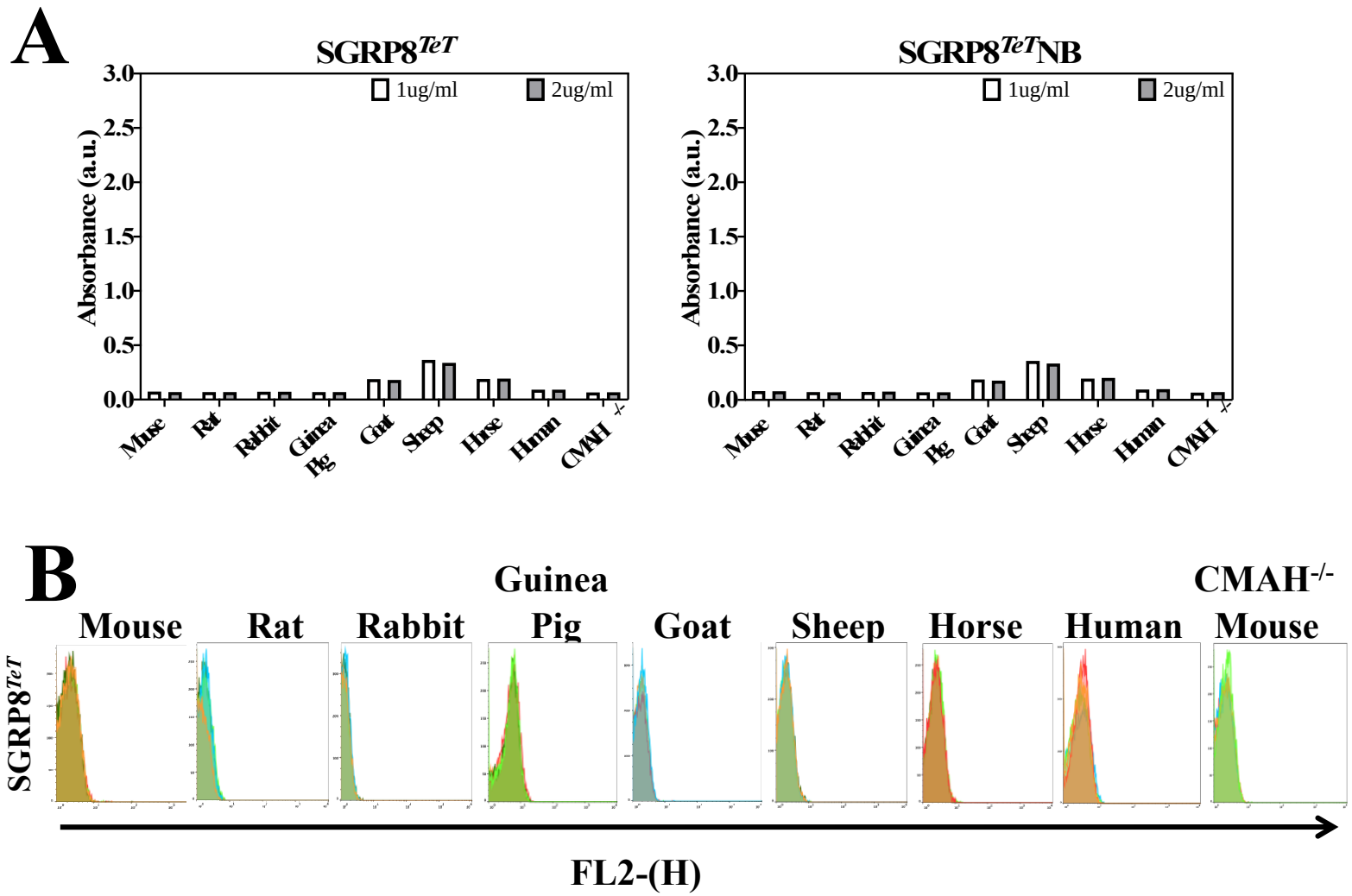

Figure S13. SGRP8^{TeT} does not exhibit nonspecific binding to serum contents, or on erythrocytes: Figure demonstrates the no binding to SGRP8TeT to tested sera (Panel A) and erythrocytes from 9 mammalian sources (Panel B). SGRP8^{TeT} ELISA with mammalian serum suggest that SGRP8^{TeT} can does not exhibit any affinity for diverse sialoglycan population present in mammalian samples. Also, the results confirm that SGRP8TeT and its nonbinding mutant do not possess any preferential binding towards protein structures in general, highlighting their utility in exclusive recognition of di-sia-linkages.

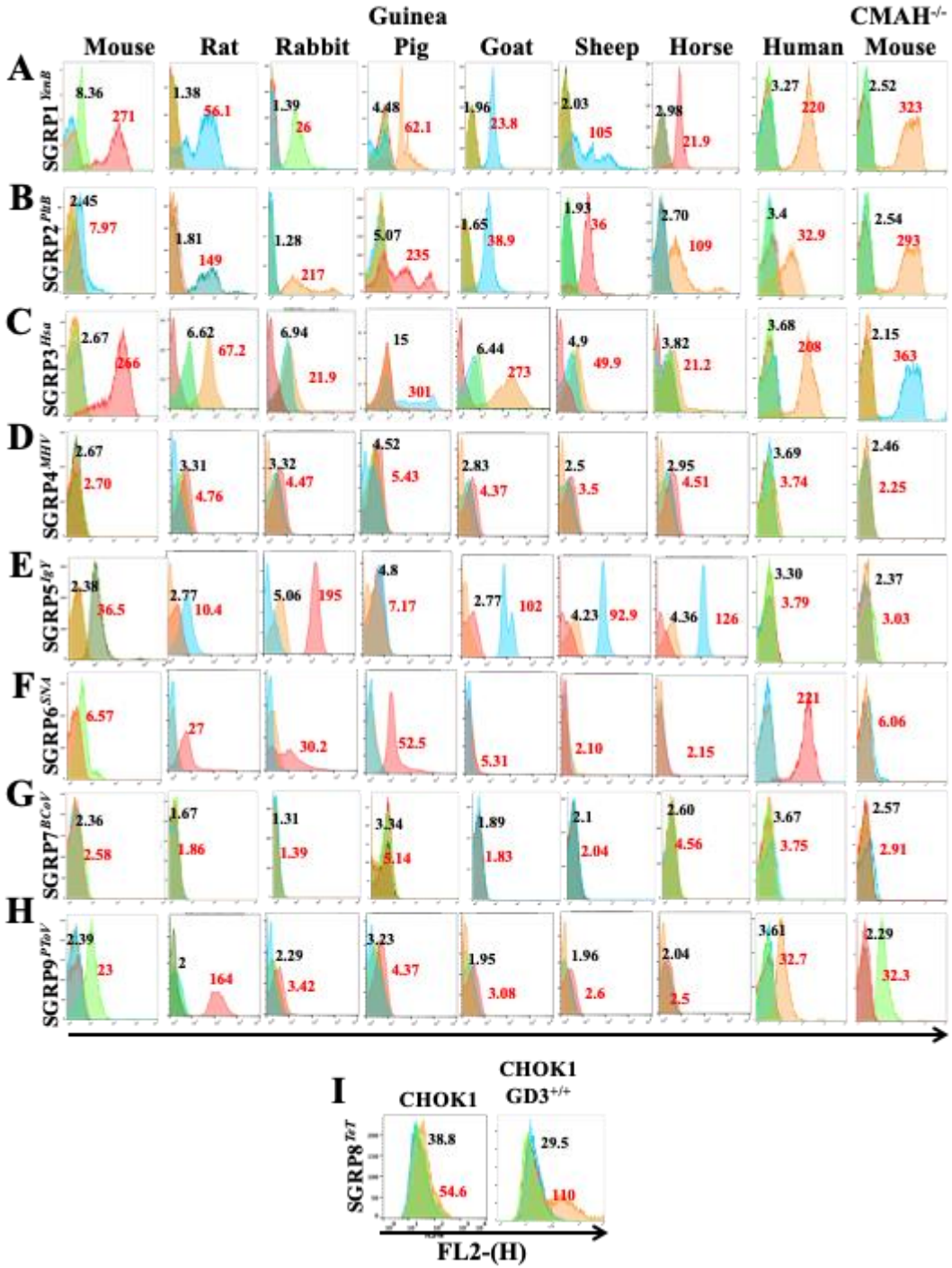
Mouse
Rat
Rabbit
Guinea Pig
Goat
Sheep
Horse
Human
CMAH-/- Mouse
A
SGRP1 VenB
8.36
271
1.38
56.1
1.39
26
4.48
62.1
1.96
23.8
2.03
105
2.98
21.9
3.27
220
2.52
323
B
SGRP2 PhiB
2.45
7.97
1.81
149
1.28
217
5.07
235
1.65
38.9
1.93
36
2.70
109
3.4
32.9
2.54
293
C
SGRP3 Hsa
2.67
266
6.62
67.2
6.94
21.9
15
301
6.44
273
4.9
49.9
3.82
21.2
3.68
208
2.15
363
D
SGRP4 MHV
2.67
2.70
3.31
4.76
3.32
4.47
4.52
5.43
2.83
4.37
2.5
3.5
2.95
4.51
3.69
3.74
2.46
2.25
E
SGRP5 IgV
2.38
36.5
2.77
10.4
5.06
195
4.8
7.17
2.77
102
4.23
92.9
4.36
126
3.30
3.79
2.37
3.03
F
SGRP6 SNA
6.57
27
30.2
52.5
5.31
2.10
2.15
221
6.06
G
SGRP7 BCoV
2.36
2.58
1.67
1.86
1.31
1.39
3.34
5.14
1.89
1.83
2.1
2.04
2.60
4.56
3.67
3.75
2.57
2.91
H
SGRP9 PToV
2.39
23
2
164
2.29
3.42
3.23
4.37
1.95
3.08
1.96
2.6
2.04
2.5
3.61
32.7
2.29
32.3
I
CHOK1
CHOK1 GD3+/+
SGRP8 ToT
38.8
54.6
29.5
110
FL2-(H)

Figure S14. SGRPs recognize Specific sialoglycans on mammalian erythrocytes: The panels, as marked in figure represent SGRPs binding with RBCs for 9 animal sources. The mean fluorescence intensities (MFI) values for SGRPs; binding and non-binding versions are mentioned for each type of erythrocyte. Panel A represents SGRP1^{YenB} (5 μg/ml) binding with all tested RBCs. Panel B represents SGRP2^{PltB} (5 μg/ml) binding with RBCs in accordance to the fractional representation of Neu5Ac-sialoglycans. Panel C shows SGRP3^{Hsa} (5 μg/ml) binding with all RBCs, while Panel D suggest SGRP4^{MHV} does not specifically bind to RBCs, suggesting lack of its ligand. SGRP5^{IgY} (2 μg/ml) binds prominently with all RBCs except rat and guinea pig (Panel E) while SGRP6^{SNA} (2 μg/ml) lacks binding to goat, sheep and horse RBCs (Panel F). Panel G suggest the RBCs do not express SGRP7^{BCoV}'s specific ligand 7,9-diOAc-Sias, resulting into negligible binding of the probe (5 μg/ml). Panel H shows SGRP9^{PToV} (5 μg/ml) affinity towards surface glycans terminating in 9-OAc-Sias on RBC surfaces. Panel I represent significantly enhanced binding of SGRP8TeT (5 μg/ml) towards disialogangliosides expressed by GD3 transfected CHO cell in comparison to native CHOK1 cells. MFIs of binding probes are marked in RED, while MFIs for non-binding versions are shown in BLACK in each panel.

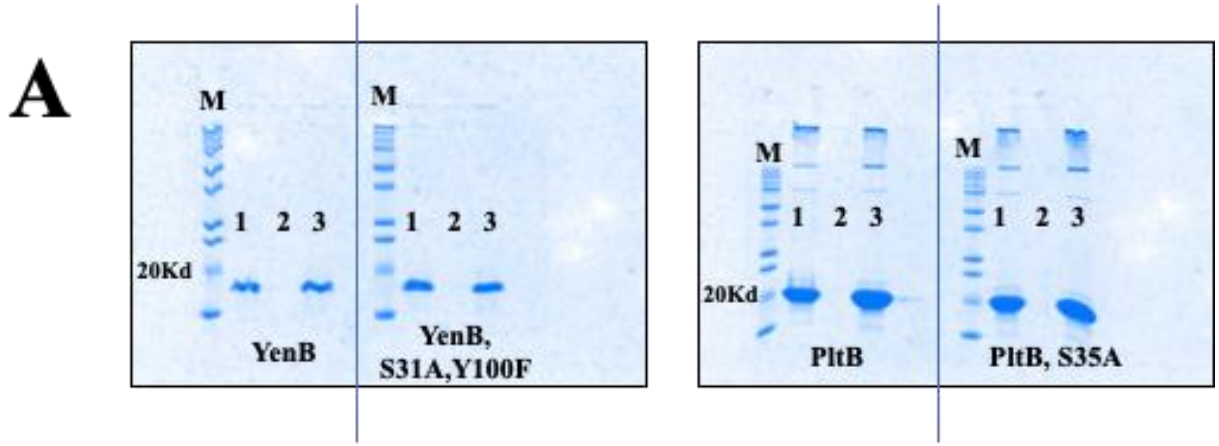
A
M
1 2 3
20Kd
YenB
M
1 2 3
YenB,
S31A,Y100F
M
1 2 3
20Kd
PltB
M
1 2 3
PltB, S35A

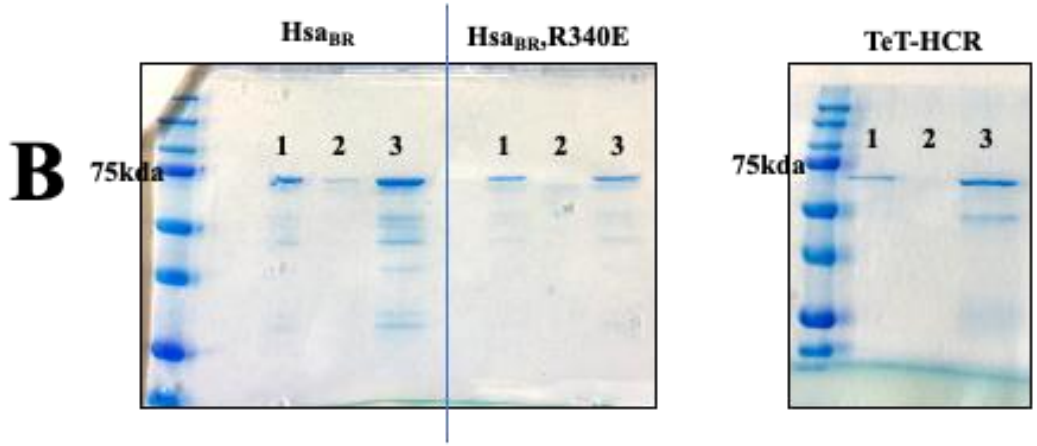
B
Hsa$_{BR}$
Hsa$_{BR}$,R340E
75kda
1 2 3 1 2 3
TeT-HCR
75kda
1 2 3

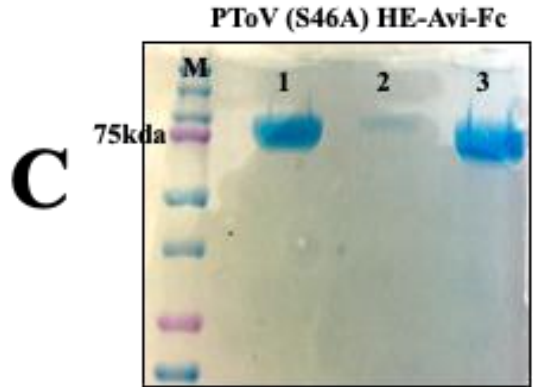
C
PToV (S46A) HE-Avi-Fc
M
75kda
1 2 3

Figure S15. Assays to confirm efficiency of biotinylation of proteins. Figure demonstrates the high efficiency of biotinylation of proteins by streptavidin-beads pull down assay in order to derive final biotinylated SGRPs. *Panel A* displays the efficacy of NHS-biotin tagging using examples of YenB and its non-binding mutant, and PltB and its non-binding mutant (set of SGRP1 and 2). *Panel B* displays the efficacy of SNAP tag biotinylation using examples of HsaBr and TeT-HCR (SGRP3 and 8). *Panel C* shows the efficacy of Avi-tag biotinylation using examples of PToV-HE-Avi-Fc (SGRP9). Lanes marked 1 indicates the biotinylated protein pulled down from streptavidin beads, lane 2 indicates the non-biotinylated protein incubated and pulled down from SA-beads (mock) and lane 3 is the initial amount of protein as reference. A comparison between Lane 1 and 3 suggest towards fraction of protein tagged with biotin out of total amount taken. Lane 2 serves as reference of goodness of experiment.

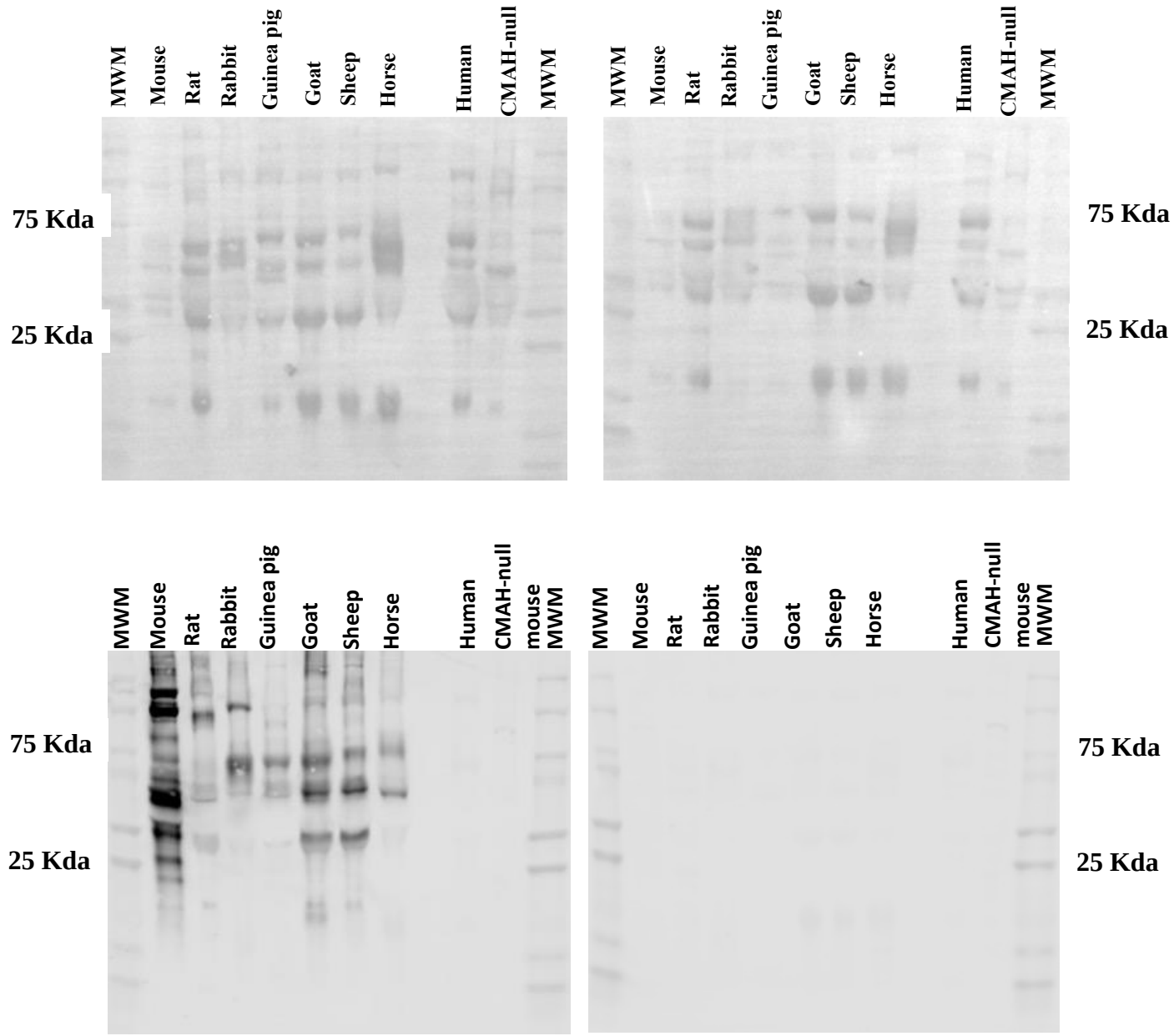

Figure S16. Ponceau S staining of western blots and their corresponding probing with SGRP5^{IgY} and SGRP5^{IgY}NB.

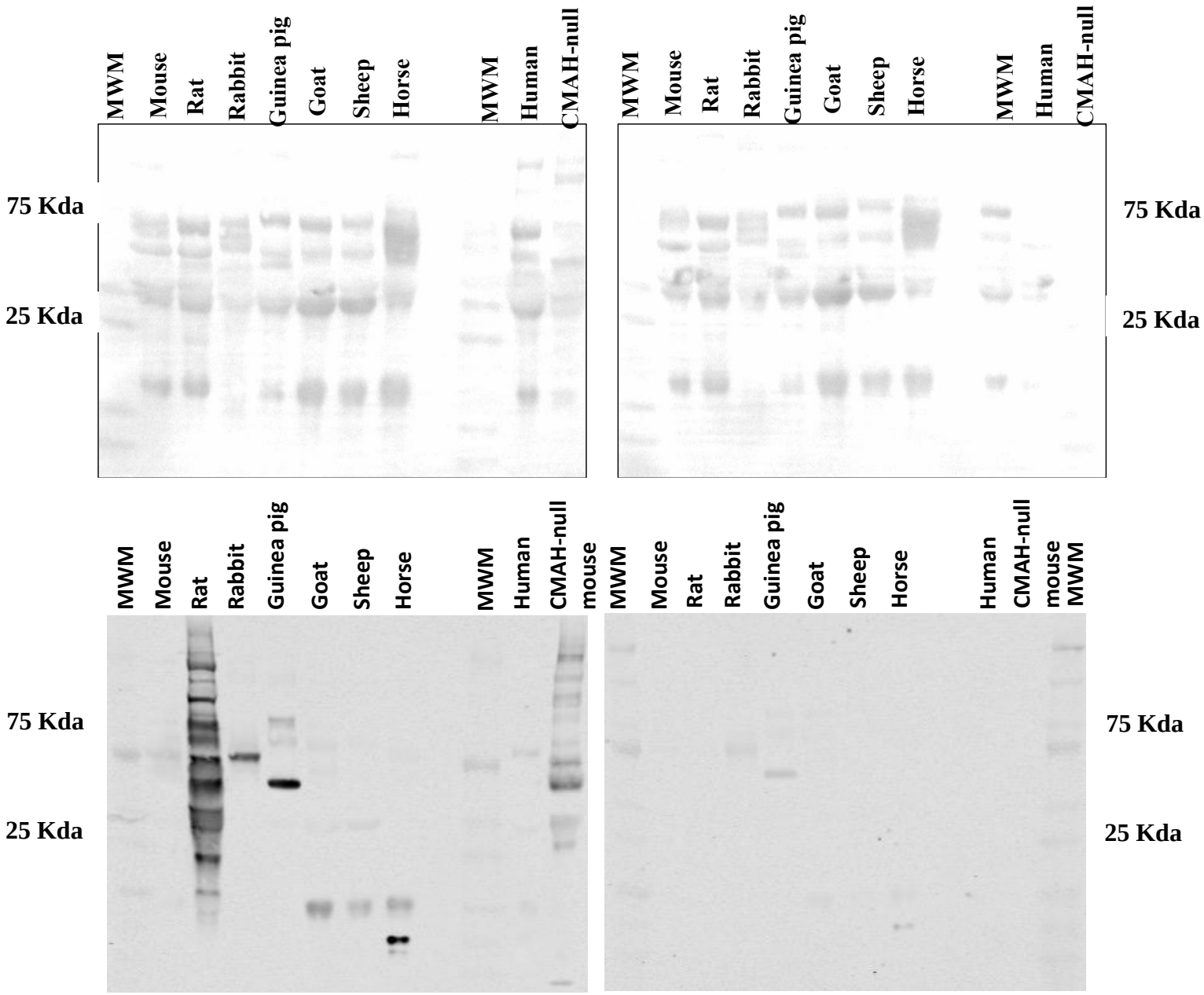

Figure S17. Ponceau S staining of western blots and their corresponding probing with SGRP9^{PToV} and SGRP9^{PToV}NB.

Supporting Information S18
FASTA Sequences of proteins characterized as SGRPs

SGRP1^{YenB} – YESubB WT (pBad18)

MAIMKIKAIALASLLVSSVTSAAMKDYDTYYSNVIINNFSSGVYNSGGKDTTFFCIGYTR
VGNKPDINNACKVDVYGKYKNGFSAMMDTAKFYYSTGLQVRVYIKKDVWYDPAFRTGFSA
NELIAITSCSSHDYCVGPKLKHHHHHH

SGRP1^{YenB}NB – YESubB S31A;Y100F (pBad18)

MAIMKIKAIALASLLVSSVTSAAMKDYDTYYANVIINNFSSGVYNSGGKDTTFFCIGYTR
VGNKPDINNACKVDVYGKYKNGFSAMMDTAKFYYSTGLQVRVFIKKDVWYDPAFRTGFSA
NELIAITSCSSHDYCVGPKLKHHHHHH

SGRP2^{PltB} – PltB WT (pET28b)

M Y M S K Y V P V Y T L L I L I Y S F N A S A E W T G D N T N A Y Y S D E V I S E L H V G Q I D T S P Y F C I K T V K A N G S G T P
V V A C A V S K Q S I W A P S F K E L L D Q A R Y F Y S T G Q S V R I H V Q K N I W T Y P L F V N T F S A N A L V G L S S C S A T Q
C F G P K K L A A A L E H H H H H H

SGRP2^{PltB}NB – PltB S35A (pET28b)

M Y M S K Y V P V Y T L L I L I Y S F N A S A E W T G D N T N A Y Y A D E V I S E L H V G Q I D T S P Y F C I K T V K A N G S G T P
V V A C A V S K Q S I W A P S F K E L L D Q A R Y F Y S T G Q S V R I H V Q K N I W T Y P L F V N T F S A N A L V G L S S C S A T Q
C F G P K K L A A A L E H H H H H H Stop

SGRP3^{Hsa} – hsaBR (pGEX-3X_SNAPf-His6)

S L N T N Q S V S A R N Q N A R V R T R R A V A A N D T E A P Q V K S G D Y V V Y R G E S F E Y Y A E I T D N S G Q V N R V V I R
N V E G G A N S T Y L S P N W V K Y S T E N L G R P G N A T V Q N P L R T R I F G E V P L N E I V N E K S Y Y T R Y I V A W D P S G
N A T Q M V D N A N R N G L E R F V L T V K S Q N E K Y D P A D P S V T Y V N N L S N L S T S E R E A V A A A V R A A N P N I P P
T A K I T V S Q N G T V T I T Y P D K S T D T I P A N R V V K D L Q I S K S N S N S T M D K D C E M K R T T L D S P L G K L E L S G C

E Q G L H R I I F L G K G T S A A D A V E V P A P A A V L G G P E P L M Q A T A W L N A Y F H Q P E A I E E F P V P A L H H P V F Q
Q E S F T R Q V L W K L L K V V K F G E V I S Y S H L A A L A G N P A A T A A V K T A L S G N P V P I L I P C H R V V Q G D L D V G
G Y E G G L A V K E W L L A H E G H R L G K P G L G P A G G S H H H H H H

SGRP3^{Hsa}NB – hsaBR R340E (pGEX-3X_SNAPf-His6)

S L N T N Q S V S A R N Q N A R V R T R R A V A A N D T E A P Q V K S G D Y V V Y R G E S F E Y Y A E I T D N S G Q V N R V V I R
N V E G G A N S T Y L S P N W V K Y S T E N L G R P G N A T V Q N P L R T R I F G E V P L N E I V N E K S Y Y T E Y I V A W D P S G
N A T Q M V D N A N R N G L E R F V L T V K S Q N E K Y D P A D P S V T Y V N N L S N L S T S E R E A V A A A V R A A N P N I P P
T A K I T V S Q N G T V T I T Y P D K S T D T I P A N R V V K D L Q I S K S N S N S T M D K D C E M K R T T L D S P L G K L E L S G C
E Q G L H R I I F L G K G T S A A D A V E V P A P A A V L G G P E P L M Q A T A W L N A Y F H Q P E A I E E F P V P A L H H P V F Q
Q E S F T R Q V L W K L L K V V K F G E V I S Y S H L A A L A G N P A A T A A V K T A L S G N P V P I L I P C H R V V Q G D L D V G
G Y E G G L A V K E W L L A H E G H R L G K P G L G P A G G S H H H H H H

SGRP4^{MHV} – MHV-S HE_Fc S45A Avitag_(pcDNA3.1)

M P M G S L Q P L A T L Y L L G M L V A S V L A F N E P L N I V S H L N D D W F L F G D A R S D C T Y V E N N G H P K L D W L D L
D P K L C N S G R I S A K S G N S L F R S F H F I D F Y N Y S G E G D Q V I F Y E G V N F S P S H G F K C L A Y G D N K R W M G N K
A R F Y A R V Y E K M A Q Y R S L S F V N V S Y A Y G G N A K P T S I C K D K T L T L N N P T F I S K E S N Y V D Y Y Y E S E A N F
T L Q G C D E F I V P L C V F N G H S K G S S S D P A N K Y Y T D S Q S Y Y N M D T G V L Y G F N S T L D V G N T V Q N P G L D L
T C R Y L A L T P G N Y K A V S L E Y L L S L P S K A I C L R K P K S F M P V Q V V D S R W N S T R Q S D N M T A V A C Q L P Y C F
F R N T S A D Y S G G T H D V H H G D F H F R Q L L S G L L Y N V S C I A Q Q G A F V Y N N V S S S W P A Y G G Y G H C P T A A N I
G Y M A P V C I Y D L V P R G S D K T H T C P P C P A P E L L G G P S V F L F P P K P K D T L M I S R T P E V T C V V V D V S H E D P
E V K F N W Y V D G V E V H N A K T K P R E E Q Y N S T Y R V V S V L T V L H Q D W L N G K E Y K C K V S N K A L P A P I E K T I
S K A K G Q P R E P Q V Y T L P P S R E E M T K N Q V S L T C L V K G F Y P S D I A V E W E S N G Q P E N N Y K T T P P V L D S D G
S F F L Y S K L T V D K S R W Q Q G N V F S C S V M H E A L H N H Y T Q K S L S L S P G K K L G G G S G L N D I F E A Q K I E W H E

SGRP4^{MHV}NB – MHV-S HE_Fc S45A;F121A_Avitag (pcDNA3.1)

M P M G S L Q P L A T L Y L L G M L V A S V L A F N E P L N I V S H L N D D W F L F G D A R S D C T Y V E N N G H P K L D W L D L
D P K L C N S G R I S A K S G N S L F R S F H F I D F Y N Y S G E G D Q V I F Y E G V N F S P S H G F K C L A Y G D N K R W M G N K
A R F Y A R V Y E K M A Q Y R S L S F V N V S Y A Y G G N A K P T S I C K D K T L T L N N P T F I S K E S N Y V D Y Y Y E S E A N F
T L Q G C D E F I V P L C V A N G H S K G S S S D P A N K Y Y T D S Q S Y Y N M D T G V L Y G F N S T L D V G N T V Q N P G L D L
T C R Y L A L T P G N Y K A V S L E Y L L S L P S K A I C L R K P K S F M P V Q V V D S R W N S T R Q S D N M T A V A C Q L P Y C F

F R N T S A D Y S G G T H D V H H G D F H F R Q L L S G L L Y N V S C I A Q Q G A F V Y N N V S S S W P A Y G Y G H C P T A A N I
G Y M A P V C I Y D L V P R G S D K T H T C P P C P A P E L L G G P S V F L F P P K P K D T L M I S R T P E V T C V V V D V S H E D P
E V K F N W Y V D G V E V H N A K T K P R E E Q Y N S T Y R V V S V L T V L H Q D W L N G K E Y K C K V S N K A L P A P I E K T I
S K A K G Q P R E P Q V Y T L P P S R E E M T K N Q V S L T C L V K G F Y P S D I A V E W E S N G Q P E N N Y K T T P P V L D S D G
S F F L Y S K L T V D K S R W Q Q G N V F S C S V M H E A L H N H Y T Q K S L S L S P G K K L G G G S G L N D I F E A Q K I E W H E

SGRP7^{BCoV} – BCoV HE_Fc_S40A_His 6-Avi (pFastBac1)

M V S A I V L Y V L L A A A A H S A F A A E F D N P P T N V V S H L N G D W F L F G D A R S D C N H V V N T N P R N Y S Y M D L N
P A L C D S G K I S S K A G N S I F R S F H F T D F Y N Y T G E G Q Q I I F Y E G V N F T P Y H A F K C T T S G S N D I W M Q N K G L
F Y T Q V Y K N M A V Y R S L T F V N V P Y V Y N G S A Q S T A L C K S G S L V L N N P A Y I A R E A N F G D Y Y Y K V E A D F Y
L S G C D E Y I V P L C I F N G K F L S N T K Y Y D D S Q Y Y F N K D T G V I Y G L N S T E T I T T G F D F N C H Y L V L P S G N Y L
A I S N E L L L T V P T K A I C L N K R K D F T P V Q V V D S R W N N A R Q S D N M T A V A C Q P P Y C Y F R N S T T N Y V G V Y
D I N H G D A G F T S I L S G L L Y D S P C F S Q Q G V F R Y D N V S S V W P L Y S Y G R C P T A A D I N T P D V P I C V Y D L V P R
G S D K T H T C P P C P A P E L L G G P S V F L F P P K P K D T L M I S R T P E V T C V V V D V S H E D P E V K F N W Y V D G V E V
H N A K T K P R E E Q Y N S T Y R V V S V L T V L H Q D W L N G K E Y K C K V S N K A L P A P I E K T I S K A K G Q P R E P Q V Y
T L P P S R E E M T K N Q V S L T C L V K G F Y P S D I A V E W E S N G Q P E N N Y K T T P P V L D S D G S F F L Y S K L T V D K S
R W Q Q G N V F S C S V M H E A L H N H Y T Q K S L S L S P G K H H H H H H R I P G K L P A G G G L N D I F E A Q K I E W H E

SGRP7^{BCoV}NB – BC0V HE_Fc_ S40A;F211A_His 6-Avi (pFastBac1)

M V S A I V L Y V L L A A A A H S A F A A E F D N P P T N V V S H L N G D W F L F G D A R S D C N H V V N T N P R N Y S Y M D L N
P A L C D S G K I S S K A G N S I F R S F H F T D F Y N Y T G E G Q Q I I F Y E G V N F T P Y H A F K C T T S G S N D I W M Q N K G L
F Y T Q V Y K N M A V Y R S L T F V N V P Y V Y N G S A Q S T A L C K S G S L V L N N P A Y I A R E A N F G D Y Y Y K V E A D F Y
L S G C D E Y I V P L C I F N G K A L S N T K Y Y D D S Q Y Y F N K D T G V I Y G L N S T E T I T T G F D F N C H Y L V L P S G N Y L
A I S N E L L L T V P T K A I C L N K R K D F T P V Q V V D S R W N N A R Q S D N M T A V A C Q P P Y C Y F R N S T T N Y V G V Y
D I N H G D A G F T S I L S G L L Y D S P C F S Q Q G V F R Y D N V S S V W P L Y S Y G R C P T A A D I N T P D V P I C V Y D L V P R
G S D K T H T C P P C P A P E L L G G P S V F L F P P K P K D T L M I S R T P E V T C V V V D V S H E D P E V K F N W Y V D G V E V
H N A K T K P R E E Q Y N S T Y R V V S V L T V L H Q D W L N G K E Y K C K V S N K A L P A P I E K T I S K A K G Q P R E P Q V Y
T L P P S R E E M T K N Q V S L T C L V K G F Y P S D I A V E W E S N G Q P E N N Y K T T P P V L D S D G S F F L Y S K L T V D K S
R W Q Q G N V F S C S V M H E A L H N H Y T Q K S L S L S P G K H H H H H H R I P G K L P A G G G L N D I F E A Q K I E W H E

SGRP8^{TeT} -Tetanus Toxin SNAPf-His6 (pGEX-3X)

Y T S Y L S I T F L R D F W G N P L R Y D T E Y Y L I P V A S S S K D V Q L K N I T D Y M Y L T N A P S Y T N G K L N I Y Y R R L Y
N G L K F I I K R Y T P N N E I D S F V K S G D F I K L Y V S Y N N N E H I V G Y P K D G N A F N N L D R I L R V G Y N A P G I P L Y
K K M E A V K L R D L K T Y S V Q L K L Y D D K N A S L G L V G T H N G Q I G N D P N R D I L I A S N W Y F N H L K D K I L G C D
W Y F V P T D E G W T N D G G G G S M D K D C E M K R T T L D S P L G K L E L S G C E Q G L H R I I F L G K G T S A A D A V E V P
A P A A V L G G P E P L M Q A T A W L N A Y F H Q P E A I E E F P V P A L H H P V F Q Q E S F T R Q V L W K L L K V V K F G E V I S
Y S H L A A L A G N P A A T A A V K T A L S G N P V P I L I P C H R V V Q G D L D V G G Y E G G L A V K E W L L A H E G H R L G K
P G L G P A G G S H H H H H H

SGRP8^{TeT}NB -Tetanus Toxin W1289A_SNAPf-His6 (pGEX-3X)

Y T S Y L S I T F L R D F W G N P L R Y D T E Y Y L I P V A S S S K D V Q L K N I T D Y M Y L T N A P S Y T N G K L N I Y Y R R L Y
N G L K F I I K R Y T P N N E I D S F V K S G D F I K L Y V S Y N N N E H I V G Y P K D G N A F N N L D R I L L V G Y N A P G I P L Y
K K M E A V K L R D L K T Y S V Q L K L Y D D K N A S L G L V G T H N G Q I G N D P N R D I L I A S N A Y F N H L K D K I L G C D
W Y F V P T D E G W T N D G G G G S M D K D C E M K R T T L D S P L G K L E L S G C E Q G L H R I I F L G K G T S A A D A V E V P
A P A A V L G G P E P L M Q A T A W L N A Y F H Q P E A I E E F P V P A L H H P V F Q Q E S F T R Q V L W K L L K V V K F G E V I S
Y S H L A A L A G N P A A T A A V K T A L S G N P V P I L I P C H R V V Q G D L D V G G Y E G G L A V K E W L L A H E G H R L G K
P G L G P A G G S H H H H H H

SGRP9^{PToV} –PToV HE_Fc_S46A_His6_Avitag (pFastBac1)

M V S A I V L Y V L L A A A A H S A F A A E A K P I T P H Y G P G H I T S D W C G F G D A R S D C T N P S S P K S L D I P Q Q L C P K
F S S K T G S S M F I S L H W N N S N T F T V F N Y S N C G V E K V F Y E G V N F S P Y R N Y T C Y H E G S S G W V N N K A G F Y
T K L Y Q M S T T S R C I K L I T L E P P E N I P S H S P G M C N P Q T N K M P D N P R L I T L T N N A S V S I Q F S L P A E F N G T N
C T K H L V P F C Y I D G G C F Q T S G F C H P F G Y S Y S S S A F Y Y G F Y T E G T P V G K H N Y I C D Y L E M K P G V Y N A T T
F G K F L L Y P T K T Y C M D T M N I T V P V Q A V Q S I W S Q S R Q S D D A I G M A C K S P Y C I F Y N K T R P Y L A P N G A D G
N H G D E E V R Q M M Q G L L V N S S C V S P Q G S T P L A L Y S T E M I Y T P N Y G S C P Q Y Y K L F E I S S D E N V L V P R G S
D K T H T C P P C P A P E L L G G P S V F L F P P K P K D T L M I S R T P E V T C V V V D V S H E D P E V K F N W Y V D G V E V H N
A K T K P R E E Q Y N S T Y R V V S V L T V L H Q D W L N G K E Y K C K V S N K A L P A P I E K T I S K A K G Q P R E P Q V Y T L P
P S R E E M T K N Q V S L T C L V K G F Y P S D I A V E W E S N G Q P E N N Y K T T P P V L D S D G S F F L Y S K L T V D K S R W Q
Q G N V F S C S V M H E A L H N H Y T Q K S L S L S P G K H H H H H H R I P G K L P A G G G L N D I F E A Q K I E W H E

SGRP9^{PToV}NB – PToV HE_Fc_S46A;F271A_His6_Avitag (pFastBac1)

M V S A I V L Y V L L A A A A H S A F A A E A K P I T P H Y G P G H I T S D W C G F G D A R S D C T N P S S P K S L D I P Q Q L C P K
F S S K T G S S M F I S L H W N N S N T F T V F N Y S N C G V E K V F Y E G V N F S P Y R N Y T C Y H E G S S G W V N N K A G F Y
T K L Y Q M S T T S R C I K L I T L E P P E N I P S H S P G M C N P Q T N K M P D N P R L I T L T N N A S V S I Q F S L P A E F N G T N
C T K H L V P F C Y I D G G C F Q T S G F C H P F G Y S Y S S S A F Y Y G F Y T E G T P V G K H N Y I C D Y L E M K P G V Y N A T T
F G K A L L Y P T K T Y C M D T M N I T V P V Q A V Q S I W S Q S R Q S D D A I G M A C K S P Y C I F Y N K T R P Y L A P N G A D G
N H G D E E V R Q M M Q G L L V N S S C V S P Q G S T P L A L Y S T E M I Y T P N Y G S C P Q Y Y K L F E I S S D E N V L V P R G S
D K T H T C P P C P A P E L L G G P S V F L F P P K P K D T L M I S R T P E V T C V V V D V S H E D P E V K F N W Y V D G V E V H N
A K T K P R E E Q Y N S T Y R V V S V L T V L H Q D W L N G K E Y K C K V S N K A L P A P I E K T I S K A K G Q P R E P Q V Y T L P
P S R E E M T K N Q V S L T C L V K G F Y P S D I A V E W E S N G Q P E N N Y K T T P P V L D S D G S F F L Y S K L T V D K S R W Q
Q G N V F S C S V M H E A L H N H Y T Q K S L S L S P G K H H H H H H R I P G K L P A G G G L N D I F E A Q K I E W H E

Supporting Information S19

Methods

Preparation of constructs:

SGRP-1 – Y. enterocolitica Toxin B5; Y. enterocolitica Toxin B5 (Non-Binding): The full-length coding region of YESubB (423 bp) incorporating a 3' Hisx6 tag in the bacterial expression vector pBAD18 was kindly provided by James Paton and is described elsewhere. The corresponding non-binding mutant YESubB (S31A; Y100F) was engineered from the wt template above using the Q5 Site-Directed Mutagenesis Kit (New England BioLabs) and sequence verified.

***SGRP-2 – S. typhi toxin B5; S. typhi toxin B5 (Non-Binding)*:** The Toxoid sequence pltB_pltA(E133A)_cdtB(H160Q)-6xHis and its corresponding non-binding control pltB(S35A)_pltA_cdtB-6xHis in the bacterial expression vector pET28b (Novagen) was kindly provided by Jorge Galan and described elsewhere. PltB or PltB(S35A) (411 bp) were amplified from the above respective constructs by PCR using pfu polymerase and primers 5' GCGCGCCATGGATGTATATGAGTAAGTATGTACC 3'; Nco1 site underlined and 5' ATATAAAGCTTCTTGGGTCCAAAGCATTGTGTCG; HindIII site underlined. PCR products were digested with Nco1 and HindIII and sub-cloned into the corresponding sites of pET28b. Constructs were sequence verified.

SGRP-3 – S. gordonii hemagglutinin surface adhesion BR; S. gordonii hemagglutinin surface adhesion BR (Non-Binding): The Hsa_{BR} sequence and its corresponding non-binding control Hsa_{BR}(R340E) (709 bp) in the bacterial expression vector pGEX-3X (Millipore Sigma) was cloned by Paul Sullam's Laboratory and described elsewhere. Hsa_{BR}/pGEX-3X and Hsa_{BR}(R340E)/pGEX-3X were subsequently modified to incorporate a 3' SNAPf_His_6 tag. Briefly, a His_6 sequence tag was inserted into the BamH1 and Xho1 sites of MCS2 of pSNAPf (New England Biolabs) to create

pSNAPf_His_6. SNAPf_His_6 was amplified from this construct by PCR using the forward primer 5'- AAAAGAATTCAACCATGGACAAAGACTGCGAAA-3' and reverse primer 5'- TTTTGAATTCATTAGTGATGGTGATGGTGATGGGA-3';

EcoR1 site underlined. PCR products were digested with EcoR1 and sub-cloned into the EcoR1 site of Hsa_{BR}/pGEX-3X and Hsa_{BR}(R340E)/pGEX-3X above. Constructs were sequence verified.

SGRP-4 – Mouse Hepatitis Virus-S Hemagglutinin Esterase (Inactive); Mouse Hepatitis Virus-S Hemagglutinin Esterase (Non-Binding): The coding sequence of MHV-S Hemagglutinin Esterase inactive (S45A) (1218bp) fused to human IgG-Fc followed by a His_6 tag in the mammalian expression vector pcDNA3.1(-) (Invitrogen) was kindly provided by Colin Parrish (MHV-S-HE_Fc_His_6) and described elsewhere. The Hisx6 and associated stop codon was deleted by Q5 site directed mutagenesis (New England Biolabs). Two complimentary oligonucleotides corresponding to the Avi-tag (Avidity) sequence GGTCTGAACGACATCTTCGAGGCTCAGAAAATCGAATGGCACGAA incorporating HindIII overlapping ends were synthesized (Integrated DNA Technologies) and annealed at 100 °C for 5 mins followed by slow cooling. The annealed oligos were cloned into the HindIII cut site of MHV-S-HE_Fc to produce MHV-S_HE_Fc_Avitag. Non-binding mutant (F212A) was generated from template MHV-S_HE_Fc_Avitag using the Q5 Site-Directed Mutagenesis Kit (New England BioLabs)

SGRP-7 – Bovine Coronavirus-Hemagglutinin Esterase (Inactive); Bovine Corona virus-Hemagglutinin Esterase (non-binding): The BCoV-Mebus HE ORF was amplified by PCR in junction overlap with a PCR amplification of the pFastBac1 clone of PToV-P4 He-Fc/Avi (see SGRP-9), but minus PToV HE sequence. Gibson assembly allowed for in-frame addition of BCoV-Mebus HE into the construct in direct replacement of PToV-P4 HE. This strategy maintained all vector, signal, and Fc-fusion/Avi architecture between constructs. Non-binding mutant F211A was generated by Q5 site-directed mutagenesis (New England Biolabs)

SGRP-8 – Clostridium tetani Heavy Chain/B Subunit; Clostridium tetani Heavy Chain/B Subunit (non-binding) mutant R1226L/W1289A; ***Clostridium tetani Heavy Chain/B Subunit (non-binding) mutant W1289A*** **-** The optimal receptor-binding domain (OBD) (Halpern and Loftus, 1993; Halpern and Loftus, 1993) of Tetanus Toxin (Heavy Chain/B Subunit) was synthesized by GENEWIZ (incorporating flanking 5' Hindlll and 3' Nco1 restriction sites) and codon optimized for expression in *E. coli* (a.a 1105>1315). pGEX-3X containing an irrelevant gene (IG) was engineered to contain a SNAPf_His_6 tag in the EcoR1 restriction site for use as an intermediate template (pGEX-3X_IG_SNAPf_His_6) and described elsewhere. Briefly, a His_6 sequence tag was inserted into the BamH1 and Xho1 sites of MCS2 of pSNAPf (New England Biolabs) to create pSNAPf_His_6. SNAPf_His_6 was amplified from this construct by PCR using VENT Polymerase (NEB), forward primer 5'- AAAAGAATTCAACCATGGACAAAGACTGCGAAA-3' and reverse primer 5'- TTTTGAATTCATTAGTGATGGTGATGGTGATGGGA-3'

(EcoR1 site are underlined). PCR products were digested with EcoR1 and sub-cloned into the EcoR1 site of the pGEX-3X_IG). pGEX-3X_IG_SNAPf_His_6 was then cut with Hindlll and Nco1 to directly replace IG with Hindlll and Nco1 cut B Subunit (OBD). Non-binding double mutant R1226L/W1289A and non-binding single mutant W1289A were generated by Q5 site-directed mutagenesis (New England Biolabs). Constructs were sequence verified.

SGRP-9 - Porcine Torovirus Hemagglutinin Esterase (inactive);Porcine Torovirus Hemagglutinin Esterase (non-binding): The coding sequence of PToV Hemagglutinin Esterase inactive (S46A) and PToV Hemagglutinin Esterase non-binding (F271A) (1176 bp) fused to human IgG-Fc followed by a 6xHis tag in the Insect expression vector pFastBac1 (ThermoFisher) was kindly provided by Colin Parrish (PToV-HE_S46A-Fc_His_6/pFastBac1; PToV-HE_F271A-Fc_His_6/pFastBac1) and described elsewhere. Both PToV-HE_S46A-Fc_His_6 and PToV-HE_F271A-Fc_His_6 were sub-cloned into pAC6 (Avidity) in-frame with the 3'Avitag (Avidity) sequence GGTCTGAACGACATCTTCGAGGCTCAGAAAATCGAATGGCACGAA. The resulting Avi-tagged constructs were amplified by PCR using pfu polymerase and the primers 5' ATATAGCGGCCGCTTTCTCGAGGCATAAGGAACACAC; Not1 site underlined and 3' CGCGCGGTACCTTATTCGTGCCATTCGATTTTCTGAG; Kpn1 site underlined. PCR products were digested with Not1 and Kpn1 and sub-cloned

into the corresponding sites of PToV-HE_S46A-Fc_His_6/pFastBac1 and PToV-HE_F271A-Fc_Hisx6/pFastBac1, which were cut with Not1 and Kpn1 thus removing the original untagged sequences. The final constructs were sequence verified.

Y.Pestis SubB - The full-length coding region of YPSubB (420 bp) incorporating a 3' Hisx6 tag in the bacterial expression vector pBAD18 was kindly provided by James Paton and is described elsewhere.

GspBBR; GSpBBR (non-binding); UB10712BR; UB10712BR (non-binding):: pGEX3X-GspBBRΔcnaA (containing just the Siglec and Unique domains of GspBBR) and pGEX3x-10712BR were constructed previously (2016 Glycobiology). The SNAPf_His_6 coding sequence was inserted in-frame into the EcoRI site at the 3'end of the BR sequences as described for SGRP-3 above. The non-binding mutant BR- SNAPf_His6 sequences were synthesized (LifeTechnologies) and then used to replace the BR segment (HindIII-NcoI) of pGEX3X-GspBBRΔcnaA- SNAPf_His_6.

E. coli SubB; E. coli Sub); E.coli SubB (non-binding): The coding region of *E. coli* SubB (423 bp) in pET-23 (+) bacterial expression vector was provided by Michael Jennings. Deletion of S106 and T107 was performed from the wt template above using the Q5 Site-Directed Mutagenesis Kit (New England BioLabs) and sequence verified. Mutant S106;T107 was cloned into pET28b which had been modified to contain a 3' SNAPf_His_6 tag. This was subsequently engineered to contain an S12A mutation (non-binding) using Q5 mutagenesis.

CD22-Fc_ACP - A CD22 cDNA fragment encoding the first two Ig-like domains fused to an EK-hIgG-Fc fragment was amplified by PCR and cloned into the mammalian expression vector pACP-tag(m)-2 (New England Biolabs).

Expression and purification of proteins in bacterial systems:

***Overexpression and purification of YenB and its nonbinding mutant*:** A single colony of BL21(DE3) competent cells (NEB, C2527H), transformed with YenB (or its mutant YenB S31A/Y100F) was inoculated in 25 ml of LB media in presence of 100 μg/ml ampicillin (Millipore, 171254-25GM) and

grown overnight at 37 °C with mild shaking of 225 rpm. 20 ml of this primary culture was added to 1 liter of LB media supplemented with 100 μg/ml ampicillin and grown at 37 °C until optical density at 600 nm reached to 0.2–0.3. To induced protein overexpression, arabinose (Sigma, A3256-25G) was added to the culture to make final concentrations 0.2% v/v, and the culture was incubated at 25 °C for 5–6 hours with mild shaking of 225 rpm. Bacteria was pelleted at 5000 g, 20 min, 4 °C and suspended in resuspension buffer (50 mM Tris-HCl, pH 8, 300 mM NaCl, 2 mg/ml lysozyme (Sigma, L6876), 1 mM EDTA, 10% glycerol in presence of DNAse (Sigma, D4263-5VL) and Protease inhibitors (Millipore, 5393134) at 4 g/ml. Pellet was resuspended, sonicated (30 secs ON/OFF, 10 cycles) and centrifuged (10000 g, 4 °C, 30 min) to exclude insoluble fractions. The soluble fraction was resuspended with preequilibrated Ni-NTA resin (Qiagen, 1018600) and incubated for 1 hr at 4 °C with end-to-end rotation. This slurry was passed through purification column (Biorad, PolyPrep 731-1550) and washed with 5 ml of 50 mM Tris-HCl, 300 mM NaCl, pH 8, followed by 2 washes with 5 ml of 50 mM Tris-HCl, 300 mM NaCl, pH 8.0, 30 mM Imidazole (Sigma, I2399-100G). The protein was eluted in 7 aliquots of 700 μl each with elution buffer (50 mM Tris-HCl, 100 mM NaCl, 300 mM Imidazole supplemented with protease inhibitors) and analyzed by SDS-PAGE. Aliquots with optimal protein concentrations were collected and transferred to PBS (Millipore, Amicon ultra centrifuge filter), supplemented with protease inhibitors, quantified (BCA, Pierce, Thermo Scientific 23225) and saved at -80 °C until further steps.

***Overexpression and purification of PltB and its nonbinding mutant*:** A single colony of BL21DE competent cells (NEB, C2527H), transformed with PltB (or its mutant- PltB S35A) was inoculated in 25 ml of LB media in presence of 50 μg/ml kanamycin (Sigma, K1377-5G) and grown overnight at 37 °C with mild shaking of 225 rpm. 10 ml of this primary culture was added to 0.5 l of LB media (Millipire, 1.10285.0500) supplemented with 50 μg/ml kanamycin and grown at 37 °C until optical density at 600 nm reached to 0.6–0.7. PltB overexpression was induced by 0.5 mM IPTG (Apex, 20-109) at 29 °C for 12–14 hours with shaking of 250 rpm. Bacteria was pelleted at 5000 g, 20 min, 4 °C and suspended in resuspension buffer (50 mM Tris-HCl, pH 8, 150 mM NaCl, 2 mg/ml lysozyme, 1 mM EDTA, DNAse and protease inhibitors) at 4 g/ml. Pellet was resuspended, sonicated (30

secs ON/OFF, 10 cycles, Fischer Scientific, 550 Sonic Dismembrator) and centrifuged (10000 g, 4 °C, 30 min) to exclude insoluble fractions (Sorvall, RC6 plus, Thermo). The soluble fraction was resuspended with preequilibrated Ni-NTA resin (Qiagen, 1018600) and incubated for 1 hr at 4 °C with end to end rotation. This slurry was passed through purification column (Biorad, PolyPrep 731-1550) and washed with 5 ml of 50 mM Tris-HCl, 150 mM NaCl, pH 8.0, followed by 2 washes with 5 ml of 50 mM Tris-HCl, 300 mM NaCl, pH 8.0, 50 mM Imidazole (Sigma, I2399-100G). The protein was eluted in 7 aliquots of 700 μl each with elution buffer (50 mM Tris-HCl, 100 mM NaCl, 300 mM Imidazole supplemented with protease inhibitors) and analyzed by SDS-PAGE. Aliquots with optimal protein concentrations were collected and transferred to PBS, supplemented with protease inhibitors, quantified (BCA, Pierce, Thermo Scientific 23225) and saved at -80 °C until further steps.

***Overexpression and purification of Hsa_{BR} and its nonbinding mutant*:** A single colony of BL21(DE3) competent cells, transformed with Hsa_{BR} (or its mutant Hsa_{BR} R340E) was inoculated in 25 ml of LB media in presence of 100 μg/ml ampicillin (Millipore, 171254-25GM) and grown overnight at 37°C with mild shaking of 225 rpm. 10 ml of this primary culture was added to 0.5lit of LB media supplemented with 100μg/ml ampicillin and grown at 37 °C until optical density at 600 nm reached to 0.7–0.8. Protein overexpression was induced by 0.5 mM IPTG (Apex, 20-109) at 24 °C for 12–14 hours (or 37 °C, 3 hrs) with shaking of 250 rpm. Bacteria was pelleted at 5000 g, 20 min, 4 °C and suspended in resuspension buffer (50 mM Tris-HCl, pH 7.5, 150 mM NaCl, 2 mg/ml lysozyme, 1% Triton X-100, 1 mM EDTA, DNAse and protease inhibitors) at 4 g/ml. Pellet was resuspended, sonicated (30 secs ON/OFF, 8 cycles) and centrifuged (10000 g, 4 °C, 30 min) to exclude insoluble fractions. The soluble fraction was resuspended with preequilibrated GST Sepharose resin (Thermo, 17-0756-01) and incubated for 1 hr at 4 °C with end to end rotation. This slurry was passed through purification column (Biorad, PolyPrep 731-1550) and washed with 10 bed volumes of resin by 50 mM Tris-HCl, pH 7.5, 150 mM NaCl, 1 mM PMSF, 0.5% Triton X-100 twice, followed by 2 washes with 10-bed-volume with 50 mM Tris-HCl, pH 7.5, 150 mM NaCl, 1 mM PMSF. The protein was eluted in 7 aliquots of 700 μl each with elution buffer (10 mM reduced glutathione (Sigma 4251-5G in 50 mM Tris-HCl, pH 8, 150 mM NaCl,

supplemented with protease inhibitors) and analyzed by SDS-PAGE. Aliquots with optimal protein concentrations were collected and transferred to PBS, supplemented with protease inhibitors, quantified by BCA and saved at -80 °C until further steps. Similar procedures were followed for expression and purification of $GspB_{BR}$, $UB10712_{BR}$ and their nonbinding mutants.

***Overexpression and purification of TeT-HCR, TeT-HCR 1226L, TeT-HCR W1289A and its nonbinding mutant*:** The procedure to purify TeT-HCR and its variant proteins remained comparable to protocol adopted for Hsa_{BR}, except for the IPTG induction conditions. For TeT-HCR, proteins were overexpressed at 26 °C for 4 hr with shaking at 250rpm.

Expressions and purification of proteins in mammalian expression system:

***Overexpression and purification of MHV-HE-Fc and hCD22_Fc*:**

HEK293 cells were transiently transfected by endotoxin free construct of MHV-Fc virolectin or its mutant in presence of polyethyleneimine (PEI, Polyscience Inc, 23966). Precisely, 18 μg DNA was vortexed with 54 μl of 1 mg/ml PEI in 2.4 ml of advanced DMEM (no serum, Gibco-12491-015) and added to each of 15cm dish of 80–90% confluent cell in 20 ml (advanced DMEM, 2% FCS, 1X P/S, 1X glutamine) and incubated 24 hr at 37 °C in incubator. Post incubation, the media was replaced by 20 ml basal media (96 ml RPMI 1640 (Invitrogen 11875-135), 96 ml DMEM (Invitrogen 12430-104), 2 ml of antibiotics 100X, 2 ml 200 mM L-glutamine, 2 ml 100 × Nutridoma (Nalgene, Nutridoma-SP, 11011375001), 2 ml of 100 mM sodium pyruvate) per plate and incubated for 4 days. The media was gently collected and centrifuged at 1000 g, 15 min, 4 °C to remove cell debris. The supernatant was adjusted to 10 mM Tris-HCl, pH 8, filtered with a 0.2 μM filter unit (Corning, 430320) and incubated with 0.5 ml protein-A-sepharose (nProtein A Sepharose 4 Fast flow, GE healthcare #1705280) at 4 °C for 24 hr. Resin was collected in purification column, washed with 10 ml of 10 mM Tris-HCl, pH 8.0, 150 mM NaCl twice and then resin was resuspended in 2 ml of 20 mM HEPES pH 7.0. Resin was treated with 25 mU of

Arthrobacter ureafaciens sialidase (EY laboratory, EC-32118-5) at room temperature for 1 hr and then washed with 10 ml of 10 mM Tris-HCl, pH 8.0, 150 mM NaCl to remove sialidase. MHV-Fc protein was eluted with 2 ml of 0.1 M glycine pH 3.0 in a tube, already containing 0.3 ml of cold 1 M Tris-HCl, pH 8.0, to neutralize pH. The elutant was buffer exchanged to PBS, supplemented with protease inhibitors, quantified by BCA assay and saved at -80 °C until further steps. Similar procedure was followed for expression and purification of hCD22-Fc.

Expressions and purification of proteins in insect expression system:

Clones of pFastBac1 constructs were used to generate recombinant bacmids in DH10Bac following the manufacturers protocol (ThermoFisher). Recombinant baculoviruses were recovered by transfection of the bacmids into Sf9 insect cells using TransIt-Insect reagent (Mirus). Viruses were then used to infect suspension High Five cells grown in Express5 media and supernatants harvested ~60–72 hours post-infection. Proteins were purified from the infected cell culture supernatants by binding to a HiTrap ProteinG HP column (GE Healthcare Life Sciences, Piscataway, NJ) and eluted with 0.1 M citrate, pH 3.0 (pH neutralization to 7.8 with 1 M Tris-HCl, pH 9.0) using ÄKTA FPLC system (GE Healthcare Life Sciences). The HE-Fc containing fractions were dialyzed in PBS and concentrated using 30 kD Amicon Ultra-15 filters (EMD Millipore). Purified proteins were observed by SDS gel migration as well as anti-human IgG Fc probing by Western. Protein concentrations were determined from A280 readings and MicroBCA Assay. Proteins were primarily aliquoted and stored at -80 °C.

Biotinylation of Proteins: Biotinylation of SNAP tagged proteins and Avi-tagged proteins were performed as suggested by manufactures (NEB, Avidity). Direct biotinylation of proteins for example-YenB, PltB and Neu5Gc-IgY was achieved by NHS mediated biotin tagging at 20:1 molar ratio as per manufacturer's protocol (Thermo scientific, EZ-Link Sulfo-NHS-LC Biotin, Cat#21326). Biotinylated proteins were concentrated, and buffer exchanged to PBS with microcon centrifugation columns according to the molecular weights of proteins. Finally, elutions were estimated for protein concentration and stored in -80 °C freezer. In addition to the functional assays on sialoglycan microarray and sera ELISA experiments, high efficiency

of biotinylation was also confirmed by a pull-down assay using streptavidin beads (Thermo, 20347). Briefly, proteins biotinylated and mock biotinylated were tested for their affinity and subsequently elution from streptavidin beads. Pulled down biotinylated proteins were also compared parallelly to the initial concentration of protein to observe the approximate fractions of proteins acquiring biotin in biotinylation tagging procedures.

Sialic acid release, DMB derivatization, and HPLC analysis: Bound Sias from serum samples were released using 2 M acetic acid hydrolysis, 80 °C for 3 hour. The hydrolyzed samples were passed through a Microcon-10 filter (Sigma-Millipore); the released Sias were recovered in the filtrate. The Sias were derivatized with DMB (Hara et al., 1989). Briefly, 7 mM DMB, 1.4 M acetic acid, 0.75 M β-mercaptoethanol, 18 mM sodium hydrosulfite, at 50 °C for 2.5 hrs, in the dark. The DMB-Sias were separated on a Gemini C18 column, 4.6 × 250 mm, 5 µm particle size (Phenomenex; Torrance, CA). Isocratic elution was employed using 7% methanol, 8% acetonitrile, 85% water for 50 min at 0.9 ml/min flow. The eluant was monitored by fluorescence with Ex373 and Em448. Sialic acid quantitation was done by derivatizing commercial Neu5Ac (Nacalai, USA; San Diego, CA) and comparing the area under the peak of known amounts.

Mild Periodate and Base treatment of sera: To remove *O*-acetyl esters and render all Sias sensitive to mild periodate treatment, serum-coated ELISA plates were expose to strong NH_4OH vapors for 24 hrs at room temperature. In parallel, another plate coated with sera were incubated in humidified chamber filled with triple distilled water at room temperature as control set of base treated sera. Wells were washed 3 times with PBS briefly to remove any residual NH_4Cl. Subsequently, plates were washed three times with PBS pH 6.5 to pre-equilibrate for mild periodate treatment, if required. To ascribe Sia specificity, serum-coated ELISA plates were treated with mild periodate to selectively cleave the Sia side- chain. For sodium periodate treatment in base treated/untreated plate, wells were incubated with 200 µl of freshly prepared cold 2 mM sodium metaperiodate (Fischer, S398-100) in PBS, pH 6.5 in dark, 4°C, precisely for 20min. The reaction was stopped by the addition of 50 µl of 100 mM sodium borohydride (Fischer, S678-25) in PBS, pH 6.5 (final concentration of 20 mM), followed by a 10-min incubation at room temperature with gentle shaking (the

borohydride inactivates the periodate). Concurrently, as a mock control, periodate and borohydride solutions were premixed (4:1), and wells were incubated with 250 µl/well side by side with the periodate-treated wells. To remove resulting borates, wells were then washed three times (10 min each wash) with 50 mM sodium acetate, pH 5.5, containing 100 mM NaCl, followed by three washes with PBS, pH 7.4. Base and/or mild periodate treated sera were used to determine Sia- specific serum binding, or OAc-Sia-specific binding in SGRPs or lectins. (Padler-Karavani et al., 2013)

References

Halpern, JL and A Loftus (1993), 'Characterization of the receptor-binding domain of tetanus toxin.', *J Biol Chem*, 268 (15), 11188-92.

Hara, S, et al. (1989), 'Determination of mono-O-acetylated N-acetylneuraminic acids in human and rat sera by fluorometric high-performance liquid chromatography', *Anal Biochem*, 179 162-66.

Padler-Karavani, V, et al. (2013), 'A simple method for assessment of human anti-Neu5Gc antibodies applied to Kawasaki disease.', *PLoS One*, 8 (3), e58443.

Glycan ID	Type	Glycan Structure	SGRP1 *VenB*	StDev	SGRP2 *PltB*	StDev	SGRP3 *Hsa*	StDev	SGRP4 *MHV*	StDev	SGRP5 *IgY*	StDev	SGRP6 *SNA*	StDev	SGRP7 *BCoV*	StDev	SGRP8 *TeT*	StDev	SGRP9 *PTox*	StDev
46	Non-sialosides	Galβ-NH2	530.5	177.3	137.3	22.5	187.3	11.2	102.0	17.8	99.3	57.8	33.3	4.9	96.5	9.0	262.3	68.6	163.3	22.3
48		GalβR2	425.0	28.8	55.5	13.2	127.5	8.0	16.5	4.1	16.8	16.4	50.5	10.5	64.3	13.6	243.5	76.8	95.5	15.1
49		GalβR1	371.8	69.9	54.3	13.9	192.4	6.1	65.5	7.6	12.0	11.0	28.3	33.5	175.5	7.1	376.5	86.9	83.5	14.2
78		Galα3Galβ4GlcNAcβR1	401.8	356.9	47.0	7.4	147.8	34.7	109.8	32.3	141.3	100.8	46.8	19.7	129.5	14.0	344.0	20.0	53.5	22.1
52		Galβ3GalNAcαR1	501.0	53.1	121.0	28.4	317.8	28.1	171.0	181.7	22.3	27.2	144.8	12.4	31.5	22.8	272.5	34.6	47.5	25.9
51		Galβ3GalNAcβR1	224.8	11.6	55.0	10.6	149.8	20.7	23.8	6.4	5.3	1.7	9.8	9.8	12.0	17.2	342.0	38.5	48.8	13.3
53		Galβ3GlcNAcβR1	361.3	107.3	70.0	17.8	396.3	49.2	72.8	27.5	3.8	1.5	28.3	9.9	185.5	15.2	289.3	86.9	71.8	21.9
236		Galβ3(Fucα4)GlcNAcβR1	193.0	61.2	56.5	30.8	271.8	33.2	52.4	33.0	41.5	21.1	160.0	28.1	33.5	25.4	370.8	43.1	74.0	11.5
43		Galβ4GlcβR1	245.5	32.1	71.0	17.3	531.5	47.8	44.0	10.7	11.5	9.0	150.8	16.0	53.0	15.8	293.0	15.6	82.5	21.7
44		Galβ4Glcβ-NH2	1334.5	185.3	184.0	63.3	217.0	32.1	28.0	23.8	82.8	18.1	189.5	29.8	127.3	22.4	198.3	28.7	82.8	11.9
50		Galβ4GlcβR2	44.5	30.6	35.5	27.7	107.3	8.5	107.8	20.6	40.0	14.9	78.5	35.7	22.3	11.6	215.3	86.8	57.0	20.5
45		Galβ4GlcNAcβR1	284.8	51.7	48.5	15.4	524.3	42.8	86.8	64.0	208.5	74.0	56.3	5.0	126.0	14.4	448.3	35.6	128.3	20.2
89		Galβ4GlcNAcβ3Galβ4GlcβR1	328.3	106.4	1901.3	637.4	74.0	12.0	44.8	25.7	35.3	22.5	576.0	37.3	61.0	15.2	248.0	48.8	65.3	20.3
54		Galβ4GlcNAc6SβR1	554.8	188.5	47.3	5.2	132.3	7.7	69.5	23.6	15.8	2.2	6.8	1.4	47.0	8.7	455.3	35.8	177.3	54.7
237		(Fucα2)Galβ3(Fucα4)GlcNAcβR1	63.3	7.0	29.3	13.8	223.5	14.6	66.1	14.2	12.3	5.3	27.3	0.4	41.3	2.1	280.3	21.1	56.0	36.0
242		(GalNAcβ4)Galβ4GlcβR1	132.3	55.9	55.0	14.9	65.3	10.7	65.2	5.3	3.5	1.3	6.3	1.1	77.3	14.2	213.0	21.0	46.3	24.5
83		Gal6Sβ4(Fucα3)GlcNAcβR1	141.8	59.7	33.3	17.4	507.5	49.3	96.5	19.3	27.0	21.9	160.8	26.3	31.0	16.9	333.5	39.9	67.5	25.3
86		Gal6Sβ4(Fucα3)GlcNAc6SβR1	347.3	68.6	56.0	8.9	260.5	37.3	78.3	40.0	6.3	1.7	31.5	7.8	134.3	13.4	102.8	35.8	77.8	7.5
47		GalNAcαR1	358.8	150.6	31.0	3.8	107.0	11.6	20.5	5.4	22.3	12.2	34.5	9.0	48.5	14.7	121.0	81.0	88.8	24.8
25	α2-3 Neu5Ac	Neu5Acα3GalβR1	5597.5	729.5	12261.5	698.8	22489.5	594.3	55.3	10.3	292.0	86.3	20.2	6.3	239.5	13.4	394.3	49.0	49.3	12.8
15		Neu5Acα3Galβ3GalNAcαR1	3462.0	318.3	9163.5	798.4	19780.3	968.3	15.0	4.5	40.0	8.8	136.3	34.5	48.3	15.6	317.3	29.3	62.3	38.5
33		Neu5Acα3Galβ3GalNAcβR1	5618.5	363.3	10075.8	475.0	14821.0	550.5	52.8	20.4	32.8	6.1	13.5	0.2	104.8	13.6	229.8	38.1	63.3	20.7
250		Neu5Acα3Galβ3GlcNAcαR1	6256.8	759.2	19121.0	541.0	13113.5	801.4	89.2	17.1	8.3	2.6	10.8	6.4	108.8	12.6	89.8	25.6	24.8	5.6
13		Neu5Acα3Galβ3GlcNAcβR1	4371.5	919.1	10721.3	285.1	15490.3	728.9	72.8	26.4	61.5	40.4	134.8	29.5	99.3	19.9	443.3	27.3	78.3	32.9
60		Neu5Acα3Galβ3GlcNAcβ3Galβ4GlcβR1	4404.5	997.7	11799.8	1004.9	9754.0	644.4	52.0	13.0	13.0	4.5	33.0	5.0	21.5	20.2	141.8	29.0	39.5	3.8
238		Neu5Acα3Galβ3(Fucα4)GlcNAcβR1	4830.0	125.3	10740.5	704.1	8606.8	519.6	87.2	20.4	47.5	18.9	91.5	17.5	67.8	11.8	158.8	92.0	36.5	12.8
21		Neu5Acα3Galβ4GlcβR1	4158.5	494.3	11054.5	112.2	10129.0	679.2	55.5	16.8	9.0	0.8	110.5	23.5	163.3	21.1	525.5	46.8	108.0	18.2
80		Neu5Acα3Galβ4GlcβR3	5308.5	322.0	9964.0	447.5	13250.5	222.4	29.5	5.8	30.5	10.5	241.5	10.9	37.3	29.1	321.3	30.9	40.8	15.1
126		Neu5Acα3Galβ4GlcβR5	6429.3	406.0	12071.8	329.0	13812.8	459.3	88.5	31.0	26.5	20.3	19.8	0.1	65.8	25.0	159.8	6.4	93.5	43.4
11		Neu5Acα3Galβ4GlcNAcβR1	3544.0	583.5	6716.5	476.0	12905.3	897.2	39.5	18.2	18.0	5.9	156.3	44.5	29.8	22.6	322.8	24.6	82.8	25.2
123		Neu5Acα3Galβ4GlcNAcβR5	6517.0	300.6	12176.0	815.0	11244.3	689.9	121.5	64.5	9.5	1.0	94.0	37.7	45.3	24.2	154.0	48.8	46.5	17.6
90		Neu5Acα3Galβ4GlcNAcβ3Galβ4GlcβR1	5800.3	632.3	11923.5	435.6	9770.8	905.2	95.5	10.2	36.0	38.1	854.0	13.0	108.5	35.2	218.3	17.8	56.0	7.5
62		Neu5Acα3Galβ4GlcNAc6SβR1	4900.8	663.8	12612.8	416.0	12627.8	749.2	89.3	34.8	32.0	22.8	67.0	9.9	122.8	26.2	231.0	35.3	248.3	29.2
55		Neu5Acα3Galβ4(Fucα3)GlcNAcβR1	5425.0	482.0	10676.0	441.0	7392.8	432.2	27.8	18.6	8.5	3.4	21.3	25.1	16.3	31.6	693.3	78.9	74.0	22.0
57		Neu5Acα3Galβ4(Fucα3)GlcNAc6SβR1	4599.5	639.6	9234.0	518.5	6375.0	474.1	78.5	15.8	33.5	27.4	21.5	3.0	82.5	22.1	147.0	37.3	28.8	3.6
96		Neu5Acα3(GalNAcβ4)Galβ4GlcβR1	5073.0	493.9	10135.5	551.1	2483.3	29.2	27.0	7.8	11.0	3.4	133.8	17.6	22.8	29.5	144.3	56.4	35.0	23.1

84		Neu5Acα3Gal6Sβ4(Fucα3)GlcNAcβR1	2992.8	133.6	9823.0	577.3	390.8	18.4	51.5	16.9	5.0	2.6	3.8	0.6	12.0	22.4	146.5	43.2	51.0	33.6
87		Neu5Acα3Gal6Sβ4(Fucα3)GlcNAc6SβR1	3945.3	532.2	8384.3	950.0	945.0	57.1	59.0	27.0	60.3	93.2	196.3	7.5	44.0	13.9	413.8	87.9	63.8	29.1
27	α 2-6 Neu5Ac	Neu5Acα6GalβR1	3039.5	348.9	5274.5	396.7	473.3	26.5	34.3	5.7	8.0	3.6	7138.8	709.2	72.0	13.7	285.8	38.9	49.0	9.6
253		Neu5Acα6Galβ3GalNAcβR1	7112.8	158.1	24258.8	1655.4	291.5	34.1	99.8	20.3	39.0	29.4	10023.5	15.3	67.3	23.5	152.8	24.7	112.0	58.5
251		Neu5Acα6Galβ3GlcNAcβR1	7850.8	103.6	13330.0	762.6	389.0	29.9	112.2	9.2	27.8	14.1	9813.3	369.2	105.3	17.7	85.8	10.7	27.8	4.6
19		Neu5Acα6Galβ4GlcβR1	2634.3	421.3	6523.3	649.9	764.0	64.3	55.3	25.0	4.8	2.5	12023.8	926.8	35.5	19.6	351.0	79.7	78.5	23.0
125		Neu5Acα6Galβ4GlcβR5	6945.5	576.4	9651.3	344.7	153.5	17.1	46.3	25.0	10.0	3.6	7798.8	143.5	52.8	14.8	101.3	35.3	28.5	13.0
17		Neu5Acα6Galβ4GlcNAcβR1	4149.0	374.5	12132.3	564.8	117.3	25.1	42.0	16.0	6.0	2.4	16690.5	729.3	81.3	13.2	380.3	39.0	82.0	13.1
124		Neu5Acα6Galβ4GlcNAcβR5	6646.3	460.9	12769.8	1174.4	294.5	28.1	28.8	7.9	8.5	3.4	24226.0	169.4	3.0	0.5	72.3	24.2	16.3	5.1
5		Neu5Acα6GalNAcαR1	4578.5	694.3	6154.8	859.8	107.3	9.7	21.8	1.7	509.5	328.7	6233.5	32.5	151.8	19.4	345.3	37.6	120.0	26.5
41	α2-8 Neu5Ac	Neu5Acα8Neu5Acα3Galβ4GlcβR1	3687.0	534.7	8305.0	864.7	95.8	17.1	53.3	21.7	190.3	43.8	40.2	3.9	135.5	7.4	2139.0	136.1	68.0	8.8
64		Neu5Acα8Neu5Acα3Galβ4GlcβR4	6076.0	402.5	20345.3	1046.2	337.0	18.7	23.5	6.8	22.5	15.0	132.2	12.5	16.5	21.0	3524.3	208.9	31.5	12.9
98		Neu5Acα8Neu5Acα3(GalNAcβ4)Galβ4GlcβR1	7009.8	761.2	16925.8	1004.7	131.3	35.8	58.0	15.1	5.0	2.9	18.5	4.1	83.3	21.2	799.0	64.8	47.8	41.7
76		Neu5Acα8Neu5Acα6Galβ4GlcβR1	6771.3	602.4	8663.0	609.1	163.5	9.9	37.0	10.2	8.0	3.2	3449.0	414.6	32.5	27.9	773.0	49.1	48.5	9.1
42		Neu5Acα8Neu5Acα8Neu5Acα3Galβ4GlcβR1	5322.5	296.2	14090.0	824.8	62.3	20.9	63.8	22.4	14.0	1.8	40.8	9.0	172.5	19.1	994.8	77.7	90.3	24.8
65		Neu5Acα8Neu5Acα8Neu5Acα3	6885.0	530.4	20933.0	965.7	394.0	29.2	22.0	2.2	7.8	4.1	99.5	36.7	42.3	35.8	2008.0	304.7	71.3	43.2
72		Neu5Acα8Neu5Gcα3Galβ4GlcβR1	5782.8	424.1	14310.8	868.5	316.8	24.8	28.5	22.1	630.5	57.5	36.8	7.5	205.0	15.5	226.0	36.7	41.5	8.6
73		Neu5Acα8Neu5Gcα6Galβ4GlcβR1	4203.0	94.5	15641.5	858.4	74.5	8.5	22.5	4.4	265.0	23.4	21.5	5.1	77.3	14.8	203.5	42.4	35.5	6.2
71		Neu5Acα8Kdnα6Galβ4GlcβR1	3889.0	896.1	12735.8	1063.9	222.8	18.7	65.0	14.0	13.3	2.9	935.0	38.0	32.5	25.7	518.0	33.0	66.8	14.9
255	8-OMe Neu5Ac	Neu5Ac8Meα3Galβ4GlcβR1	6719.8	205.5	174.5	41.7	519.0	22.2	72.3	8.5	32.3	8.0	320.5	31.6	101.3	18.9	104.5	7.2	56.3	12.0
256		Neu5Ac8Meα6Galβ4GlcβR1	4162.8	564.5	69.5	38.2	185.5	9.9	59.8	2.9	2.8	1.3	78.0	8.6	97.3	11.0	144.0	16.1	43.5	36.3
104	4-OAc Neu5Ac	Neu4,5Ac2α3Galβ3GalNAcαR1	7135.8	776.5	13177.3	1056.2	12690.5	496.0	6523.8	328.0	6.5	1.3	172.3	22.4	4.0	7.6	116.3	69.8	40.5	17.4
103		Neu4,5Ac2α3Galβ3GalNAcβR1	7944.3	415.9	21455.3	2239.1	13367.8	476.6	3429.3	561.3	7.5	1.3	386.5	53.4	26.3	16.1	150.0	19.3	56.0	34.0
102		Neu4,5Ac2α3Galβ3GlcNAcαR1	7552.8	541.5	18864.5	1374.7	4168.8	64.9	2607.3	285.6	6.0	1.2	127.0	20.3	43.0	15.0	134.5	56.2	38.3	19.9
101		Neu4,5Ac2α3Galβ3GlcNAcβR1	7202.5	484.9	12174.8	478.8	5305.3	56.1	4193.3	667.0	4.0	3.4	11.3	4.1	25.5	6.4	185.5	35.2	34.8	26.4
99		Neu4,5Ac2α3Galβ4GlcβR1	6236.8	709.7	19729.5	1738.3	16058.3	188.5	1541.3	161.3	10.3	3.3	383.8	20.6	86.5	39.7	288.3	74.2	76.8	36.5
79		Neu4,5Ac2α3Galβ4GlcNAcβR1	5639.0	426.3	17190.5	861.1	10950.0	246.7	1781.3	27.5	10.0	3.5	171.8	21.2	120.3	16.1	298.3	53.6	75.0	50.3
100		Neu4,5Ac2α3Galβ4GlcNAcβ3Galβ4GlcβR1	4675.3	397.4	14328.0	868.1	10068.8	135.4	2032.8	201.1	4.8	1.3	56.5	9.7	2.3	16.0	154.3	26.9	23.0	15.3
29	Ac Neu5Ac	Neu5,9Ac2α3GalβR1	4285.8	592.2	7011.5	256.2	9808.3	581.6	76.3	33.9	37.0	23.9	33.0	8.3	124.0	10.5	414.8	52.1	379.8	20.5
9		Neu5,9Ac2α3Galβ3GalNAcαR1	3833.3	973.1	11159.8	838.6	24528.0	960.3	56.8	15.8	89.5	106.9	101.0	11.0	214.3	13.6	393.3	32.8	1055.5	141.5
35		Neu5,9Ac2α3Galβ3GalNAcβR1	3965.3	833.4	11015.0	545.6	19351.5	832.8	55.0	29.7	31.3	6.4	140.8	50.7	24.5	9.0	394.8	64.9	588.8	21.5
7		Neu5,9Ac2α3Galβ3GlcNAcβR1	3049.8	306.6	8960.3	628.2	4057.0	399.9	22.0	12.0	24.8	11.0	826.8	48.9	68.0	6.2	421.3	30.0	618.5	22.5
240		Neu5,9Ac2α3Galβ3(Fucα4)GlcNAcβR1	7452.5	688.7	14599.5	627.6	7585.0	427.1	210.1	26.9	4.5	1.3	1.3	0.0	76.3	9.9	223.5	14.5	1202.8	151.1
39		Neu5,9Ac2α3Galβ4GlcβR1	4967.3	582.1	13037.0	1058.2	11877.3	928.7	19.5	11.1	17.0	10.7	122.8	8.8	31.0	37.1	361.5	39.5	904.8	58.3

1	9-O	Neu5,9Ac2α3Galβ4GlcNAcβR1	5839.3	342.4	13794.8	1044.2	18829.5	295.0	24.5	3.7	17.8	17.6	30.5	2.7	109.8	33.1	404.3	57.6	783.8	19.3
92		Neu5,9Ac2α3Galβ4GlcNAcβ3Galβ4GlcβR1	5006.5	391.1	9095.0	671.3	8798.5	253.6	55.3	15.6	13.8	5.9	1345.0	139.8	11.5	28.2	255.5	29.2	4528.3	414.1
31		Neu5,9Ac2α6GalβR1	3393.5	669.1	4531.0	543.2	311.0	87.2	22.5	4.7	53.3	37.5	10567.5	288.1	42.5	15.6	378.0	80.4	582.8	55.8
37		Neu5,9Ac2α6Galβ4GlcβR1	4141.3	640.5	12416.8	636.6	78.8	5.1	69.8	13.5	9.3	5.3	19260.0	1044.3	144.3	22.1	289.8	23.1	1099.0	86.4
3		Neu5,9Ac2α6Galβ4GlcNAcβR1	3578.5	231.4	13582.5	1114.8	247.5	39.3	135.5	15.9	7.8	1.7	23729.3	1309.4	73.8	24.6	539.0	66.2	768.3	48.4
23		Neu5,9Ac2α6GalNAcαR1	4358.8	873.5	4252.3	415.0	337.3	28.2	37.8	33.2	11.0	5.8	1749.5	178.3	33.5	23.7	299.3	10.3	3635.5	748.8
243		Neu5,9Ac2α8Neu5Acα3Galβ4GlcβR1	6972.0	589.7	13636.8	836.3	849.3	37.6	198.3	8.2	4.0	2.2	20.3	51.4	27.3	20.5	1899.0	300.7	2646.0	224.6
26	α2-3 Neu5Gc	Neu5Gcα3GalβR1	4514.5	542.5	2056.0	289.5	11601.5	654.1	68.5	21.3	41435.3	3022.5	70.3	34.9	285.3	21.5	652.8	48.7	87.5	13.6
16		Neu5Gcα3Galβ3GalNAcαR1	3448.8	322.9	438.3	127.0	20061.5	1080.3	25.0	7.9	41405.5	1715.3	136.5	12.5	94.5	17.7	395.5	82.5	57.3	20.8
34		Neu5Gcα3Galβ3GalNAcβR1	4894.0	359.1	1871.5	148.0	20902.8	1267.2	93.8	16.1	35987.0	2926.5	28.0	3.0	46.0	44.5	386.8	19.1	64.5	22.6
14		Neu5Gcα3Galβ3GlcNAcβR1	4960.3	233.9	846.0	178.0	14246.5	862.7	74.8	24.2	34309.5	2455.3	90.3	7.0	91.8	20.3	596.8	36.7	88.5	24.6
61		Neu5Gcα3Galβ3GlcNAcβ3Galβ4GlcβR1	5450.8	852.3	1111.0	236.7	9735.0	317.4	29.3	12.5	34988.3	3942.8	135.8	22.0	68.0	34.0	143.0	16.9	42.0	9.1
239		Neu5Gcα3Galβ3(Fucα4)GlcNAcβR1	5770.0	340.6	328.0	55.0	8933.8	433.5	107.3	21.9	41263.3	2811.9	116.5	1.8	68.8	27.2	128.5	72.6	33.8	15.6
22		Neu5Gcα3Galβ4GlcβR1	4763.0	905.4	6561.8	269.2	11094.0	411.6	56.0	8.9	32183.8	5677.4	111.0	42.4	51.8	25.3	493.3	61.6	157.0	38.1
12		Neu5Gcα3Galβ4GlcNAcβR1	4458.8	862.4	3419.8	233.9	11003.0	707.6	37.5	7.7	50362.3	3174.3	23.3	32.3	84.5	22.5	367.0	60.8	59.5	16.1
91		Neu5Gcα3Galβ4GlcNAcβ3Galβ4GlcβR1	3337.3	699.0	2594.0	563.8	10991.8	688.7	118.3	56.2	43622.3	3348.9	998.8	15.3	64.5	17.7	243.3	73.6	74.3	35.8
63		Neu5Gcα3Galβ4GlcNAc6SβR1	4143.3	454.4	1955.8	889.7	14325.0	579.7	112.5	20.3	36866.3	2937.4	70.5	5.3	90.5	26.8	463.0	57.9	60.5	7.2
56		Neu5Gcα3Galβ4(Fucα3)GlcNAcβR1	5403.5	851.8	2159.3	132.2	8287.0	354.7	23.5	5.4	34731.8	3078.8	80.8	16.3	67.0	31.5	230.0	22.5	91.0	44.4
58		Neu5Gcα3Galβ4(Fucα3)GlcNAc6SβR1	5347.8	660.0	7726.0	457.8	6429.0	265.7	79.8	29.4	48057.3	5410.2	20.5	9.0	44.5	14.5	349.0	41.8	64.8	6.8
97		Neu5Gcα3(GalNAcβ4)Galβ4GlcβR1	5646.3	415.6	115.8	54.0	100.0	12.3	25.5	8.3	21921.5	2495.7	20.3	1.1	105.0	36.0	114.0	37.0	18.5	3.4
85		Neu5Gcα3Gal6Sβ4(Fucα3)GlcNAcβR1	3596.0	809.3	280.3	110.0	87.3	30.8	224.5	155.8	28225.5	2996.0	4.1	10.7	53.8	30.5	139.3	57.6	42.8	18.9
88		Neu5Gcα3Gal6Sβ4(Fucα3)GlcNAc6SβR1	1200.3	203.4	77.5	19.0	395.0	163.1	26.3	12.9	5.0	0.8	22.0	0.0	38.5	41.8	404.8	83.3	74.8	25.5
28	α2-6 Neu5Gc	Neu5Gcα6GalβR1	4021.3	299.0	382.8	69.9	470.8	34.0	32.8	22.6	22645.5	1025.0	3536.8	278.8	216.0	21.8	503.5	28.6	87.8	8.8
254		Neu5Gcα6Galβ3GalNAcβR1	5277.3	544.2	723.0	79.4	355.5	26.1	87.8	27.8	32376.8	4757.0	11005.5	439.8	89.0	24.4	167.5	30.4	85.5	40.8
252		Neu5Gcα6Galβ3GlcNAcβR1	6979.8	402.6	695.8	349.9	340.3	12.8	107.3	23.3	52848.8	5597.5	9230.3	944.9	57.5	12.3	213.5	35.6	65.5	27.4
20		Neu5Gcα6Galβ4GlcβR1	2801.5	362.2	392.3	64.0	937.5	82.1	22.5	10.8	30604.5	1579.6	10983.3	885.1	98.3	7.5	419.3	37.8	39.5	3.0
18		Neu5Gcα6Galβ4GlcNAcβR1	3796.5	383.2	928.0	234.5	187.5	33.1	51.3	11.2	34435.8	4758.1	20148.3	1087.7	87.3	12.7	409.0	25.4	62.8	4.2
6		Neu5Gcα6GalNAcαR1	5852.3	685.5	163.0	26.5	230.8	38.0	46.8	9.3	27507.8	1375.2	42.0	36.9	213.8	8.3	523.8	23.1	140.5	36.9
69	α2-8 Neu5Gc	Neu5Gcα8Neu5Acα3Galβ4GlcβR1	4200.8	375.7	15150.0	761.9	84.3	18.6	36.0	8.6	30943.3	4381.4	19.5	31.0	82.5	27.3	800.0	97.3	36.5	13.8
75		Neu5Gcα8Neu5Gcα3Galβ4GlcβR1	5462.8	438.9	732.8	187.6	967.0	101.2	105.3	15.5	29980.3	2397.0	18.0	3.3	246.3	26.6	434.5	80.1	93.5	32.0
257	8-OMe Neu5Gc	Neu5GcMeα3Galβ4GlcβR1	7393.3	202.0	72.8	9.3	9701.8	497.1	57.3	21.8	8.0	2.2	0.0	1.5	78.3	15.1	102.5	13.3	30.0	13.5
258		Neu5GcMeα6Galβ4GlcβR1	5308.5	661.7	147.5	57.0	413.0	72.5	63.5	21.3	20.3	4.5	4304.5	651.8	88.2	7.4	158.3	31.1	261.0	44.9
77		Neu5GcMeα8Neu5Acα3Galβ4GlcβR1	8736.0	411.7	2931.0	490.1	35.8	12.5	56.0	24.6	49.3	83.2	34.5	2.9	94.0	6.6	1283.0	165.4	39.3	3.0
111		Neu4Ac5Gcα3Galβ3GalNAcαR1	3647.5	347.4	113.0	24.9	13857.3	718.8	105.0	26.4	27187.0	4019.4	208.8	20.4	60.5	4.7	227.3	10.2	54.8	36.0

110	4-OAc Neu5Gc	Neu4Ac5Gcα3Galβ3GalNAcβR1	5855.5	264.3	168.8	44.0	7919.5	740.5	133.8	44.5	22221.0	3163.7	112.0	39.5	52.5	10.2	206.5	31.5	55.5	44.2
109		Neu4Ac5Gcα3Galβ3GlcNAcαR1	4690.0	139.3	113.0	27.1	6969.3	57.4	44.5	12.4	26897.8	3364.5	27.5	7.5	109.5	28.3	138.5	45.1	32.0	13.5
108		Neu4Ac5Gcα3Galβ3GlcNAcβR1	4796.8	680.5	229.0	117.4	4571.3	256.8	42.8	13.6	27515.5	3176.3	23.0	3.2	6.5	11.3	111.8	53.9	20.8	9.0
106		Neu4Ac5Gcα3Galβ4GlcβR1	5513.5	693.6	161.0	58.3	5594.5	327.7	97.3	13.8	29068.8	2017.5	3.8	1.6	119.8	23.3	215.3	56.8	48.8	10.8
105		Neu4Ac5Gcα3Galβ4GlcNAcβR1	5143.5	632.0	687.3	109.1	6626.3	81.6	56.0	20.9	31642.0	4015.0	20.2	7.1	31.0	13.4	147.5	85.2	34.3	11.4
107		Neu4Ac5Gcα3Galβ4GlcNAcβ3Galβ4GlcβR1	2578.0	259.1	65.0	6.7	2215.3	85.6	116.3	35.9	22188.0	2028.0	33.0	6.0	252.5	20.5	359.0	61.6	106.5	68.5
30	9-OAc Neu5Gc	Neu5Gc9Acα3GalβR1	4532.3	241.1	172.3	20.9	8669.5	85.9	65.3	7.1	21795.0	1822.5	48.2	10.1	115.8	13.5	618.0	38.5	612.3	20.7
10		Neu5Gc9Acα3Galβ3GalNAcαR1	3923.0	389.3	71.5	6.0	18474.5	1024.8	66.8	27.2	22721.8	1524.8	219.5	40.1	73.0	1.5	618.3	78.2	491.3	15.0
36		Neu5Gc9Acα3Galβ3GalNAcβR1	3555.8	643.5	1003.8	143.3	12688.8	916.5	152.0	148.6	30014.8	2794.8	41.0	11.4	60.5	7.5	317.3	31.4	344.8	11.9
8		Neu5Gc9Acα3Galβ3GlcNAcβR1	4999.0	488.2	462.5	82.6	3491.0	351.4	24.5	2.9	47570.8	2029.2	143.0	19.4	159.8	24.3	692.0	74.6	642.3	14.9
40		Neu5Gc9Ac3Galβ4GlcβR1	4499.0	340.5	2514.3	240.9	8050.0	442.7	105.8	126.7	28760.3	3436.1	28.3	2.0	82.8	10.4	302.8	2.1	398.5	33.8
2		Neu5Gc9Acα3Galβ4GlcNAcβR1	6852.0	539.4	1355.0	306.3	15152.3	869.9	54.8	11.2	29415.0	2391.1	74.3	3.3	110.5	16.7	613.0	50.5	501.5	23.5
93		Neu5Gc9Acα3Galβ4GlcNAcβ3Galβ4GlcβR1	5725.0	813.8	452.5	84.2	8896.3	43.7	40.8	11.1	39933.5	2388.9	1052.5	104.6	87.3	29.0	247.5	25.3	455.3	8.2
32		Neu5Gc9Acα6GalβR1	3045.8	624.6	197.8	41.2	402.0	63.6	87.5	122.4	18476.8	3685.6	4453.5	166.7	127.0	34.9	476.8	44.5	360.8	21.5
38		Neu5Gc9Ac6Galβ4GlcβR1	7529.8	349.7	594.3	67.4	206.0	51.4	81.8	26.1	17761.8	2636.6	15282.8	800.4	75.5	12.5	348.0	55.4	524.5	53.8
4		Neu5Gc9Acα6Galβ4GlcNAcβR1	4993.8	339.8	555.3	55.1	280.3	46.2	27.8	5.6	33448.5	4035.7	13580.5	1027.1	126.8	24.3	700.8	95.9	611.0	10.8
24		Neu5Gc9Acα6GalNAcαR1	3668.5	655.3	469.8	59.5	368.0	23.3	30.3	8.7	32427.8	1575.5	983.8	95.2	64.3	7.5	453.0	27.6	804.3	27.6
245	Ganglioside type	Neu5Acα3(Galβ3GalNAcβ4)Galβ4GlcβR1	7241.8	497.4	13635.0	500.0	214.3	23.1	59.7	23.5	4.0	2.9	8.8	0.2	0.0	5.0	160.3	61.0	37.3	17.3
247		Neu5Acα3(Fuca2Galβ3GalNAcβ4)Galβ4GlcβR1	5741.3	352.5	11117.0	688.3	239.0	14.1	99.2	19.7	23.0	5.4	35.8	6.4	47.0	9.1	173.3	26.5	65.3	30.8
244		Neu5Acα8Neu5Acα3(Galβ3GalNAcβ4)Galβ4GlcβR1	6593.5	245.5	10313.5	777.6	301.5	27.9	102.1	18.4	6.3	3.9	6.3	4.1	140.8	16.5	1461.8	19.0	73.5	25.7
246		Neu5Gcα3(Galβ3GalNAcβ4)Galβ4GlcβR1	6429.8	364.4	55.0	6.8	281.3	14.9	78.3	10.4	13426.8	2374.7	3.8	2.9	47.3	48.6	549.3	56.9	62.3	39.9
248		Neu5Gcα3(Fuca2Galβ3GalNAcβ4)Galβ4GlcβR1	4501.5	688.0	36.5	26.7	285.8	18.0	121.2	11.8	8266.3	771.6	16.3	2.5	76.0	25.6	153.8	54.6	35.8	12.7